

Supporting information

Bio-waste Derived Ni Single-atom Catalysts with Ni-pyridine-N₄

Active Sites for Efficient N-Alkylation of Alcohols and Amines

Yuxin Zhu,^a Qiudi Zhu,^a Youjuan Tan,^a Hongqin Wang,^a Xuefei Liu,^a Wei Gong,^{*a} Dongdong Ye,^{*b} and Xianglin Pei^{*a}

^a School of Materials and Architectural Engineering, Guizhou Normal University, Guiyang 550025, China.

^b College of Materials and Chemistry, Anhui Agricultural University, Hefei 230036, China.

* Corresponding Author: X. Pei, E-mail: xianglinpei@163.com; D. Ye, E-mail: ydd@whu.edu.cn;
W. Gong, E-mail: gongw@gznu.edu.cn.

Table of contents

S1 Experimental Section	3
S1.1 Materials	3
S1.2 Characterization	3
S1.3 Supplementary Figures	5
S1.4 Supplementary Tables.....	19
S2 Computational Details	23
S3 NMR Data of the Products.....	30
S3.1 Scope of amines and alcohols	30
S3.2 Scope of heterocycles	40
S4 NMR Image of the Products	43
S5 Supplementary References.....	68

S1 Experimental Section

S1.1 Materials

Chitin was purchased from Zhejiang Golden-Shell Pharmaceutical Co., Ltd. H₂O₂ was gained from Chongqing Chuandong Chemical (Group) Co., Ltd (30%). Phytic acid was purchased from Shanghai Aladdin Biochemical Technology Co., Ltd (50% in H₂O). Nickel(II) chloride hexahydrate (NiCl₂·6H₂O, 99%) was obtained from Shanghai Titan Scientific Co., Ltd. Nano Ni was purchased from Shanghai Macklin Biochemical Technology Co., Ltd (99.99%). Nickel acetate (Ni(OAc)₂, AR), Nickel(II) Nickel (II) acetylacetone dihydrate (Ni(acac)₂, 99%) and Bis(triphenylphosphine) nickel(II) chloride (NiCl₂(pph₃)₂, 98%) were purchased from Tianjin Damao chemical reagent factory, Shanghai Titan Scientific Co., Ltd., and Bide Pharmatech Co., Ltd., respectively. Some substrates for alcohols and amines such as 3-methylaniline, 4-methoxybenzyl alcohol, 3-methoxybenzyl alcohol, *etc.* were used as received. All other reagents, such as toluene, n-hexane, DMF, *etc.*, were obtained from various commercial sources and used without further purification.

S1.2 Characterization

The morphology and EDS mapping of the samples were examined using a field emission scanning electron microscope (FESEM, Zeiss SUPRA 55 Sapphire, Germany) with an accelerating voltage of 5 kV. Nitrogen adsorption measurements were carried out using a Micromeritics AsAp2020 (USA), and Brunauer-Emmett-Teller (BET) analysis was performed automatically. Fourier-transform infrared (FT-IR) spectra were obtained on a PerkinElmer 1600 (USA) at 220V, 50Hz with a Nernst source. Scanned 16-32 times from 4000-400 cm⁻¹ using KBr pellet method. X-ray diffraction (XRD) patterns were recorded using an X-ray powder diffractometer (Rigaku Miniflex600, Japan) with Cu K α radiation ($\lambda = 1.5406 \text{ \AA}$). Raman spectroscopy was characterized by Momo Vista 2560 from Princeton, USA, and the intensity ratio (ID/IG) of D-band and G-band (ID/IG) was used to characterize the degree of disorder

of carbon materials. Transmission electron microscope (TEM) images were collected using a JEM-2010 electron microscope (JEOL, Japan) at an accelerating voltage of 200 kV. HAADF-STEM and elemental mapping of HAADF-STEM images were studied at an accelerating voltage of 300 kV. X-ray photoelectron spectroscopy (XPS) was collected using a VG Multi Lab 2000 system equipped with a monochromatic Al K α X-ray source (XPS, VG Multi Lab 2000, USA). X-ray absorption fine structure spectra (Ni K-edge) were collected on the BL14W beamline of the Shanghai Synchrotron Radiation Facility (SSRF). Ni K-edge XANES tests were recorded in transmission mode. Ni foil, NiO and NiPc were used as references. The obtained EXAFS data were extracted and processed according to the standard procedures using the ATHENA module implemented in the IFEFFIT software package. Gas chromatography (GC) yields were determined using a GC-2014 Gas Chromatograph of Shimadzu Corporation, Japan equipped with an FID detector. The loading amount of Ni was tested using ICP-OES (Prodigy 7, Leeman Labs Inc., USA). ^1H NMR spectra were recorded on Bruker AVANCE 300 and 400 spectrometers at ambient temperatures of 300.1 and 400.1 MHz, respectively, using CDCl_3 (7.26 ppm) as an internal standard. Chemical shifts and coupling constants (J) were reported in ppm and Hz, respectively. The multiplicities of peaks were denoted as follows: s (singlet), d (doublet), t (triplet), m (multiplet).

S1.3 Supplementary Figures

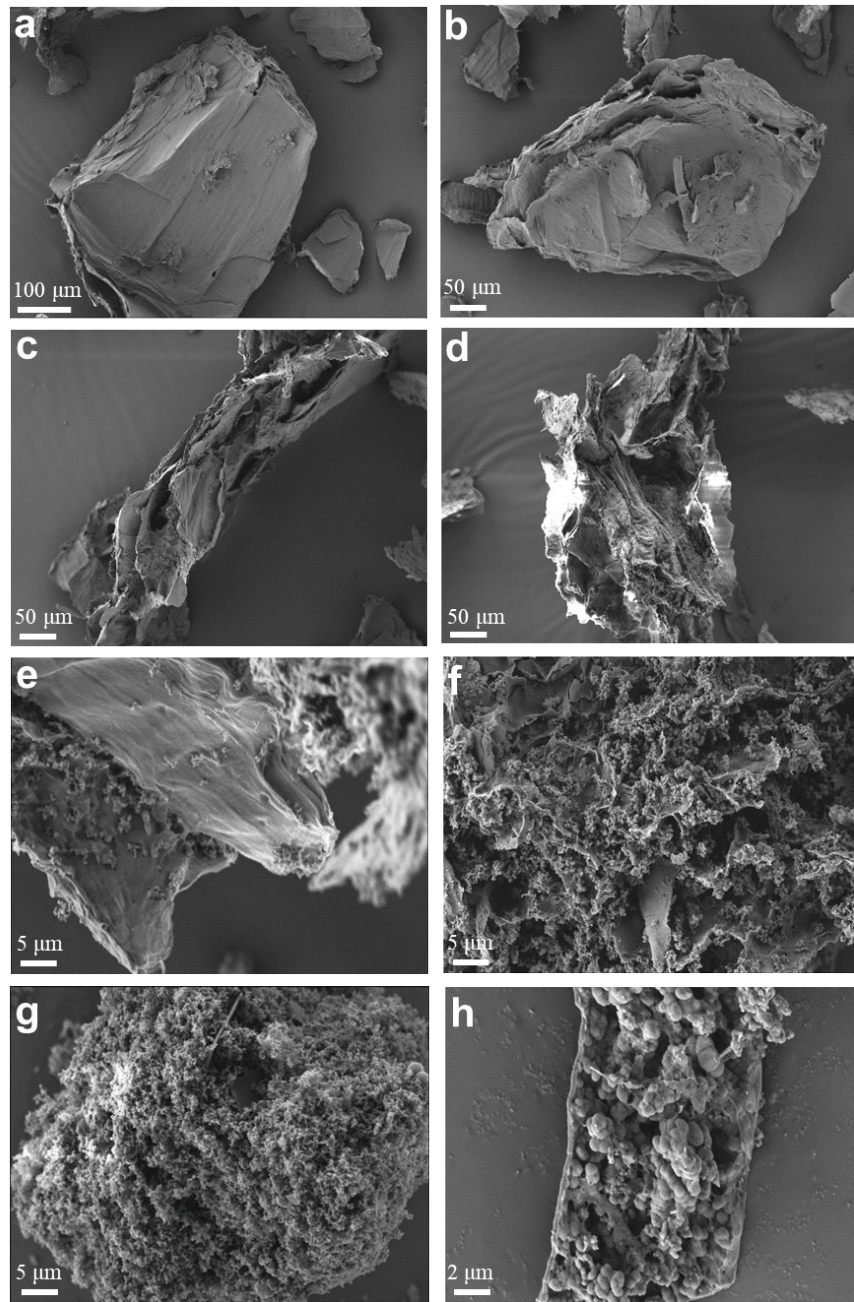


Figure S1. a-h) SEM images of the PC by adjusting the concentrations of phytic acid and H₂O₂. Reaction conditions: a) Phytic acid (5 wt %) and H₂O₂ (2 wt %). b) Phytic acid (7 wt %) and H₂O₂ (4 wt %). c) Phytic acid (9 wt %) and H₂O₂ (6 wt %). d) Phytic acid (11 wt %) and H₂O₂ (8 wt %). e) Phytic acid (13 wt %) and H₂O₂ (10 wt %). f) Phytic acid (15 wt %) and H₂O₂ (12 wt %). g) Phytic acid (20 wt %) and H₂O₂ (16 wt %). h) Phytic acid (25 wt %) and H₂O₂ (20 wt %).

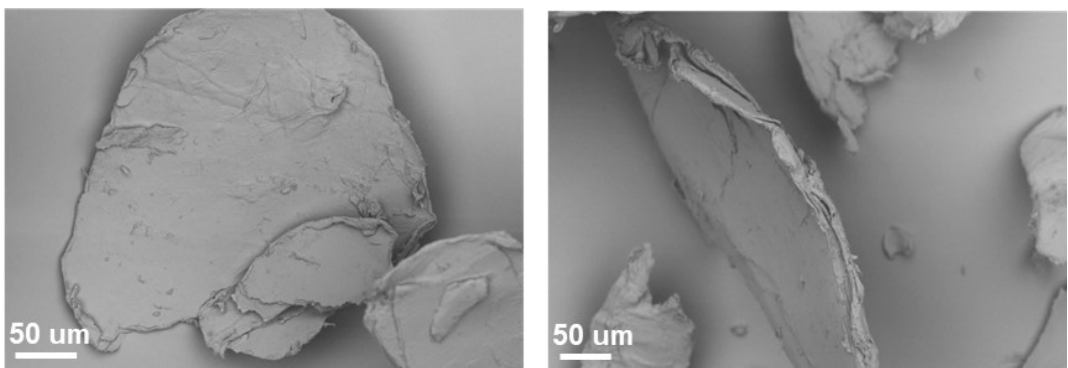


Figure S2. SEM images of the initial chitin.

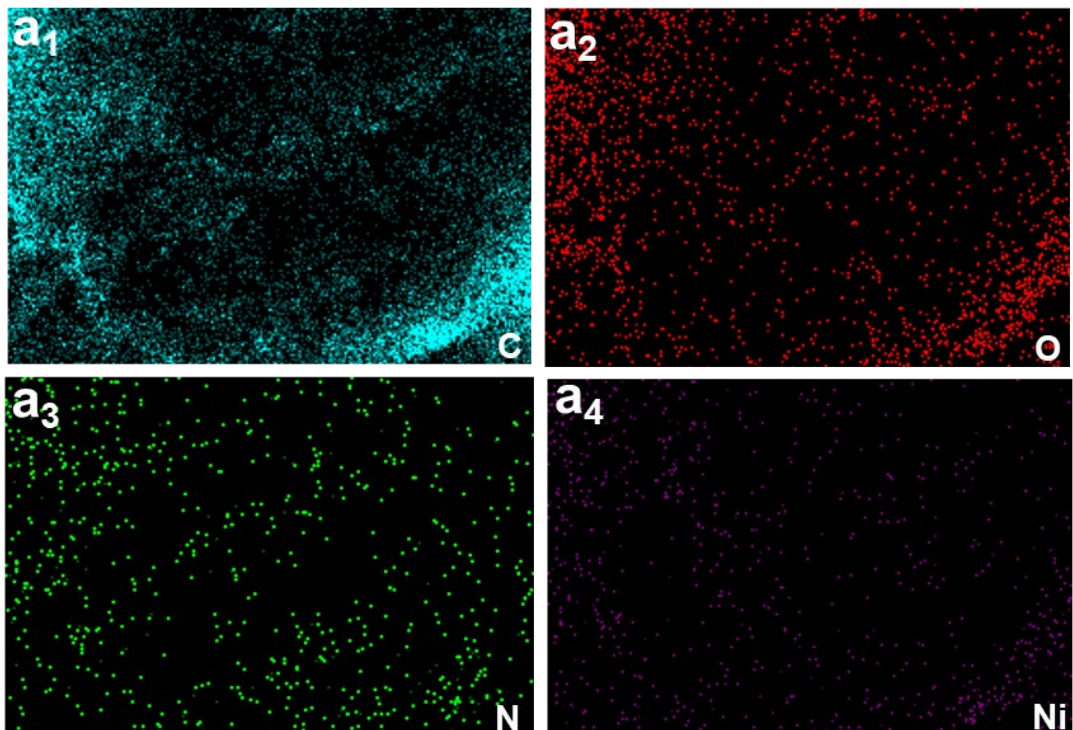


Figure S3. SEM-EDS mapping images of C a₁), O a₂), N a₃), and Ni a₄) elements in CPC@Ni catalyst.

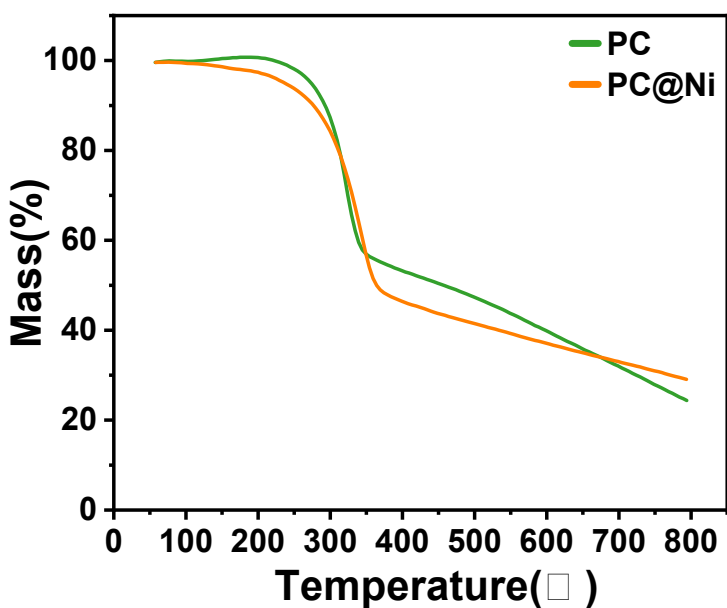


Figure S4. Thermogravimetric analysis of PC and PC@Ni.

The PC carrier did experience pyrolysis dehydration and obvious mass loss during the pyrolysis process at high temperature. Meanwhile, the loading of metallic Ni on the PC support may have a certain degradation effect on the PC support, resulting the PC@Ni sample with more obvious thermal weightlessness behavior in the temperature of 50°C to 600°C.

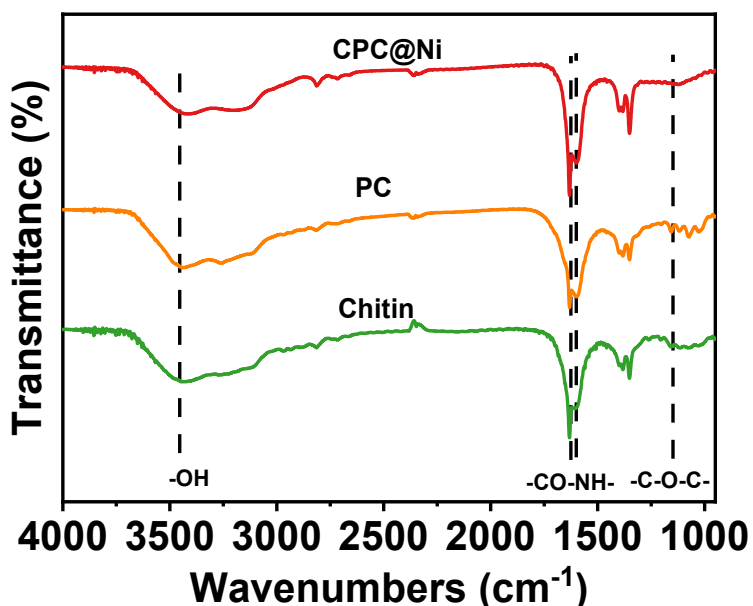


Figure S5. FT-IR spectra of the initial chitin, PC, and CPC@Ni.

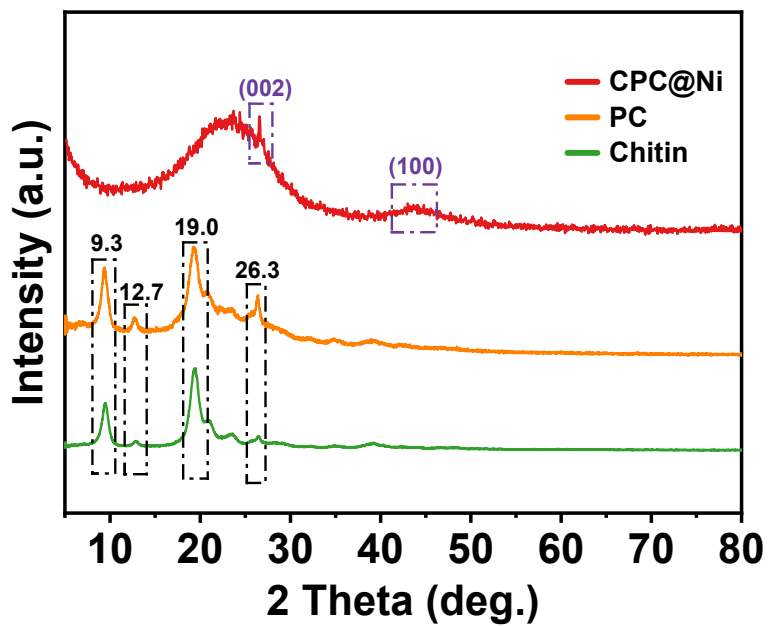


Figure S6. X-ray diffraction pattern (XRD) of the initial chitin, PC, and CPC@Ni.

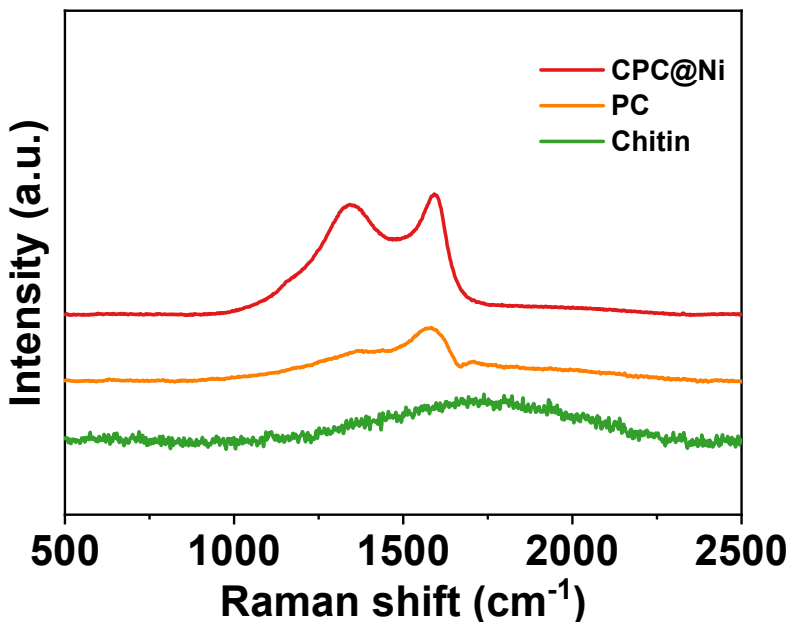


Figure S7. Raman spectra of the initial chitin, PC, and CPC@Ni.

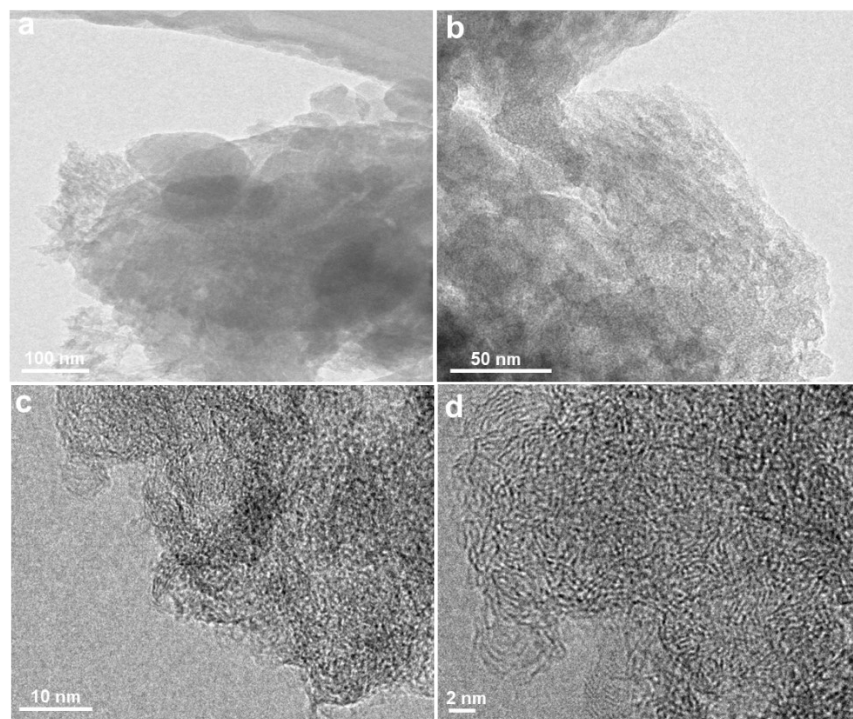


Figure S8. a-d) TEM images of the CPC@Ni.

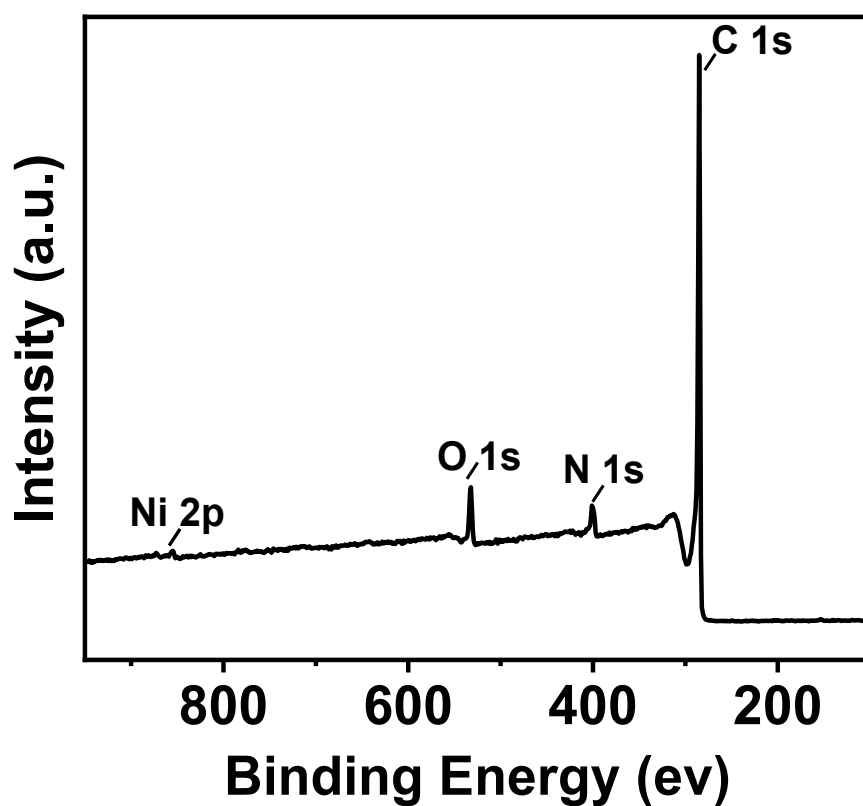


Figure S9. XPS full-size spectrum of the CPC@Ni.

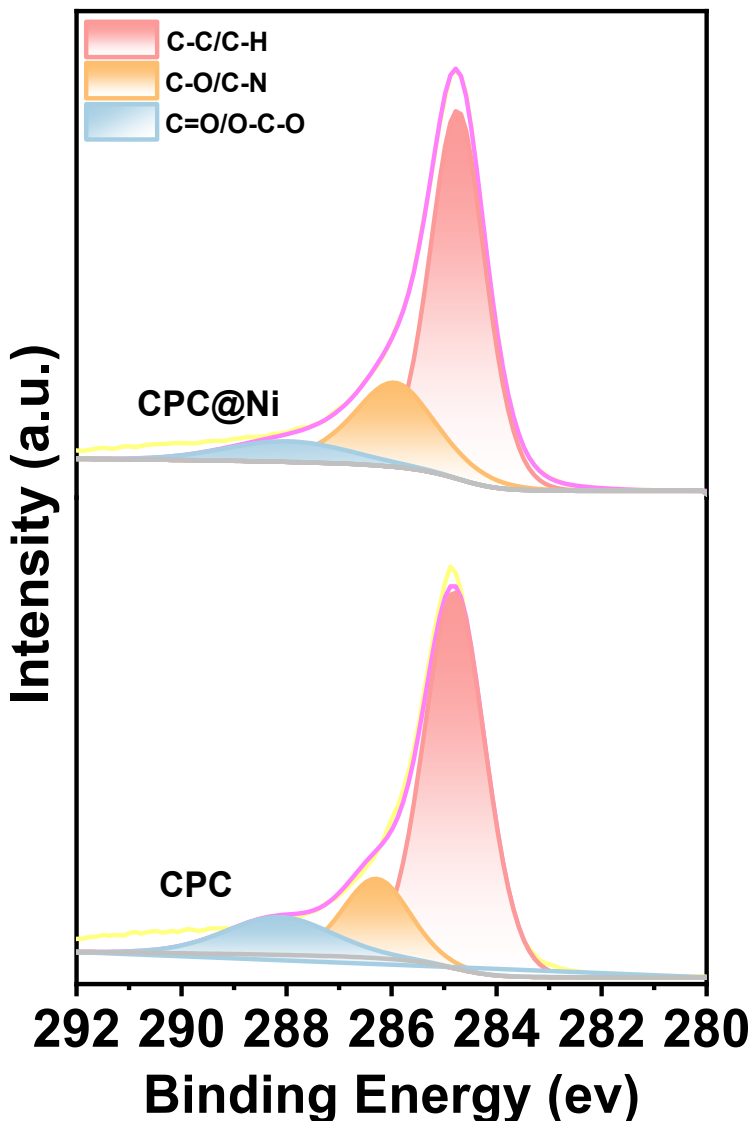


Figure S10. XPS of C1s spectra for the CPC and CPC@Ni.

The C1s spectra of CPC and CPC@Ni both exhibited peaks at 284.80 eV, 286.35 eV and 288.20 eV, corresponding to the C-C/C-H, C-O/C-N and C=O/O-C-O bonds respectively. The peaks of the C1s spectra of CPC and CPC@Ni hardly shifted, indicating that there was no interaction between Ni and C elements. Similarly, in the O1s spectra, CPC was split into three peaks corresponding to X-C=O/-C-O-C- (532.10 eV), -O-C=O (533.20 eV) and -O-N- (534.40 eV), respectively. The binding energy of CPC@Ni after loading the metal Ni also almost did not shift, indicating the no interaction between Ni and O elements.

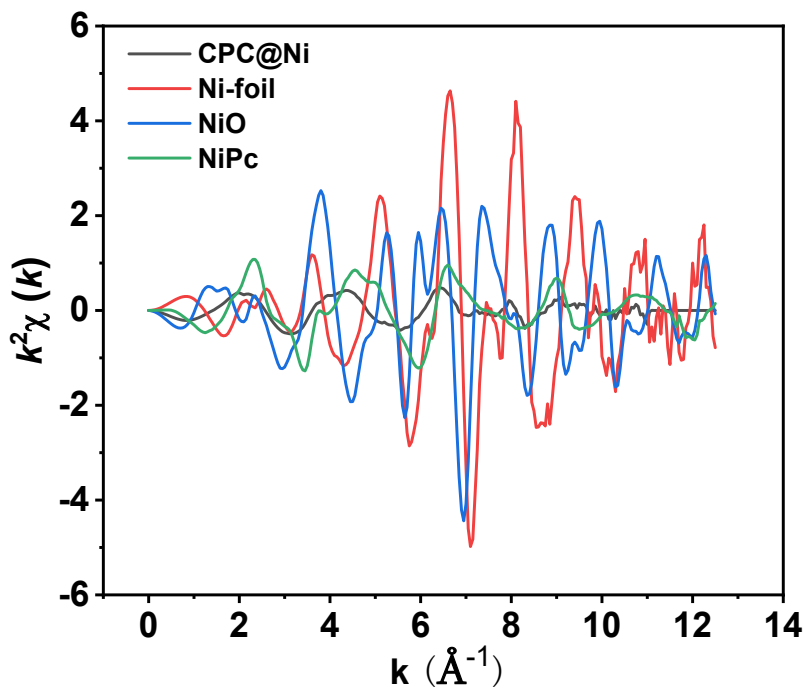


Figure S11. The k^2 -weighted EXAFS in k-space at the Ni K-edge for the CPC@Ni, Ni foil, NiO and NiPc.

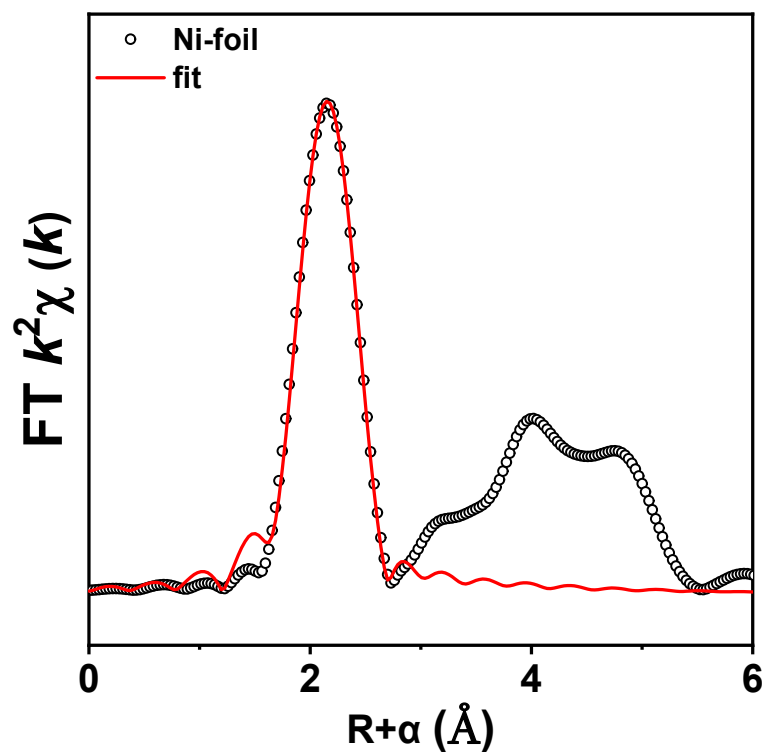


Figure S12. A typical fitting curve of the EXAFS signal in R-space for the adsorbed Ni foil.

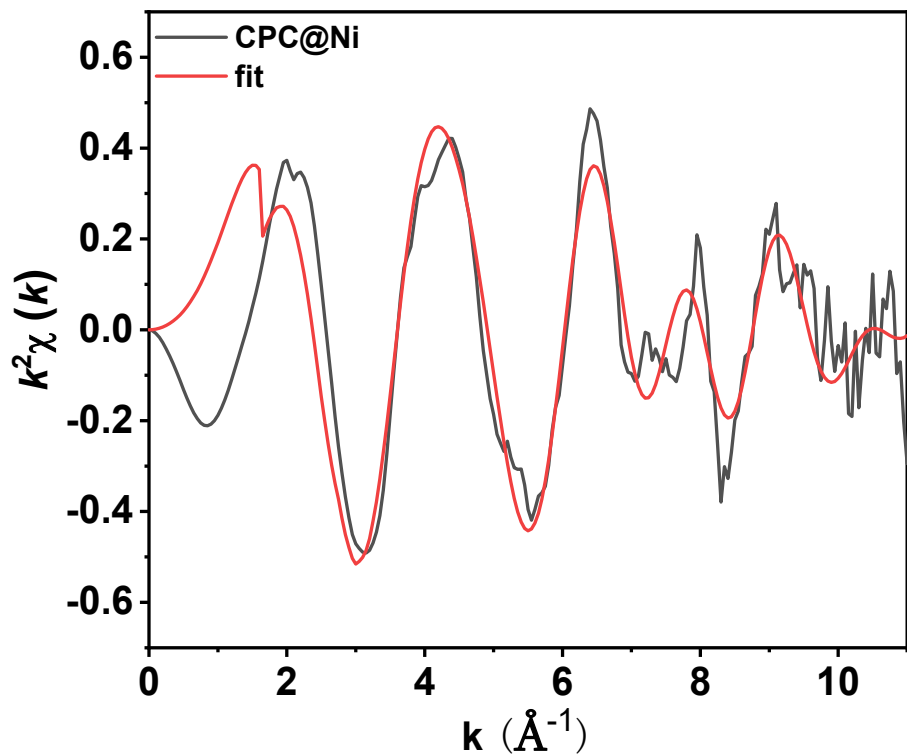


Figure S13. Ni K-edge EXAFS fitting curves of CPC@Ni at K space.

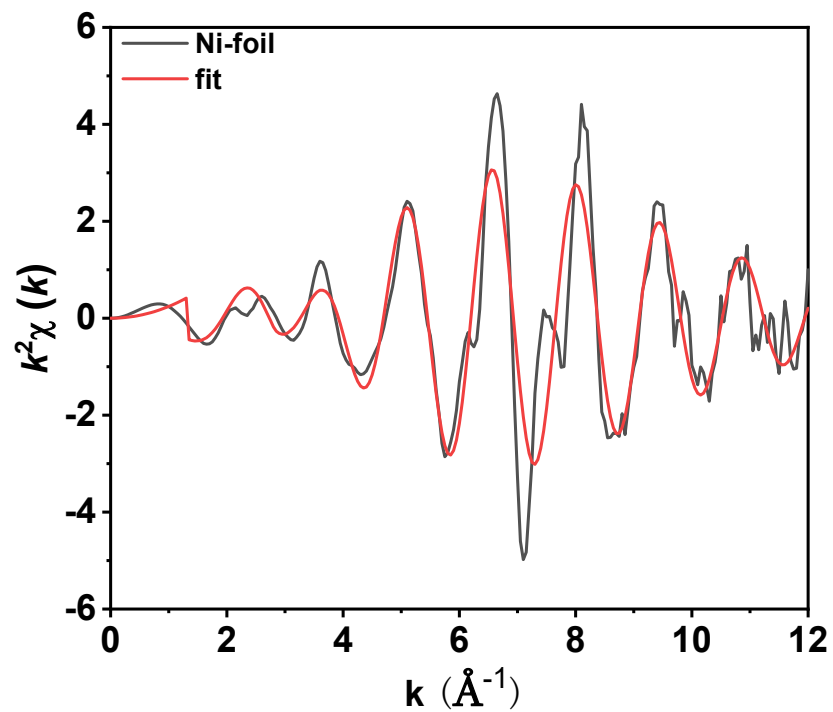


Figure S14. Ni K-edge EXAFS fitting curves of Ni foil at K space.

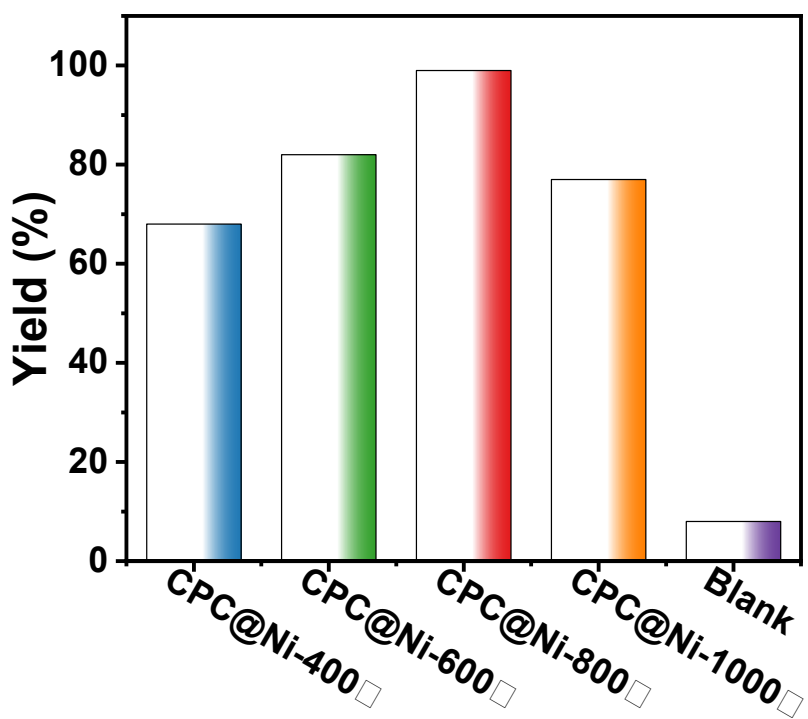


Figure S15. The impact of different pyrolysis temperatures on the activity of CPC@Ni catalyst.

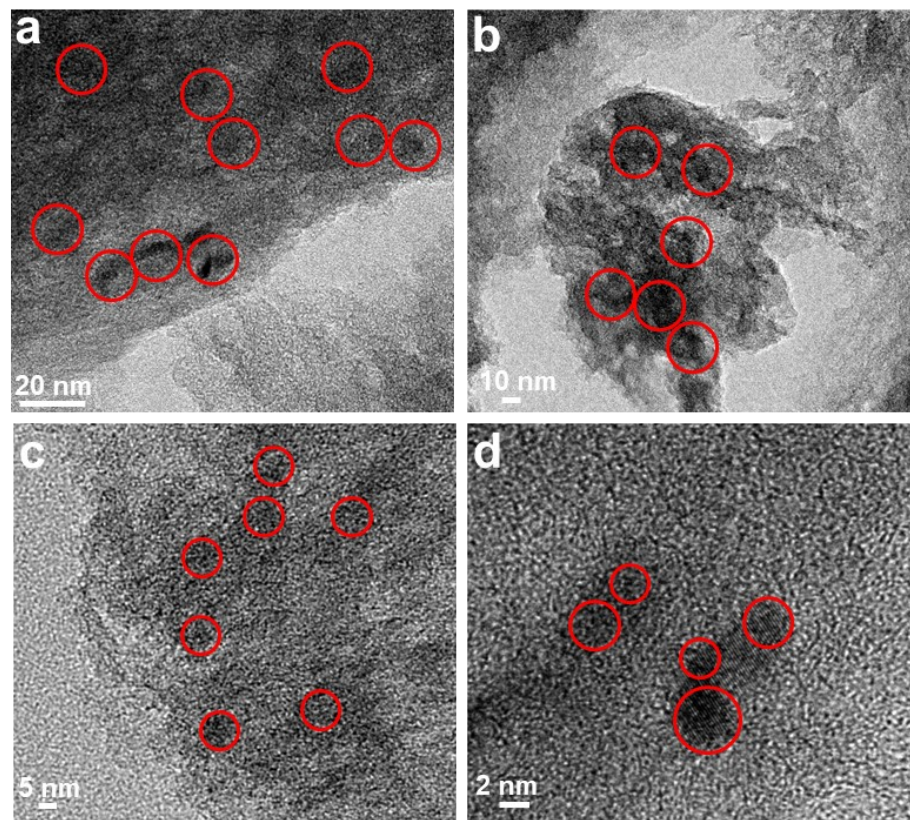


Figure S16. TEM images of the CPC@Ni-1000°C catalyst.

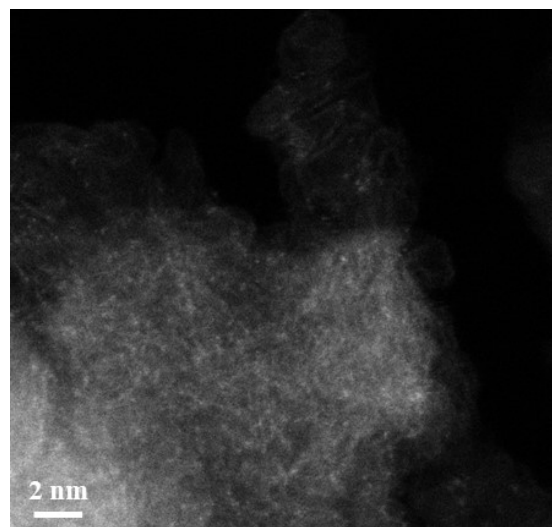


Figure S17. HAADF image of the 8-reused CPC@Ni catalyst.

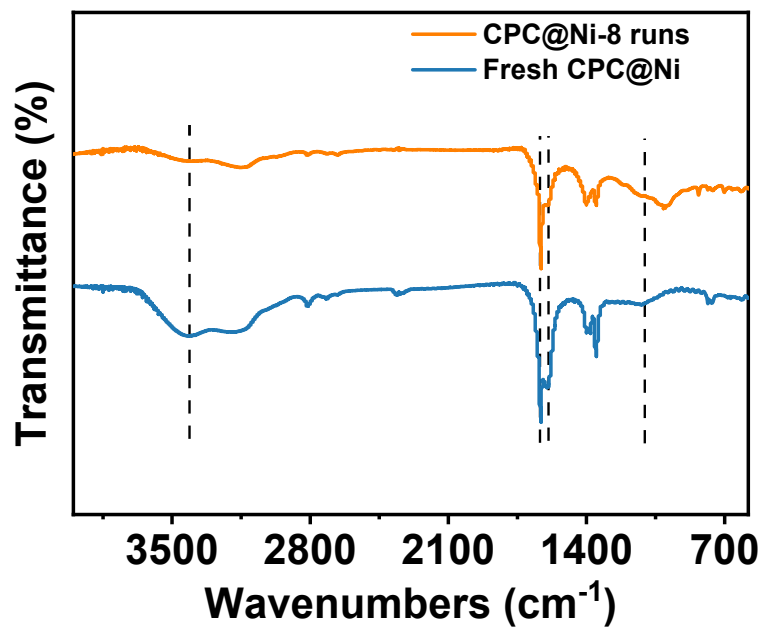


Figure S18. FT-IR spectra of the 8-reused CPC@Ni catalyst.

Deuterium labelling experiments

	3-H	C-H/H	C-H/D	C-D/D	N-H
Singnal δ	6.62	-	4.18	-	3.92
Integral value	1.00	-	0.08*2/2.08	-	0.92/0.92
Calculated ratio	-	-	8%	92%	100%

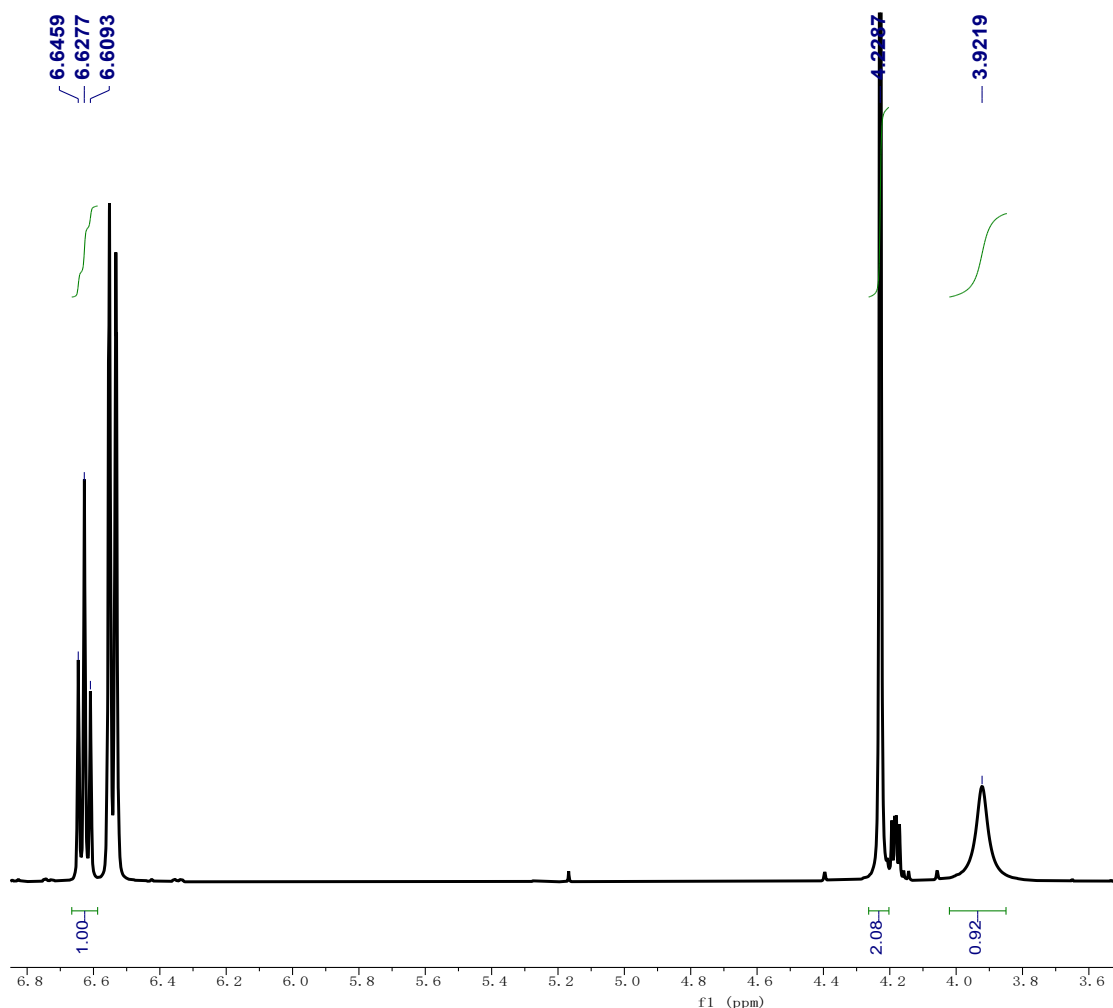
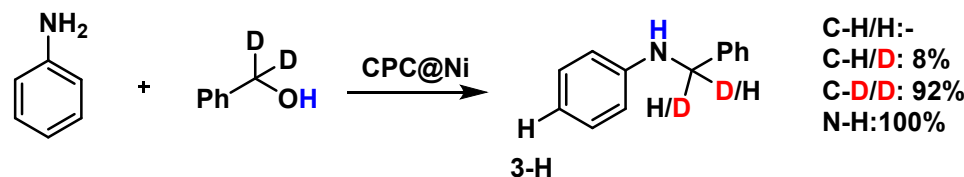


Figure S19. ^1H NMR spectrum of N-benzyldenedeuterianiline in CDCl_3 .

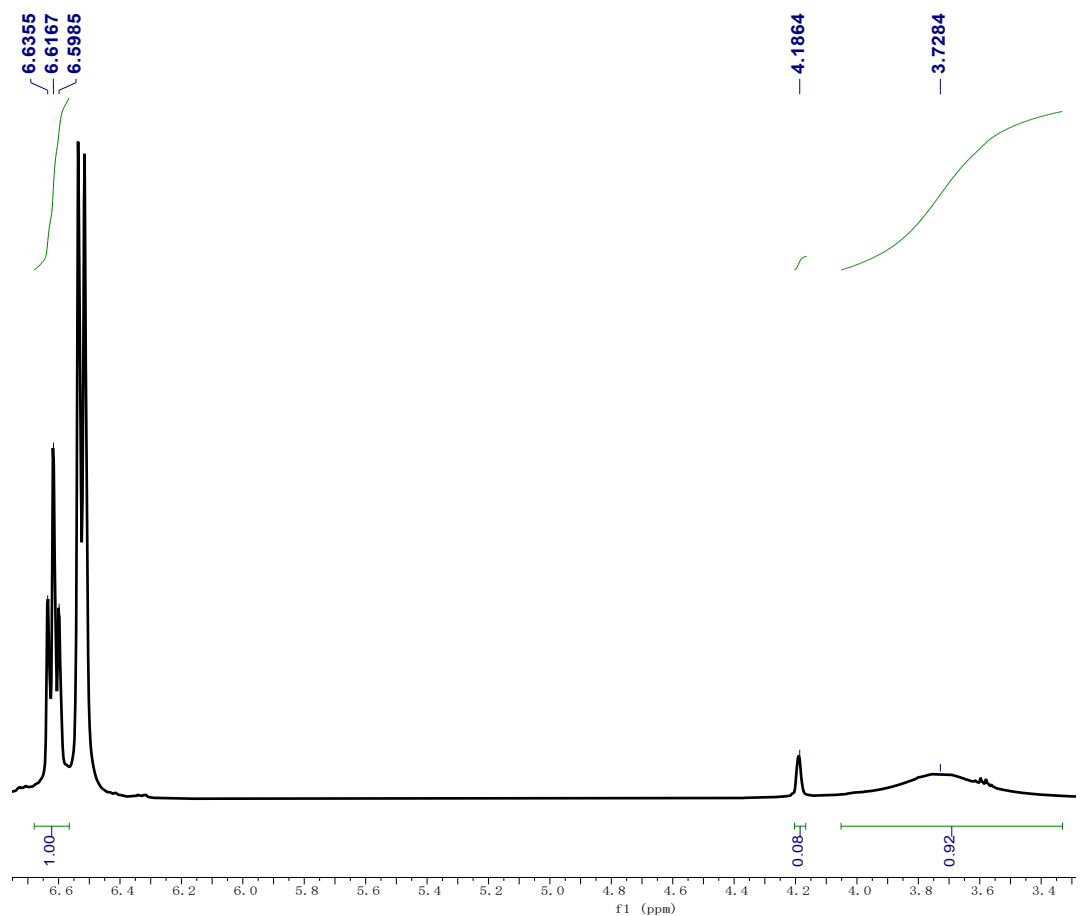


Figure S20. ¹H NMR spectrum of N-benzylaniline with types of C-H/H, C-H/D and C-D/D in CDCl₃.

ZYX #24 RT: 0.10 AV: 1 NL: 1.38E9
T: FTMS + p ESI Full ms [100.0000-1500.0000]

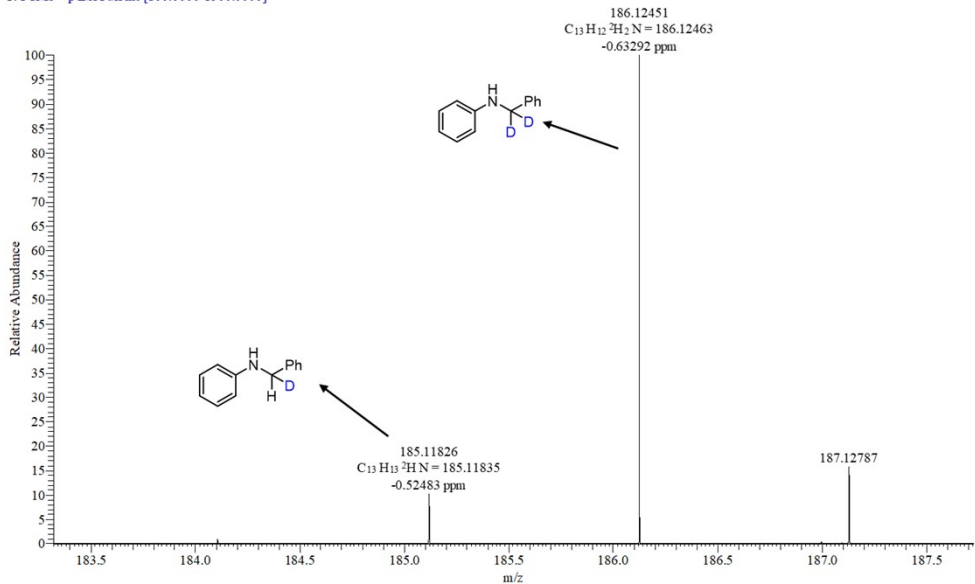


Figure S21. HR-MS spectrum for the deuterium labelling experiment by using α -C-H deuterated benzyl alcohol.

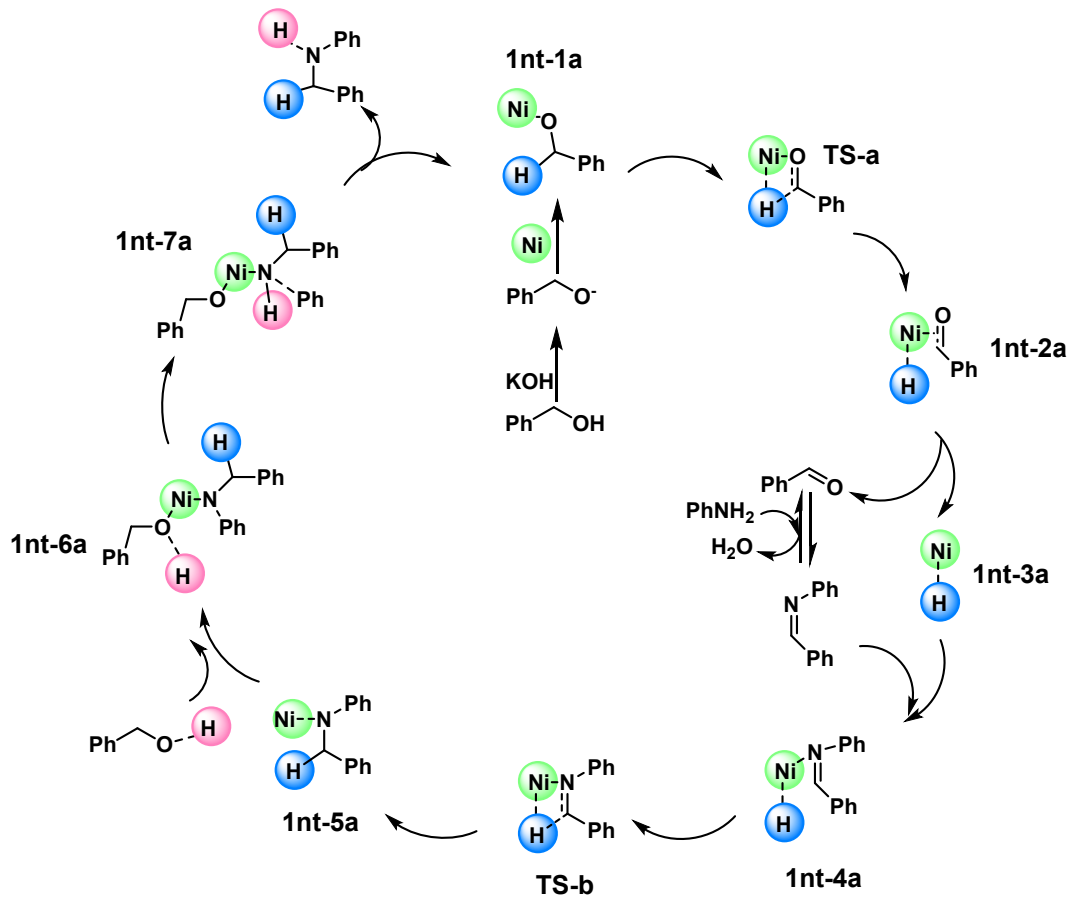


Figure S22. The proposed mechanism for the hydrogen borrowing reaction catalyzed by CPC@Ni.

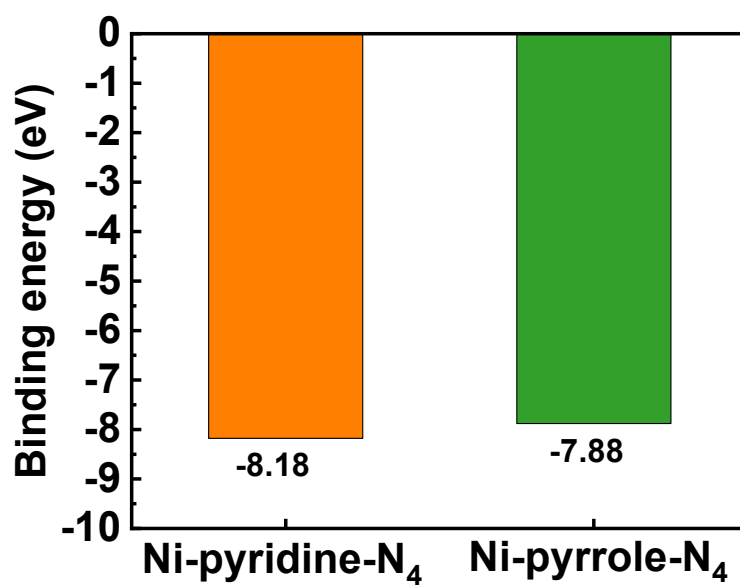


Figure S23. The binding energies of the above coordination models.

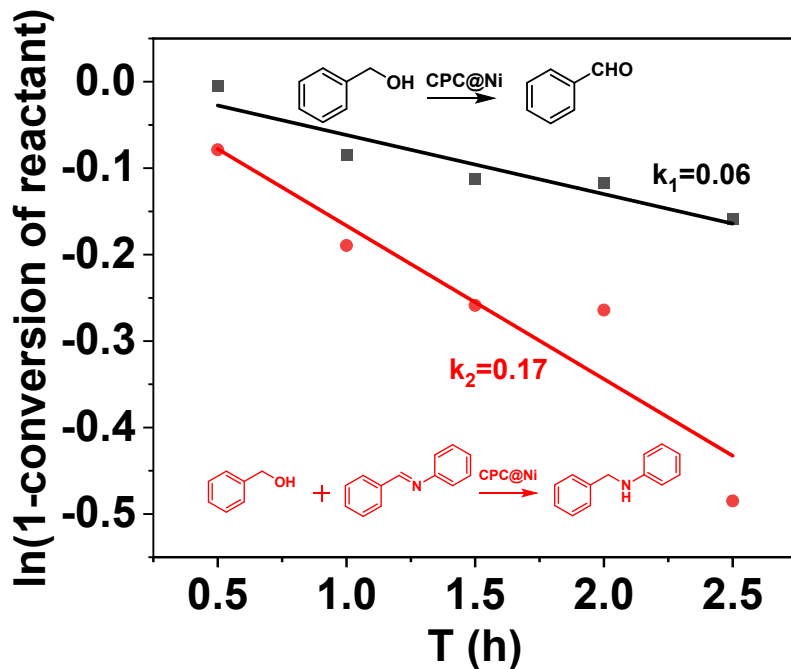


Figure S24. The kinetic plots for reaction of benzyl alcohol oxidation to benzaldehyde, and the reaction between benzyl alcohol and *N*-benzylimine. k: rate constant.

S1.4 Supplementary Tables

Table S1. EXAFS fitting parameters at the Ni K-edge for various samples ($S_0^2=0.82$ from Ni-foil).

	shell	CN ^a	R ^b (Å)	σ ^{2c} (Å ²)	ΔE ₀ ^d (eV)	R factor
Ni-foil	Ni-Ni	12	2.48±0.01	0.0063	6.7±0.9	0.0062
Ni-Sample	Ni-N	3.9±0.4	2.00±0.02	0.0064	-9.3±1.5	0.0064
	Ni-N-C	5.4±0.8	2.84±0.01	0.0034		

^aCN: coordination numbers; ^bR: bond distance; ^cσ²: Debye-Waller factors; ^d ΔE₀: the inner potential correction. R factor: goodness of fit. Error bounds that characterize the structural parameters obtained by EXAFS spectroscopy were estimated as CN ± 20%; R ± 1%; σ² ± 20%.

Table S2. Screening of solvents in the reaction between aniline and benzyl alcohol ^a

Entry	Solvent	Temperature (°C)	Base	Time (h)	Yield (%) ^b
1	Petroleum ether	120	KOH	20	55
2	n-hexane	120	KOH	20	60
3	Toluene	120	KOH	20	Trace
4	DCM	120	KOH	20	NR
5	THF	120	KOH	20	NR
6	1,4-Dioxane	120	KOH	20	21
7	MeCN	120	KOH	20	20
8	MeOH	120	KOH	20	NR
9	DMF	120	KOH	20	NR
10	H ₂ O	120	KOH	20	NR

^a Reaction conditions: aniline (0.25 mmol), benzyl alcohol (0.5 mmol), base (0.5 mmol), solvent (1.5 mL), CPC@Ni (0.4 mol% [Ni], Ni:PhNH₂), reacted at 120 °C for 20 h. ^b The yield of N-benzylaniline was determined by gas chromatography.

Table S3. The influence on the type of alkali to the reaction of aniline and benzyl alcohol ^a



Entry	Solvent	Temperature (°C)	Base	Time (h)	Yield (%) ^b
1	n-hexane	120	NaOH	21	Trace
2	n-hexane	120	KOH	21	68
3	n-hexane	120	Na ₂ CO ₃	21	NR
4	n-hexane	120	K ₂ CO ₃	21	NR
5	n-hexane	120	NaO ^t Bu	21	Trace
6	n-hexane	120	KO ^t Bu	21	NR
7	n-hexane	120	Et ₃ N	21	20

^a Reaction conditions: aniline (0.25 mmol), benzyl alcohol (0.5 mmol), base (0.5 mmol), solvent (1.5 mL), CPC@Ni (0.4 mol% [Ni], Ni:PhNH₂), reacted at 120 °C for 21 h. ^b The yield of *N*-benzylaniline was determined by gas chromatography.

Table S4. Effect of base dosage on aniline and benzyl alcohol ^a

Entry	Temperature (°C)	KOH (mmol)	Time (h)	Yield (%) ^b
1	120	0.6	21	32
2	120	0.5	21	66
3	120	0.4	21	88
4	120	0.3	21	99
5	120	0.2	21	99
6	120	0.1	21	28
7	120	-	21	0

^a Reaction conditions: aniline (0.25 mmol), benzyl alcohol (0.5 mmol), base (KOH), n-hexane (1.5 mL), CPC@Ni (0.4 mol% [Ni], Ni:PhNH₂), reacted at 120 °C for 21 h. ^b The yield of *N*-benzylaniline was determined by gas chromatography.

Table S5. Effect of reaction temperature on the reaction of aniline and benzyl alcohol

a

Entry	Temperature (°C)	Time (h)	Yield (%) ^b
1	130	21	99
2	120	21	99
3	110	21	95
4	100	21	16
5	90	21	Trace
6	60	21	NR

^a Reaction conditions: aniline (0.25 mmol), benzyl alcohol (0.5 mmol), KOH (0.2 mmol), n-hexane (1.5 mL), CPC@Ni (0.4 mol% [Ni], Ni:PhNH₂), 21 h. ^b The yield of *N*-benzylaniline was determined by gas chromatography.

Table S6. Some typical cases of supported catalysts catalyzing the hydrogen borrowing reaction of aniline and benzyl alcohol.

Catalyst	Temperature (°C)	Catalyst amount (mol %)	Time (h)	Yield (%)	Substrate scopes	TOF (h ⁻¹)	References
NbW-67%-N ₂	145	1.14	7	88	11	11	<i>J. Mol. Catal.</i> 2025 , 570: 114669.
Au-Pd@CeO ₂	150	5	8	95	5	2.38	<i>J. Chem. Sci.</i> 2024 , 136(2): 40.
OC-Ni	140	4.28	24	82	25	0.80	<i>ACS Appl. Nano Mater.</i> 2024 , 7(10): 11159-11169.
Ru@UiO-66-NH ₂	120	7	12	83	22	0.99	<i>Catal. Sci. Technol.</i> 2024 , 14(7): 1958-1966.
Cu/CeO ₂ -P	160	5.3	24	91	29	0.71	<i>J Catal.</i> 2023 , 418: 163-177.
Cu ₂ /NPC-550	140	12	12	87	31	0.60	<i>Chem.</i> 2023 , 1: 105124.
PTB-Ir@rGO (benzamide)	120	1	12	90	18	7.5	<i>ChemistrySelect.</i> 2023 , 8(45): e202303206
Pt/C	130	1.02	48	94	3	1.92	<i>J. Org. Chem.</i> 2023 , 88(4): 2245-2259.
Ru-HT (benzamide)	140	0.91	48	88	52	2.01	<i>J. Org. Chem.</i> 2022 , 87(9): 5556-5567.
Pd ₁ Cu _{0.6} -Fe ₃ O ₄ (MeOH)	140	5	24	94	18	0.78	<i>Catal. Sci. Technol.</i> 2022 (11): 3524-3533.
Pd@SiO ₂	150	1	30	97	36	3.23	<i>J Catal.</i> 2020 , 382: 141-149.
Ni/Ru@SBA	120	3	24	93	20	1.29	<i>ACS Sustain. Chem. Eng.</i> 2022 , 10(26): 8342-8349.
Bpy-UiO-Ni	140	0.85	48	100	20	2.45	<i>Tetrahedron.</i> 2022 , 124: 132993.
Ru-PNC-700	150	4.9	48	94	22	0.40	<i>New J. Chem.</i> 2021 , 45(32): 14687-14694.
Mn@NrGO	140	8	24	89	55	0.46	<i>ChemCatChem.</i> 2021 , 13(20): 4334-4341.
Hf-Beta	150	2	4.5	97.2	3	10.8	<i>ACS Catal.</i> 2021 , 11(13): 8049-8061.
Hf-MOF-808	120	12	2	85	14	3.54	<i>ACS Sustainable Chem. Eng.</i> 2021 , 9(47): 15793-15806.
Pt/C	140	1	15	92	10	6.13	<i>J Catal.</i> 2019 , 371: 47-56.
Co ₂ Rh ₂ /C	100	5	24	99	61	0.83	<i>J. Org. Chem.</i> 2018 , 83(15): 8533-8542.
Ag-Mo-22	160	20	12	93	37	0.39	<i>Chem. Eur. J.</i> 2011 , 17(3): 1021-1028.
This Work	120	0.4	21	99	42	11.79	-

TOF is defined as the number of moles of substrate transformed by 1 mol of the catalyst

$$TOF = \frac{n_{product}}{n_{catalyst} \times t}$$

present on the surface per unit time, and TOF is calculated as:

S2 Computational Details

All the DFT calculations were conducted based on the Vienna Ab-initio Simulation Package (VASP).¹ The exchange-correlation effects were described by the Perdew-Burke-Ernzerhof (PBE) functional within the generalized gradient approximation (GGA) method.² The core-valence interactions were accounted by the projected augmented wave (PAW) method.^{3,4} The energy cutoff for plane wave expansions was set to 450 eV. The structural optimization was completed for energy and force convergence set at 1.0×10^{-6} eV and 0.02 eV Å⁻¹, respectively. We applied a graphene supercell with the surface periodicity of 64 including 96 atoms as a basis to construct the Ni-pyridine and Ni-pyrrole N₄ structures. The Climbing Image-Nudged Elastic Band (CI-NEB) method was employed to obtain the initial gausses for transition state structures,⁵ followed by the Dimer method to converge to saddle points.⁶ Intermediate images were generated using the image-dependent pair potential (IDPP) interpolation scheme.⁷ Frequency calculations were carried out to ensure that all transition states possess exactly one imaginary frequency. For all models, a vacuum layer of 20 Å was applied in the z direction to avoid periodic interactions. The Brillouin zone was sampled with a $1 \times 2 \times 1$ grid centered at the gamma (Γ) point. The binding energy of Ni was calculated by following equation:

$$E_{bind} = E_{Ni - N_4 - C} - E_{N_4 - C} - E_{Ni}$$

where $E_{Ni - N_4 - C}$, $E_{N_4 - C}$, E_{Ni} is the energy of Ni-N₄-C, N₄-C, Ni. The Gibbs free energies (G) were calculated by combining the DFT total energy with zero-point energy (E_{ZPE}), heat capacity (C_p), and entropy (TS) correction, as shown in below. The standard ideal gas method was used to calculate E_{ZPE} , $\int C_p dT$, and TS from temperature (298.15 K), pressure (1 atm), and vibrational energies via the VASPKIT code.⁸

$$G = E_{DFT} + E_{ZPE} - TS + \int C_p dT$$

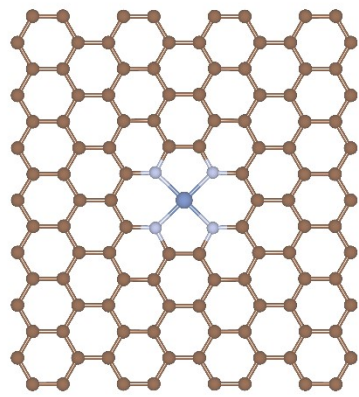


Figure S25. The model of Ni-pyridine-N₄, with binding energy of -8.18 eV.

C	0.99995	0	0.09608
C	0.12483	0.08368	0.09605
C	0.08339	0	0.09604
C	0.20818	0.08357	0.09605
C	0.24959	0	0.09605
C	0.37478	0.08297	0.09608
C	0.3331	0	0.09608
C	0.45803	0.08259	0.09608
C	0.49991	0	0.09607
C	0.6253	0.0826	0.09605
C	0.58342	0	0.09604
C	0.70854	0.08297	0.09605
C	0.75022	0	0.09605
C	0.87514	0.08356	0.09607
C	0.83372	0	0.09608
C	0.9585	0.08367	0.09607
C	0.99987	0.16747	0.09608
C	0.12548	0.25094	0.09609
C	0.08346	0.16746	0.09607
C	0.20945	0.25095	0.09609
C	0.25008	0.16697	0.09608
C	0.37548	0.24901	0.0961
C	0.33332	0.16636	0.09608
C	0.45866	0.24766	0.0961
C	0.50022	0.16484	0.0961
C	0.62468	0.24766	0.09611
C	0.58312	0.16484	0.09609
C	0.70786	0.249	0.0961
C	0.75	0.16634	0.09608

C	0.87386	0.25095	0.09608
C	0.83324	0.16698	0.09608
C	0.95783	0.25093	0.09609
C	0.99956	0.33431	0.09607
C	0.12656	0.41733	0.09603
C	0.08376	0.33432	0.09607
C	0.21085	0.41754	0.09605
C	0.25229	0.33418	0.09608
C	0.38182	0.41573	0.09605
C	0.3363	0.3336	0.09608
C	0.49999	0.32967	0.09608
C	0.58336	0.32965	0.09608
C	0.70152	0.41573	0.09608
C	0.74704	0.3336	0.09609
C	0.87249	0.41754	0.09606
C	0.83103	0.33418	0.09608
C	0.95677	0.41734	0.09607
C	0.99958	0.5	0.09607
C	0.12656	0.58267	0.09603
C	0.08377	0.5	0.09604
C	0.21085	0.58246	0.09605
C	0.25479	0.5	0.09606
C	0.38182	0.58427	0.09605
C	0.33995	0.5	0.09605
C	0.70152	0.58428	0.09608
C	0.74341	0.5	0.09609
C	0.87249	0.58246	0.09606
C	0.82856	0.5	0.09607
C	0.95677	0.58266	0.09607
C	0.99956	0.66569	0.09607
C	0.12548	0.74907	0.09609
C	0.08376	0.66569	0.09607
C	0.20945	0.74906	0.09609
C	0.25229	0.66583	0.09608
C	0.37548	0.75099	0.0961
C	0.3363	0.6664	0.09608
C	0.45866	0.75234	0.0961
C	0.49999	0.67034	0.09608
C	0.62468	0.75235	0.09611
C	0.58336	0.67035	0.09608
C	0.70786	0.751	0.0961
C	0.74704	0.66641	0.09609
C	0.87386	0.74905	0.09608
C	0.83103	0.66582	0.09608

C	0.95783	0.74907	0.09609
C	0.99987	0.83254	0.09608
C	0.12483	0.91633	0.09605
C	0.08346	0.83254	0.09607
C	0.20818	0.91643	0.09605
C	0.25008	0.83303	0.09608
C	0.37478	0.91703	0.09608
C	0.33332	0.83364	0.09608
C	0.45803	0.91741	0.09608
C	0.50022	0.83516	0.0961
C	0.6253	0.91741	0.09605
C	0.58312	0.83516	0.09609
C	0.70854	0.91703	0.09606
C	0.75	0.83366	0.09608
C	0.87514	0.91644	0.09607
C	0.83324	0.83303	0.09608
C	0.9585	0.91633	0.09607
N	0.4627	0.41195	0.09602
N	0.62066	0.41194	0.09606
N	0.4627	0.58805	0.09602
N	0.62066	0.58806	0.09606
Ni	0.54171	0.5	0.096

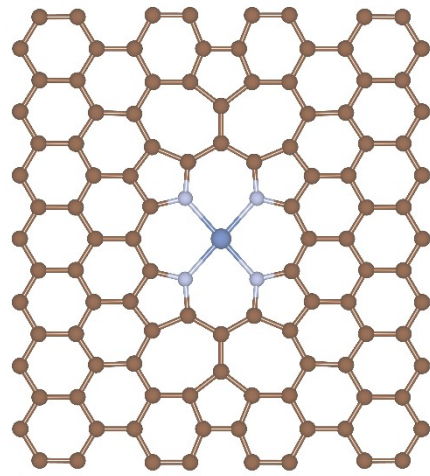


Figure S26. The model of Ni-pyrrole-N₄, with binding energy of -7.88 eV.

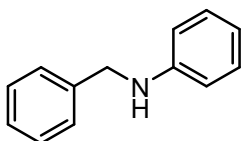
C	0.99824	0.99982	0.12805
C	0.12863	0.08283	0.12803
C	0.08487	0.99982	0.128
C	0.21496	0.0834	0.12797
C	0.25866	0.9998	0.12791
C	0.38616	0.08775	0.12789
C	0.34455	0.99979	0.12787
C	0.47089	0.08757	0.12794
C	0.50119	0.99977	0.12796
C	0.6123	0.08758	0.12805
C	0.58201	0.99977	0.12804
C	0.697	0.08777	0.12813
C	0.73861	0.9998	0.12816
C	0.86818	0.08342	0.12819
C	0.8245	0.99981	0.12815
C	0.9545	0.08284	0.12816
C	0.99887	0.16558	0.12818
C	0.12647	0.2492	0.12806
C	0.08428	0.16556	0.12811
C	0.21124	0.24968	0.1279
C	0.25731	0.16815	0.12792
C	0.38452	0.2585	0.12776
C	0.3436	0.1713	0.12786
C	0.46621	0.29754	0.12775
C	0.54158	0.15045	0.12797
C	0.61695	0.29756	0.12791
C	0.69864	0.25852	0.12802

C	0.73955	0.17134	0.12814
C	0.87194	0.2497	0.12822
C	0.82584	0.16818	0.12821
C	0.9567	0.24922	0.12822
C	0.99918	0.3329	0.12815
C	0.12632	0.41671	0.12793
C	0.08399	0.3329	0.12807
C	0.21078	0.41729	0.12774
C	0.25171	0.33359	0.12776
C	0.38069	0.41473	0.12755
C	0.33488	0.33482	0.12765
C	0.7025	0.41474	0.12776
C	0.74829	0.33483	0.12793
C	0.87238	0.4173	0.12796
C	0.83145	0.3336	0.12806
C	0.95684	0.41672	0.12804
C	0.99954	0.49983	0.1279
C	0.12632	0.58294	0.1277
C	0.08361	0.49982	0.12789
C	0.21077	0.58232	0.12754
C	0.25526	0.4998	0.12751
C	0.3807	0.58485	0.12741
C	0.34151	0.49979	0.12743
C	0.7025	0.58486	0.12768
C	0.74165	0.4998	0.12769
C	0.87238	0.58234	0.12775
C	0.8279	0.49981	0.12779
C	0.95683	0.58294	0.12779
C	0.99918	0.66675	0.12774
C	0.12646	0.75044	0.12769
C	0.08399	0.66675	0.12769
C	0.21123	0.74991	0.1276
C	0.25171	0.666	0.12748
C	0.3845	0.74107	0.12759
C	0.33487	0.66476	0.12743
C	0.4662	0.70204	0.12762
C	0.61696	0.70203	0.12782
C	0.69864	0.74108	0.12786
C	0.7483	0.66477	0.12775
C	0.87193	0.74993	0.12784
C	0.83145	0.66604	0.12776
C	0.9567	0.75044	0.12778
C	0.99887	0.83408	0.12784
C	0.12863	0.91681	0.12789

C	0.08427	0.83409	0.1278
C	0.21496	0.91621	0.12786
C	0.2573	0.83144	0.12774
C	0.38615	0.91182	0.12783
C	0.34359	0.82827	0.12772
C	0.47088	0.912	0.1279
C	0.54157	0.84909	0.1279
C	0.6123	0.912	0.12801
C	0.69701	0.91182	0.12807
C	0.73955	0.82826	0.12798
C	0.86819	0.91623	0.12804
C	0.82585	0.83145	0.12796
C	0.9545	0.91681	0.12798
C	0.54157	0.24858	0.12788
C	0.54157	0.75098	0.12779
N	0.62321	0.60611	0.12773
N	0.45999	0.60611	0.12753
N	0.45999	0.39347	0.12764
N	0.6232	0.39348	0.12776
Ni	0.54162	0.49975	0.12767

S3 NMR Data of the Products

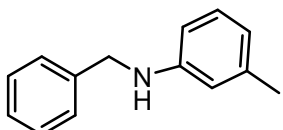
S3.1 Scope of amines and alcohols



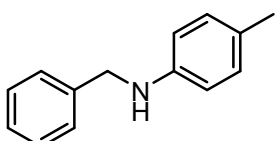
N-benzyylaniline (pro.1): Colorless oil ($m = 53$ mg, 99% isolated yield). ^1H NMR (400 MHz, Chloroform-*d*) δ 7.30 (d, $J = 6.9$ Hz, 4H), 7.26 - 7.20 (m, 1H), 7.17 - 7.08 (m, 2H), 6.68 (t, $J = 7.3$ Hz, 1H), 6.57 (d, $J = 7.5$ Hz, 2H), 4.25 (s, 2H), 3.92 (s, 1H). This spectrum was also similar to the reported (*ACS Catal.* **2018**, 8, 8525 - 8530; *ACS Catal.* **2019**, 9, 9051 - 9059; *Inorg. Chem.* **2017**, 56, 14682 - 14687).⁹⁻¹²



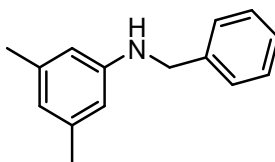
N-benzyl-2-methylaniline (pro.2): Colorless oil ($m = 54$ mg, 99% isolated yield). ^1H NMR (400 MHz, Chloroform-*d*) δ 7.26 (dt, $J = 14.9, 7.3$ Hz, 4H), 7.18 (t, $J = 7.0$ Hz, 1H), 6.99 (dd, $J = 12.8, 7.1$ Hz, 2H), 6.58 (t, $J = 7.3$ Hz, 1H), 6.51 (d, $J = 8.0$ Hz, 1H), 4.26 (s, 2H), 3.75 (s, 1H), 2.06 (s, 3H). This spectrum was also similar to the reported (*Chem. Eur. J.* **2023**, 29, e202302007; *Green Chem.* **2019**, 21, 219 - 224).^{9, 10}



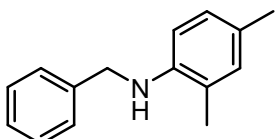
N-benzyl-3-methylaniline (pro.3): Colorless oil ($m = 49$ mg, 99% isolated yield). ^1H NMR (400 MHz, Chloroform-*d*) δ 7.30 (d, $J = 6.8$ Hz, 4H), 7.23 (d, $J = 6.5$ Hz, 1H), 7.09 - 6.99 (m, 1H), 6.52 (d, $J = 7.5$ Hz, 1H), 6.44 - 6.35 (m, 2H), 4.24 (s, 2H), 3.87 (s, 1H), 2.24 (s, 3H). This spectrum was also similar to the reported (*Eur. J. Inorg. Chem.* **2023**, 26, e202200751; *Chem. Eur. J.* **2023**, 29, e202302007).^{13, 14}



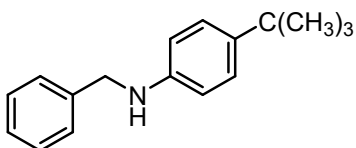
N-benzyl-4-methylaniline (pro.4): Colorless oil ($m = 52$ mg, 99% isolated yield). ^1H NMR (400 MHz, Chloroform-*d*) δ 7.29 (q, $J = 7.8$ Hz, 4H), 7.22 (d, $J = 6.8$ Hz, 1H), 6.94 (d, $J = 8.4$ Hz, 2H), 6.50 (d, $J = 8.5$ Hz, 2H), 4.22 (s, 2H), 3.80 (s, 1H), 2.20 (s, 3H). This spectrum was also similar to the reported (*Eur. J. Inorg. Chem.* **2023**, 26, e202200751; *Chem. Eur. J.* 2023, 29, e202302007; *J. Org. Chem.* **2023**, 88, 771 - 787).¹³⁻¹⁵



N-benzyl-3,5-dimethylaniline (pro.5): Colorless oil ($m = 57$ mg, 98% isolated yield). ^1H NMR (400 MHz, Chloroform-*d*) δ 7.24 (q, $J = 7.6$ Hz, 4H), 7.16 (t, $J = 6.6$ Hz, 1H), 6.29 (s, 1H), 6.17 (s, 2H), 4.18 (s, 2H), 3.76 (s, 1H), 2.13 (s, 6H). This spectrum was also similar to the reported (*ACS Catal.* **2018**, 8, 8525 - 8530; *Inorg. Chem.* **2018**, 57, 14582 - 14593).^{11, 16}

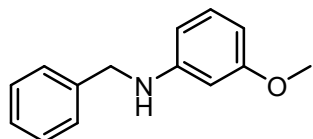


N-benzyl-2,4-dimethylaniline (pro.6): Colorless oil ($m = 60$ mg, 95% isolated yield). ^1H NMR (400 MHz, Chloroform-*d*) δ 7.41 - 7.19 (m, 4H), 7.19 - 7.10 (m, 1H), 6.80 (s, 2H), 6.42 (d, $J = 8.7$ Hz, 1H), 4.23 (s, 2H), 3.60 (s, 1H), 2.13 (s, 3H), 2.03 (s, 3H). This spectrum was also similar to the reported (*ACS Omega.* **2023**, 8(6): 5332 - 5348).¹⁷



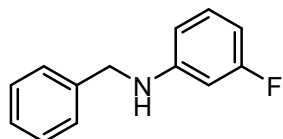
N-benzyl-4-(tert-butyl) aniline (pro.7): Colorless oil ($m = 60$ mg, 99% isolated yield).

^1H NMR (400 MHz, Chloroform-*d*) δ 7.31 - 7.21 (m, 4H), 7.19 - 7.08 (m, 3H), 6.53 - 6.47 (m, 2H), 4.20 (s, 2H), 3.78 (s, 1H), 1.19 (s, 9H). This spectrum was also similar to the reported (*Mol. Catal.* **2021**, 503: 111415).¹⁸

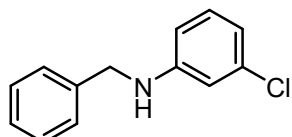


N-benzyl-3-methoxyaniline (pro.8): Colorless oil ($m = 54$ mg, 99% isolated yield).

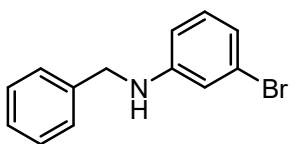
^1H NMR (400 MHz, Chloroform-*d*) δ 7.30 - 7.19 (m, 4H), 7.17 (ddd, $J = 6.5, 3.9, 1.9$ Hz, 1H), 6.97 (t, $J = 8.1$ Hz, 1H), 6.22 - 6.11 (m, 2H), 6.09 (t, $J = 2.3$ Hz, 1H), 4.20 (s, 2H), 3.94 (s, 1H), 3.64 (s, 3H). This spectrum was also similar to the reported (*ACS Catal.* **2013**, 3, 2536 - 2540; *Eur. J. Inorg. Chem.* **2023**, 26, e202200751).^{14, 19}



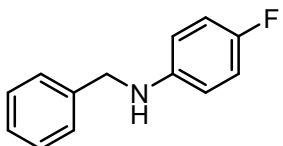
N-benzyl-3-fluoroaniline (pro.9): Yellow oil ($m = 46$ mg, 94% isolated yield). ^1H NMR (400 MHz, Chloroform-*d*) δ 7.30 (d, $J = 5.4$ Hz, 4H), 7.24 (t, $J = 4.6$ Hz, 1H), 7.07 - 6.99 (m, 1H), 6.39 - 6.29 (m, 2H), 6.25 (dd, $J = 11.6, 2.4$ Hz, 1H), 4.21 (d, $J = 5.1$ Hz, 2H), 4.05 (s, 1H). This spectrum was also similar to the reported (*Chem. Eur. J.* **2023**, 29(61): e202302007).¹³



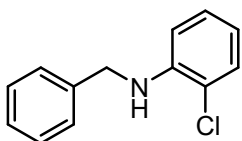
N-benzyl-3-chloroaniline (pro.10): Yellow oil. ($m = 51.7$ mg, 89% isolated yield). ^1H NMR (400 MHz, Chloroform-*d*) δ 7.31 - 7.22 (m, 5H), 6.98 (t, $J = 8.1$ Hz, 1H), 6.62 (ddd, $J = 7.9, 2.0, 0.9$ Hz, 1H), 6.58 - 6.50 (m, 1H), 6.38 (ddd, $J = 8.2, 2.4, 0.9$ Hz, 1H), 4.20 (d, $J = 22.1$ Hz, 2H), 3.96 (s, 1H). This spectrum was also similar to the reported (*Chem. Eur. J.* **2023**, 29(61): e202302007).¹³



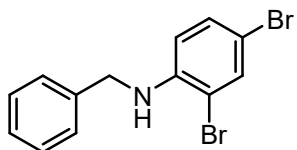
N-benzyl-3-bromoaniline (pro.11): Yellow oil ($m = 50$ mg, 92% isolated yield). ^1H NMR (400 MHz, Chloroform-*d*) δ 7.31 - 7.20 (m, 5H), 6.91 (t, $J = 8.0$ Hz, 1H), 6.76 (d, $J = 7.8$ Hz, 1H), 6.68 (s, 1H), 6.41 (d, $J = 8.3$ Hz, 1H), 4.19 (d, $J = 26.0$ Hz, 2H), 3.94 (s, 1H). This spectrum was also similar to the reported (*ChemComm.* **2011**, 47, 6981 - 6983; *J. Org. Chem.* **2023**, 88, 771 - 787).^{15, 20}



N-benzyl-4-fluoroaniline (pro.12): Colorless oil ($m = 47$ mg, 95% isolated yield). ^1H NMR (400 MHz, Chloroform-*d*) δ 7.27 (d, $J = 5.0$ Hz, 2H), 7.24 (dd, $J = 8.4, 2.5$ Hz, 2H), 7.22 - 7.11 (m, 1H), 6.83-6.73 (m, 2H), 6.50 - 6.41 (m, 2H), 4.18 (s, 2H), 3.80 (s, 1H). This spectrum was also similar to the reported (*Inorg. Chem.* **2017**, 56, 14682 - 14687; *J. Org. Chem.* **2023**, 88, 771 - 787).^{9, 15}

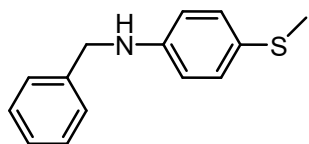


N-benzyl-2-chloroaniline (pro.13): Colorless oil ($m = 74.2$ mg, 95% isolated yield). ^1H NMR (400 MHz, Chloroform-*d*) δ 7.35 - 7.29 (m, 4H), 7.24 (d, $J = 7.1$ Hz, 2H), 7.05 (td, $J = 7.7, 1.5$ Hz, 1H), 6.60 (t, $J = 7.5$ Hz, 2H), 4.70 (s, 1H), 4.35 (s, 2H). This spectrum was also similar to the reported (*Org. Lett.* **2024**, 26, 6065-6069).²¹



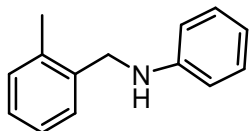
N-benzyl-2,4-dibromoaniline (pro.14): Colorless oil ($m = 81.5$ mg, 95% isolated yield). ^1H NMR (400 MHz, Chloroform-*d*) δ 7.52 (d, $J = 2.2$ Hz, 1H), 7.35 - 7.22 (m, 5H), 7.19 - 7.12 (m, 1H), 6.41 (d, $J = 8.7$ Hz, 1H), 4.74 (s, 1H), 4.32 (d, $J = 5.1$ Hz, 2H).

^{13}C NMR (101 MHz, Chloroform-*d*) δ 143.99, 138.21, 134.36, 131.31, 128.89, 127.59, 127.23, 112.72, 109.97, 108.37, 48.02.

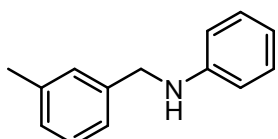


N-benzyl-4-methylthioaniline (pro.15): Yellow solid ($m = 61$ mg, 98% isolated yield). ^1H NMR (400 MHz, Chloroform-*d*) δ 7.25 (s, 2H), 7.24 (s, 2H), 7.19 (s, 1H), 7.11 (d, $J = 8.7$ Hz, 2H), 6.47 (d, $J = 8.7$ Hz, 2H), 4.20 (s, 2H), 4.08 - 3.86 (m, 1H), 2.29 (s, 3H).

^{13}C NMR (101 MHz, Chloroform-*d*) δ 147.01, 139.21, 131.51, 128.74, 127.51, 127.38, 124.53, 113.56, 48.33, 19.16.

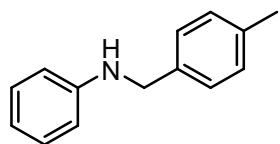


N-(2-methylbenzyl) aniline (pro.16): Colorless oil ($m = 57$ mg, 99% isolated yield). ^1H NMR (400 MHz, Chloroform-*d*) δ 7.27 (d, $J = 7.1$ Hz, 1H), 7.20 - 7.09 (m, 5H), 6.68 (t, $J = 7.3$ Hz, 1H), 6.56 (d, $J = 8.0$ Hz, 2H), 4.18 (s, 2H), 3.71 (s, 1H), 2.32 (s, 3H). This spectrum was also similar to the reported (*ACS Catal.* **2018**, 8, 8525 - 8530).¹¹



N-(3-methylbenzyl) aniline (pro.17): Colorless oil ($m = 56$ mg, 99% isolated yield).

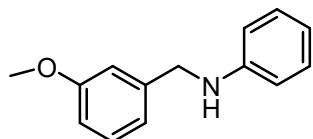
^1H NMR (400 MHz, Chloroform-*d*) δ 7.17 - 7.02 (m, 5H), 6.98 (d, $J = 7.4$ Hz, 1H), 6.61 (t, $J = 7.3$ Hz, 1H), 6.52 (d, $J = 7.3$ Hz, 2H), 4.15 (s, 2H), 3.85 (s, 1H), 2.24 (s, 3H). This spectrum was also similar to the reported (*ACS Catal.* **2018**, 8, 8525-8530).¹¹



N-(4-methylbenzyl) aniline (pro.18): Colorless oil ($m = 59$ mg, 99% isolated yield).

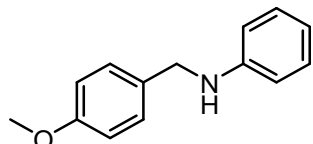
^1H NMR (400 MHz, Chloroform-*d*) δ 7.15 (d, $J = 7.9$ Hz, 2H), 7.11-6.99 (m, 4H), 6.61 (t, $J = 7.3$ Hz, 1H), 6.52 (d, $J = 7.8$ Hz, 2H), 4.16 (s, 2H), 3.84 (s, 1H), 2.24 (s, 3H).

This spectrum was also similar to the reported (*ACS Catal.* **2019**, 9, 9051-9059).¹⁰



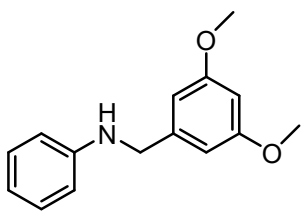
N-(3-methoxybenzyl) aniline (pro.19): Colorless oil ($m = 58$ mg, 99% isolated yield).

^1H NMR (400 MHz, Chloroform-*d*) δ 7.14 (t, $J = 7.8$ Hz, 1H), 7.06 (dd, $J = 8.6, 7.3$ Hz, 2H), 6.88-6.79 (m, 2H), 6.71 (dd, $J = 8.4, 2.6$ Hz, 1H), 6.62 (d, $J = 7.3$ Hz, 1H), 6.51 (d, $J = 7.5$ Hz, 2H), 4.18 (s, 2H), 3.91 (s, 1H), 3.67 (s, 3H). This spectrum was also similar to the reported (*RSC Adv.* **2022**, 12(4): 2436-2442).²²



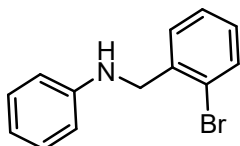
N-(4-methoxybenzyl) aniline (pro.20): Colorless oil ($m = 62$ mg, 99% isolated yield).

^1H NMR (400 MHz, Chloroform-*d*) δ 7.16 (d, $J = 8.6$ Hz, 2H), 7.10 - 7.01 (m, 2H), 6.76 (d, $J = 8.7$ Hz, 2H), 6.64 - 6.56 (m, 1H), 6.54 - 6.47 (m, 2H), 4.11 (s, 2H), 3.81 (s, 1H), 3.66 (s, 3H). This spectrum was also similar to the reported (*ACS Catal.* **2018**, 8, 8525-8530).¹¹

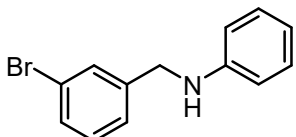


N-(3,5-dimethoxybenzyl) aniline (pro.21): Colorless oil ($m = 64$ mg, 98% isolated yield). ^1H NMR (400 MHz, Chloroform-*d*) δ 7.21 - 7.10 (m, 2H), 6.69 (t, $J = 7.4$ Hz, 1H), 6.63 - 6.57 (m, 2H), 6.52 (dd, $J = 2.2, 1.1$ Hz, 2H), 6.36 (s, 1H), 4.23 (s, 2H), 4.05 (s, 1H), 3.74 (s, 6H).

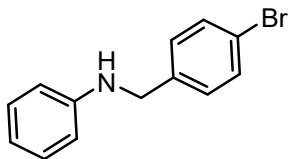
^{13}C NMR (101 MHz, Chloroform-*d*) δ 129.33, 117.69, 112.98, 105.38, 99.17, 55.37, 48.56.



N-(2-bromobenzyl) aniline (pro.22): Colorless oil ($m = 48.5$ mg, 79% isolated yield). ^1H NMR (400 MHz, Chloroform-*d*) δ 7.33 (d, $J = 7.6$ Hz, 2H), 7.29 (s, 1H), 7.17 (s, 2H), 7.10 (s, 1H), 6.64 (t, $J = 7.6$ Hz, 1H), 6.54 (d, $J = 7.9$ Hz, 2H), 4.33 (s, 2H), 4.01 (s, 1H). This spectrum was also similar to the reported (*ACS Catal.* **2019**, 9, 9051-9059; *J. Org. Chem.* **2023**, 88, 771-787).^{10, 15}

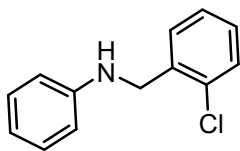


N-(3-bromobenzyl) aniline (pro.23): Yellow oil ($m = 62$ mg, 95% isolated yield). ^1H NMR (400 MHz, Chloroform-*d*) δ 7.51 (s, 1H), 7.38 (d, $J = 7.9$ Hz, 1H), 7.27 (d, $J = 7.9$ Hz, 1H), 7.21 - 7.13 (m, 3H), 6.72 (t, $J = 7.4$ Hz, 1H), 6.59 (d, $J = 7.4$ Hz, 2H), 4.28 (s, 2H), 4.04 (s, 1H). This spectrum was also similar to the reported (*Eur. J. Org. Chem.* **2022**, 2022(41): e202200982).²³



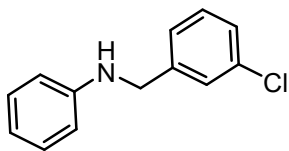
N-(4-bromobenzyl) aniline (pro.24): Yellow oil ($m = 54.6$ mg, 84% isolated yield).

^1H NMR (400 MHz, Chloroform-*d*) δ 7.44 (d, $J = 8.3$ Hz, 2H), 7.24 - 7.20 (m, 2H), 7.16 (t, $J = 7.8$ Hz, 2H), 6.71 (t, $J = 7.6$ Hz, 1H), 6.59 (d, $J = 8.1$ Hz, 2H), 4.27 (s, 2H), 4.04 (s, 1H). This spectrum was also similar to the reported (*ACS Catal.* **2018**, 8, 8525 - 8530).¹¹



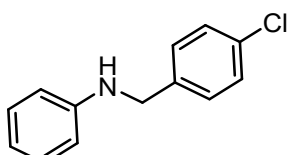
N-(2-chlorobenzyl) aniline (pro.25): Colorless oil ($m = 39$ mg, 76% isolated yield).

^1H NMR (400 MHz, Chloroform-*d*) δ 7.33 - 7.27 (m, 2H), 7.15 - 7.10 (m, 2H), 7.08 (d, $J = 7.0$ Hz, 2H), 6.64 (t, $J = 7.5$ Hz, 1H), 6.54 (d, $J = 8.2$ Hz, 2H), 4.36 (s, 2H), 3.97 (s, 1H). This spectrum was also similar to the reported (*Org. Lett.* **2024**, 26, 6065 - 6069).²¹



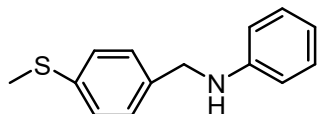
N-(3-chlorobenzyl) aniline (pro.26): Colorless oil ($m = 43$ mg, 84% isolated yield).

^1H NMR (400 MHz, Chloroform-*d*) δ 7.28 (d, $J = 1.8$ Hz, 1H), 7.18 - 7.08 (m, 5H), 6.68 (t, $J = 7.3$ Hz, 1H), 6.55 - 6.48 (m, 2H), 4.16 (s, 2H), 3.92 (s, 1H). This spectrum was also similar to the reported (*Chem. Eur. J.* **2023**, 29(61): e202302007).¹³

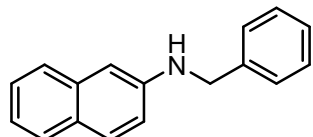


N-(4-chlorobenzyl) aniline (pro.27): Colorless oil ($m = 40$ mg, 80% isolated yield).

^1H NMR (400 MHz, Chloroform-*d*) δ 7.20 (d, $J = 2.0$ Hz, 4H), 7.08 (t, $J = 7.0$ Hz, 2H), 6.67 - 6.60 (m, 1H), 6.51 (d, $J = 8.5$ Hz, 2H), 4.21 (s, 2H), 3.92 (s, 1H). This spectrum was also similar to the reported (*ACS Catal.* **2018**, 8, 8525-8530).¹¹

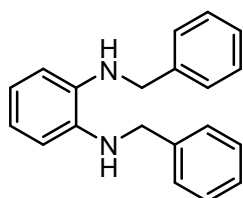


N-(4-(methylthio) benzyl) aniline (pro.28): Colorless oil ($m = 61$ mg, 99% isolated yield). ^1H NMR (400 MHz, Chloroform-*d*) δ 7.17 (d, $J = 8.4$ Hz, 2H), 7.14 - 7.10 (m, 2H), 7.06 (dd, $J = 8.6, 7.3$ Hz, 2H), 6.61 (t, $J = 7.4$ Hz, 1H), 6.51 (d, $J = 7.3$ Hz, 2H), 4.16 (s, 2H), 3.89 (s, 1H), 2.36 (s, 3H). This spectrum was also similar to the reported (*Chem. Eur. J.* 2023, 29(61): e202302007; *J. Am. Chem. Soc.* **2019**, 141(29): 11677 - 11685).^{13, 24}



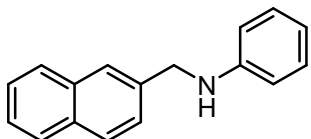
N-benzylnaphthalen-2-amine (pro.29): Yellow oil ($m = 58$ mg, 99% isolated yield).

^1H NMR (400 MHz, Chloroform-*d*) δ 7.54 (d, $J = 10.3$ Hz, 1H), 7.49 (d, $J = 5.9$ Hz, 1H), 7.26 (dt, $J = 6.9, 4.2$ Hz, 5H), 7.18 (d, $J = 7.1$ Hz, 1H), 7.13-7.03 (m, 2H), 6.79 - 6.69 (m, 2H), 4.28 (s, 2H), 4.06 (s, 1H). This spectrum was also similar to the reported (*ACS Catal.* **2019**, 9, 9051 - 9059).¹⁰

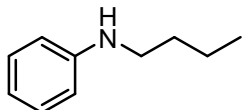


N, N-dibenzylbenzene-diamine (pro.30): Yellow oil. ($m = 57$ mg, 80% isolated yield). ^1H NMR (400 MHz, Chloroform-*d*) δ 7.22 (ddd, $J = 26.1, 14.0, 7.0$ Hz, 10H), 6.74 - 6.57 (m, 4H), 4.20 (s, 4H), 3.53 (s, 2H). This spectrum was also similar to the

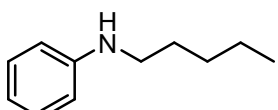
reported (*Mol. Catal.* **2021**, 503: 111415).¹⁸



N-(naphthalen-2-ylmethyl) aniline (pro.31): Colorless oil (m = 58 mg, 81% isolated yield). ^1H NMR (400 MHz, Chloroform-*d*) δ 7.78 - 7.68 (m, 4H), 7.43 - 7.35 (m, 3H), 7.17 - 7.08 (m, 2H), 6.72 - 6.64 (m, 1H), 6.57 (d, J = 8.6 Hz, 2H), 4.34 (s, 2H), 3.95 (s, 1H). This spectrum was also similar to the reported (*ACS Catal.* **2018**, 8, 8525 - 8530).¹¹

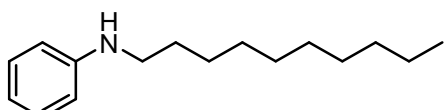


N-butylaniline (pro.32): Colorless oil (m = 26 mg, 63% isolated yield). ^1H NMR (400 MHz, Chloroform-*d*) δ 7.16 - 7.06 (m, 3H), 6.92 (d, J = 3.4 Hz, 1H), 6.89 - 6.84 (m, 1H), 6.66 (t, J = 7.3 Hz, 1H), 6.58 (d, J = 8.0 Hz, 2H), 4.41 (s, 2H), 3.88 (s, 1H). ^{13}C NMR (101 MHz, Chloroform-d) δ 148.61, 129.27, 117.11, 112.73, 43.71, 31.73, 20.36, 13.96.



N-pentylaniline (pro.33): Colorless oil (m = 45 mg, 68% isolated yield). ^1H NMR (400 MHz, Chloroform-*d*) δ 7.16 (t, J = 7.8 Hz, 2H), 6.67 (t, J = 7.3 Hz, 1H), 6.59 (d, J = 8.0 Hz, 2H), 3.57 (s, 1H), 3.08 (t, J = 7.1 Hz, 2H), 1.60 (t, J = 7.3 Hz, 2H), 1.42 - 1.33 (m, 4H), 0.94 - 0.88 (m, 3H).

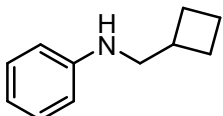
^{13}C NMR (101 MHz, Chloroform-d) δ 148.62, 117.11, 112.74, 44.02, 29.41, 29.33, 22.58.



N-decylaniline (pro.34): Colorless oil (m = 32 mg, 77% isolated yield). ^1H NMR (400

MHz, Chloroform-*d*) δ 7.19 - 7.11 (m, 2H), 6.67 (t, *J* = 7.3 Hz, 1H), 6.58 (d, *J* = 8.0 Hz, 2H), 3.54 (s, 1H), 3.07 (t, *J* = 7.1 Hz, 2H), 1.59 (t, *J* = 7.3 Hz, 2H), 1.27 (s, 14H), 0.88 (t, *J* = 6.7 Hz, 3H).

¹³C NMR (101 MHz, Chloroform-d) δ 148.63, 129.28, 117.12, 112.75, 44.07, 32.00, 29.71, 29.67, 29.56, 29.43, 27.28, 22.78, 14.20.

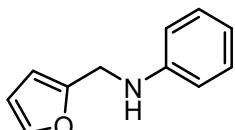


***N*-(cyclobutylmethyl)aniline (pro.35):** Colorless oil (*m* = 35 mg, 84% isolated yield).

¹H NMR (400 MHz, Chloroform-*d*) δ 7.15 (t, *J* = 7.7 Hz, 2H), 6.67 (t, *J* = 7.3 Hz, 1H), 6.58 (d, *J* = 8.0 Hz, 2H), 3.39 (s, 1H), 3.10 (d, *J* = 7.3 Hz, 2H), 2.64 - 2.50 (m, 1H), 2.10 (d, *J* = 8.3 Hz, 2H), 1.91 (q, *J* = 8.2 Hz, 2H), 1.72 (p, *J* = 8.6 Hz, 2H).

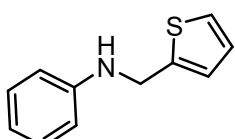
¹³C NMR (101 MHz, Chloroform-*d*) δ 148.70, 129.28, 117.20, 112.82, 49.86, 35.09, 26.16, 18.62.

S3.2 Scope of heterocycles



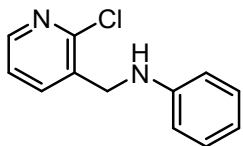
***N*-(furan-2-ylmethyl) aniline (pro.36):** Yellow oil. (*m* = 43 mg, 92% isolated yield).

¹H NMR (400 MHz, Chloroform-*d*) δ 7.33 (d, *J* = 1.9 Hz, 1H), 7.20 - 7.11 (m, 2H), 6.72 (t, *J* = 7.3 Hz, 1H), 6.63 (d, *J* = 8.6 Hz, 2H), 6.28 (d, *J* = 1.8 Hz, 1H), 6.19 (d, *J* = 3.2 Hz, 1H), 4.28 (s, 2H), 3.89 (s, 1H). This spectrum was also similar to the reported (Green Chem. 2019, 21: 219-224).²⁵



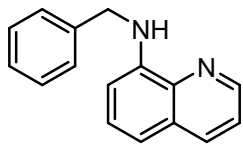
***N*-(thiophen-2-ylmethyl) aniline (pro.37):** Colorless oil (*m* = 44.6 mg, 94% isolated yield). ¹H NMR (400 MHz, Chloroform-d) δ 7.20 - 7.13 (m, 3H), 6.96 (d, *J* = 2.1 Hz,

1H), 6.92 (dd, $J = 5.1, 3.5$ Hz, 1H), 6.72 (t, $J = 7.3$ Hz, 1H), 6.65 - 6.59 (m, 2H), 4.43 (s, 2H), 3.91 (s, 1H). This spectrum was also similar to the reported (*ACS Catal.* **2018**, 8, 8525-8530; *J. Org. Chem.* **2023**, 88, 771-787).^{11, 15}

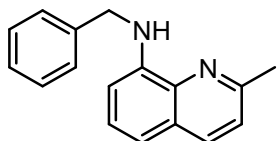


N-((2-chloropyridin-3-yl) methyl) aniline (pro.38): Yellow oil. ($m = 32$ mg, 65% isolated yield). ^1H NMR (400 MHz, CDCl_3) δ 7.19 (s, 5H), 5.57 (s, 1H), 5.54 (s, 1H), 4.05 (d, $J = 7.1$ Hz, 2H), 3.65 (s, 1H).

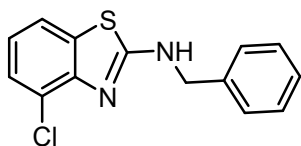
^{13}C NMR (101 MHz, Chloroform-*d*) δ 154.59, 149.69, 148.73, 137.69, 129.25, 121.01, 118.19.



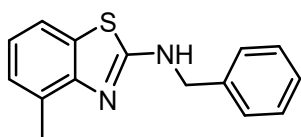
N-benzylquinolin-8-amine (pro.39): Yellow oil. ($m = 57$ mg, 94% isolated yield). ^1H NMR (400 MHz, Chloroform-*d*) δ 8.59 (dd, $J = 4.2, 1.7$ Hz, 1H), 7.91 (dd, $J = 8.2, 1.7$ Hz, 1H), 7.32 (d, $J = 7.5$ Hz, 2H), 7.28 - 7.10 (m, 5H), 6.93 (d, $J = 8.1$ Hz, 1H), 6.52 (d, $J = 7.7$ Hz, 2H), 4.43 (d, $J = 5.1$ Hz, 2H). This spectrum was also similar to the reported (*Eur. J. Inorg. Chem.* **2023**, 26(16): e202200751).¹⁴



N-benzyl-2-methylquinolin-8-amine (pro.40): Yellow oil. ($m = 63$ mg, 96% isolated yield). ^1H NMR (400 MHz, Chloroform-*d*) δ 8.08 (d, $J = 8.4$ Hz, 1H), 7.64 (d, $J = 7.6$ Hz, 2H), 7.60 - 7.42 (m, 4H), 7.36 (d, $J = 8.4$ Hz, 1H), 7.30 - 7.19 (m, 1H), 6.94 (s, 1H), 6.83 (d, $J = 7.6$ Hz, 1H), 4.72 (d, $J = 5.4$ Hz, 2H), 2.89 (s, 3H). This spectrum was also similar to the reported (*Tetrahedron*. **2018**, 74(17): 2121 - 2129).²⁶

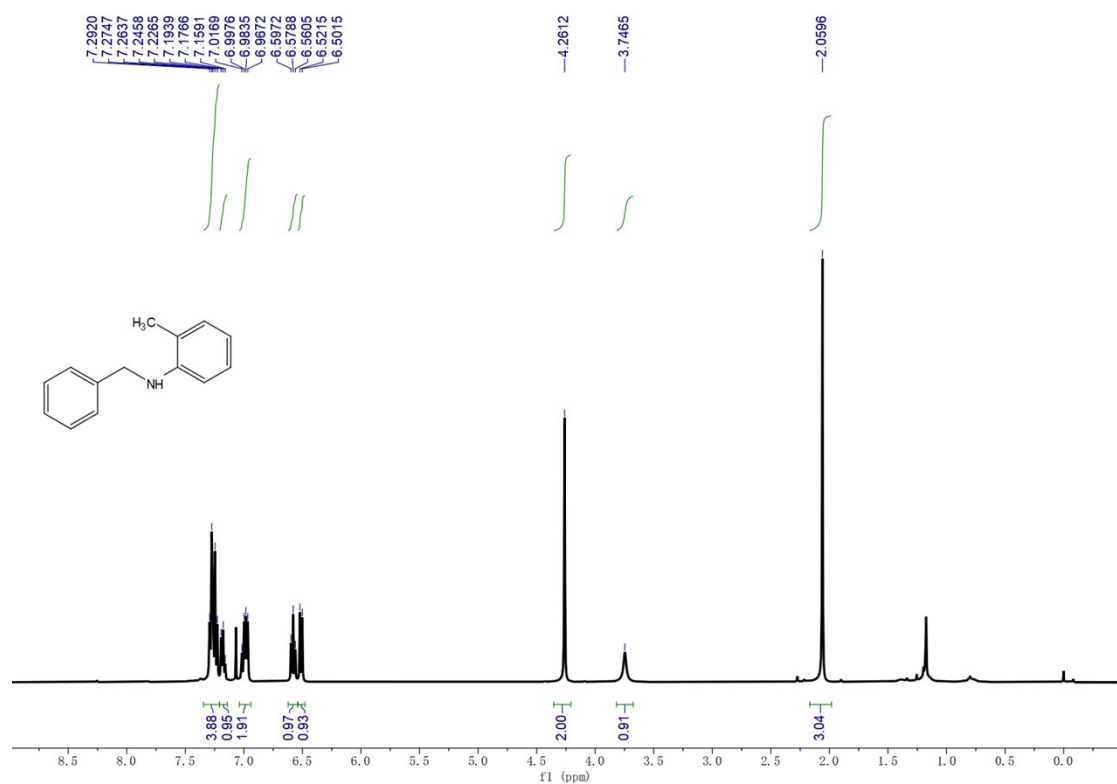
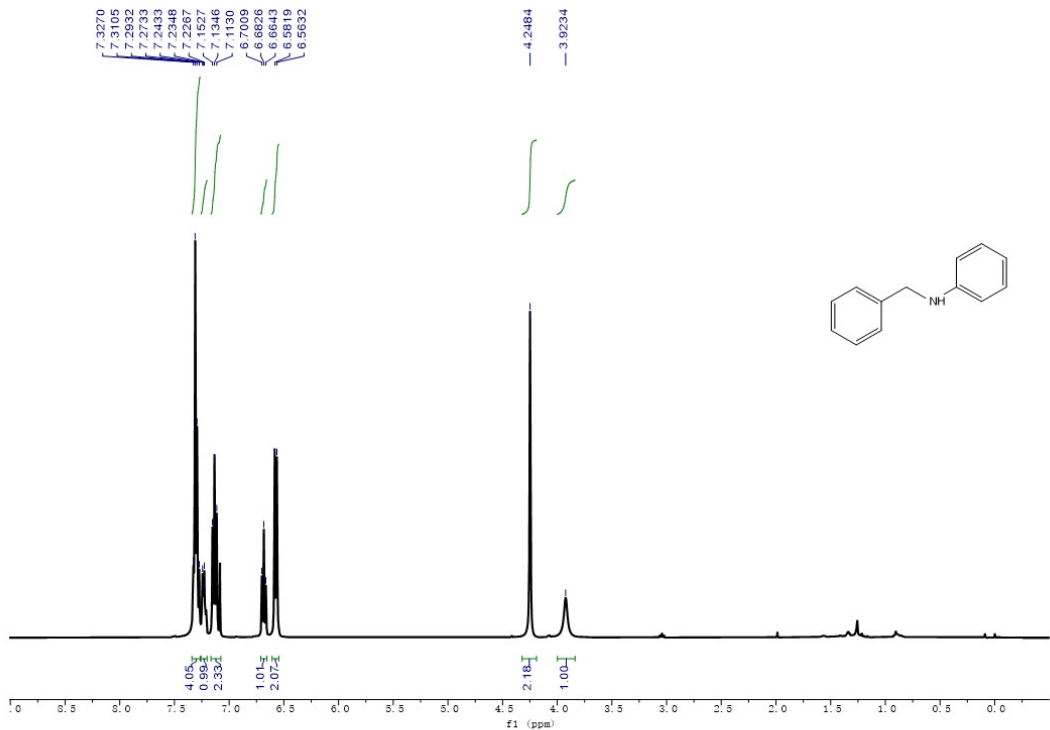


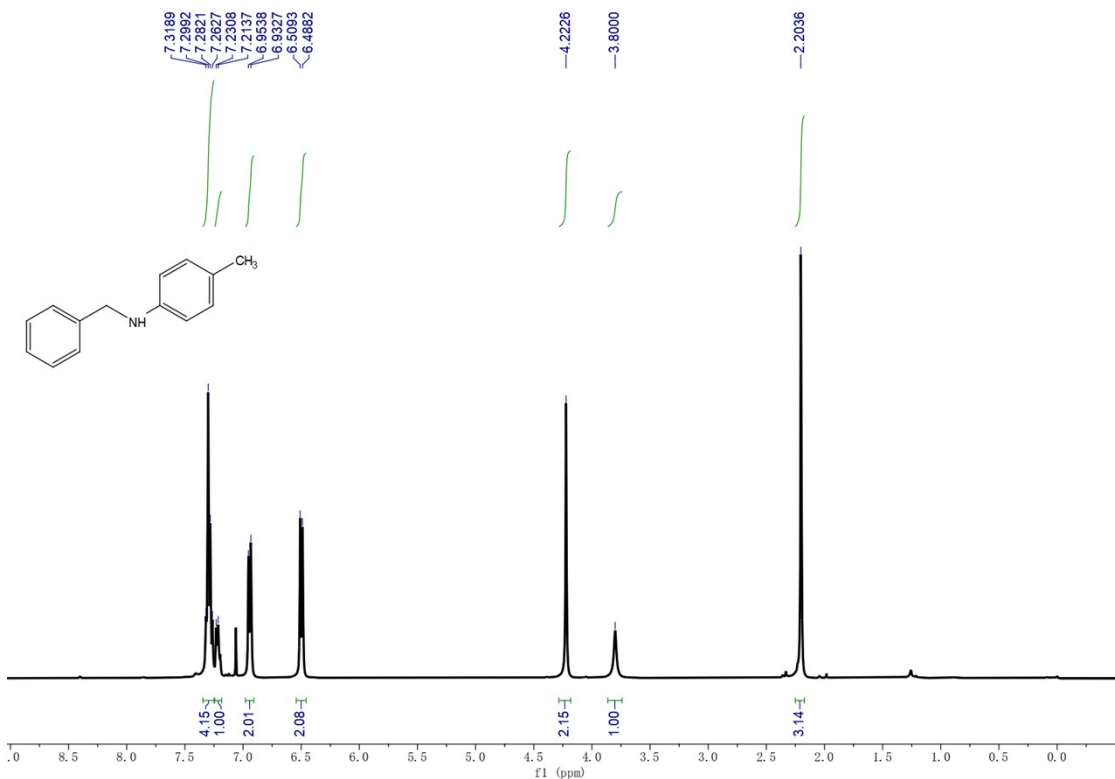
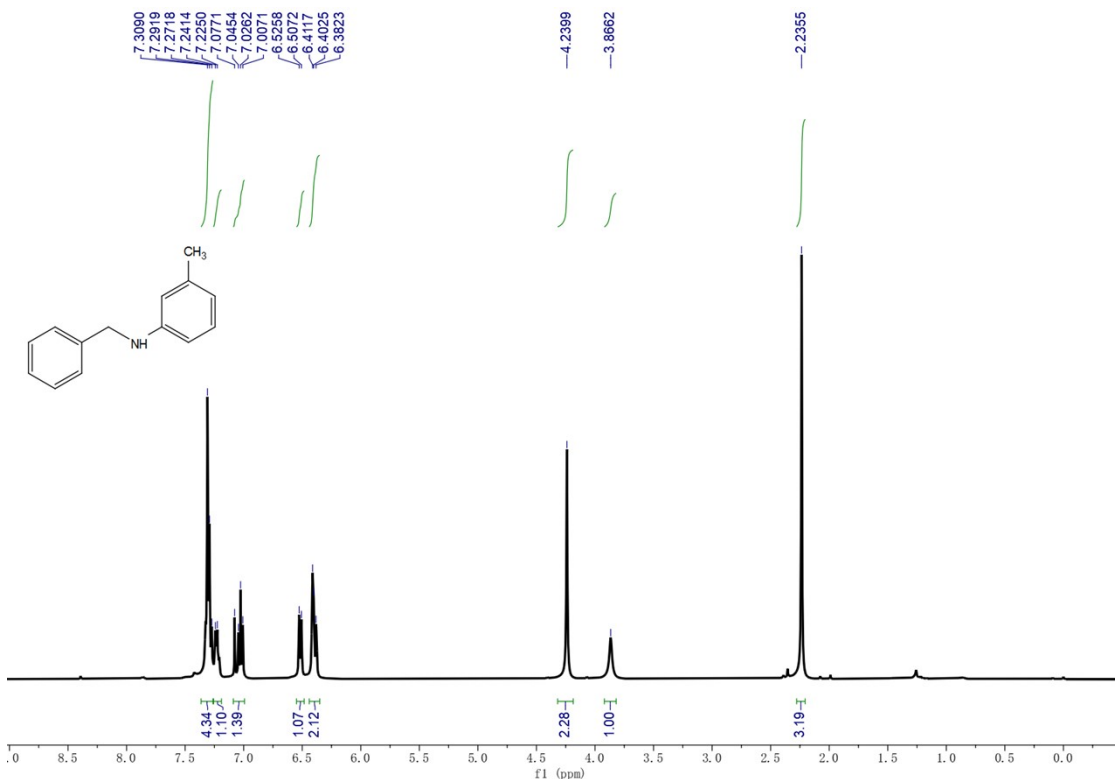
N-benzyl-4-chlorobenzo[d]thiazol-2-amine (pro.41): White solid. ($m = 68$ mg, 99% isolated yield). ^1H NMR (400 MHz, Chloroform-*d*) δ 8.07 (s, 1H), 7.30 (dd, $J = 7.8, 0.9$ Hz, 1H), 7.26 - 7.14 (m, 5H), 7.13 (t, $J = 3.4$ Hz, 1H), 6.84 (t, $J = 7.9$ Hz, 1H), 4.50 (s, 2H). This spectrum was also similar to the reported (*J. Org. Chem.* **2017**, 82(18): 9637 - 9646).²⁷

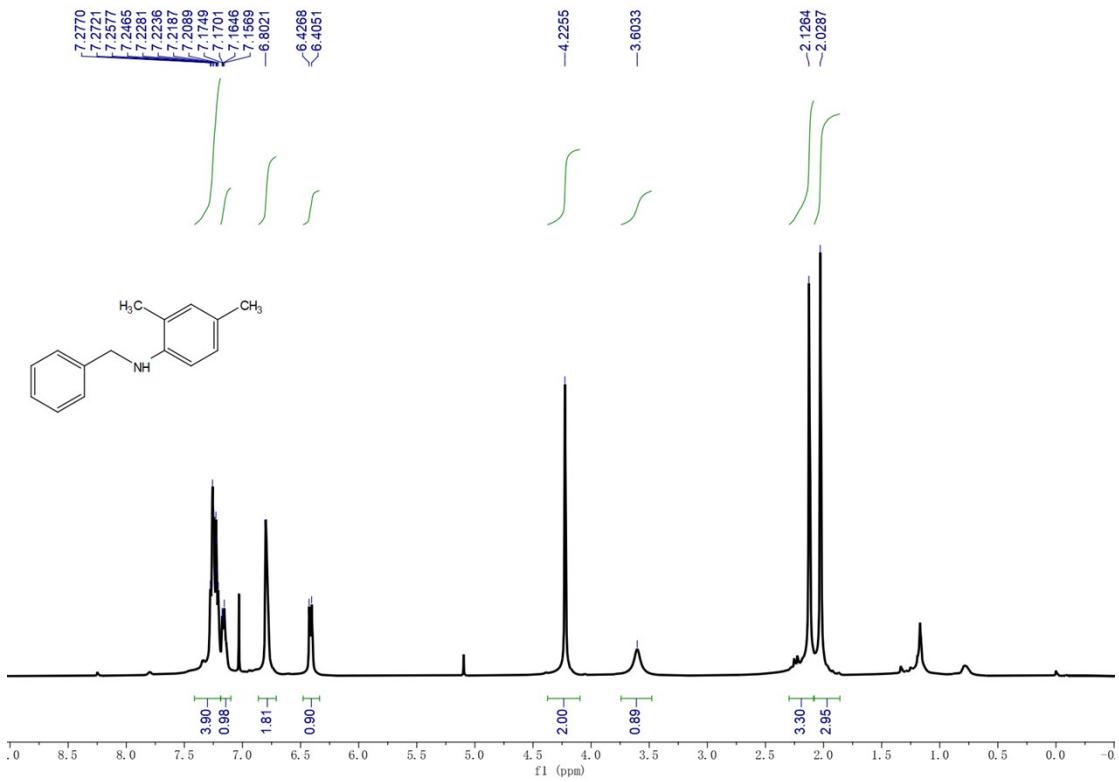
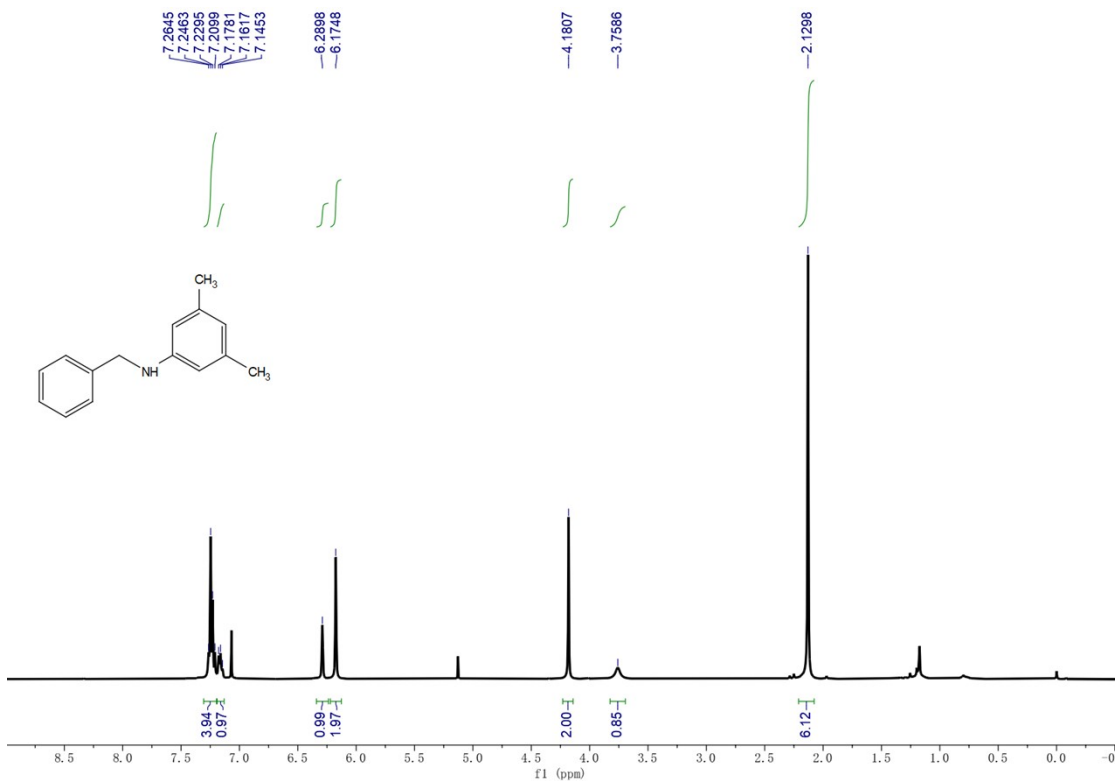


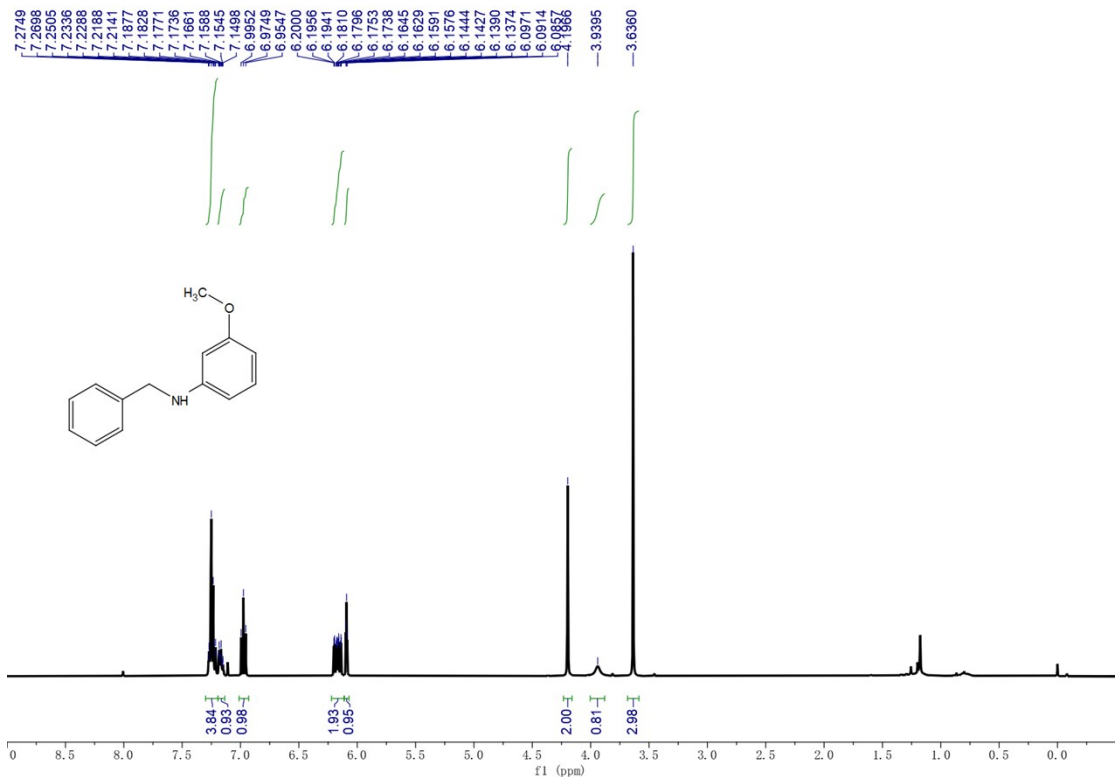
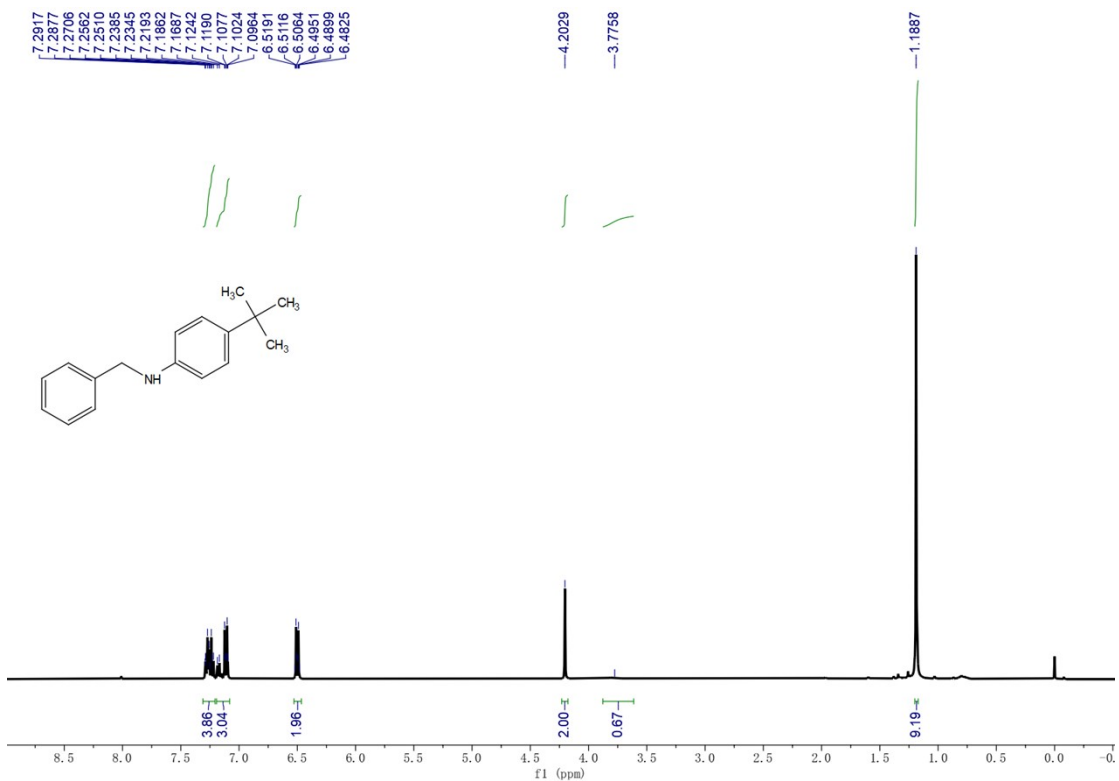
N-benzyl-4-methylbenzo[d]thiazol-2-amine (pro.42): White solid. ($m = 63$ mg, 99% isolated yield). ^1H NMR (400 MHz, Chloroform-*d*) δ 7.30 (d, $J = 7.8$ Hz, 1H), 7.26 - 7.08 (m, 5H), 6.99 (d, $J = 7.4$ Hz, 1H), 6.87 (t, $J = 7.6$ Hz, 1H), 6.37 (s, 1H), 4.44 (s, 2H), 2.44 (s, 3H). This spectrum was also similar to the reported (*J. Org. Chem.* **2017**, 82(18): 9637 - 9646).²⁷

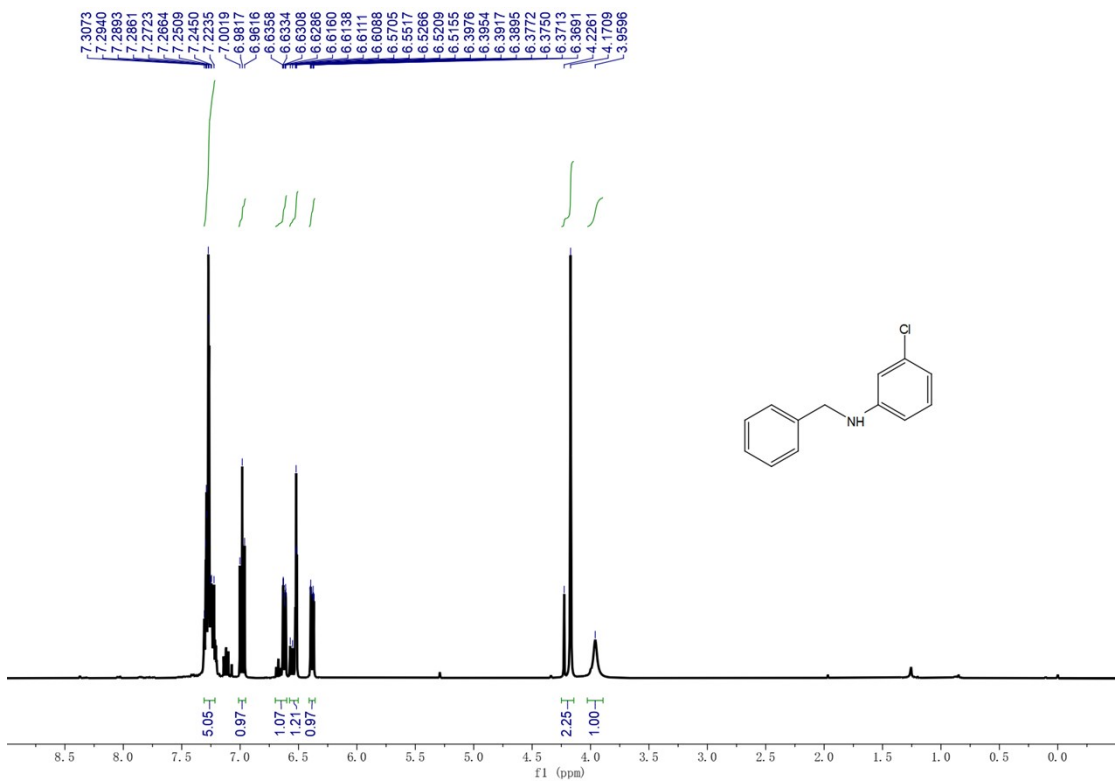
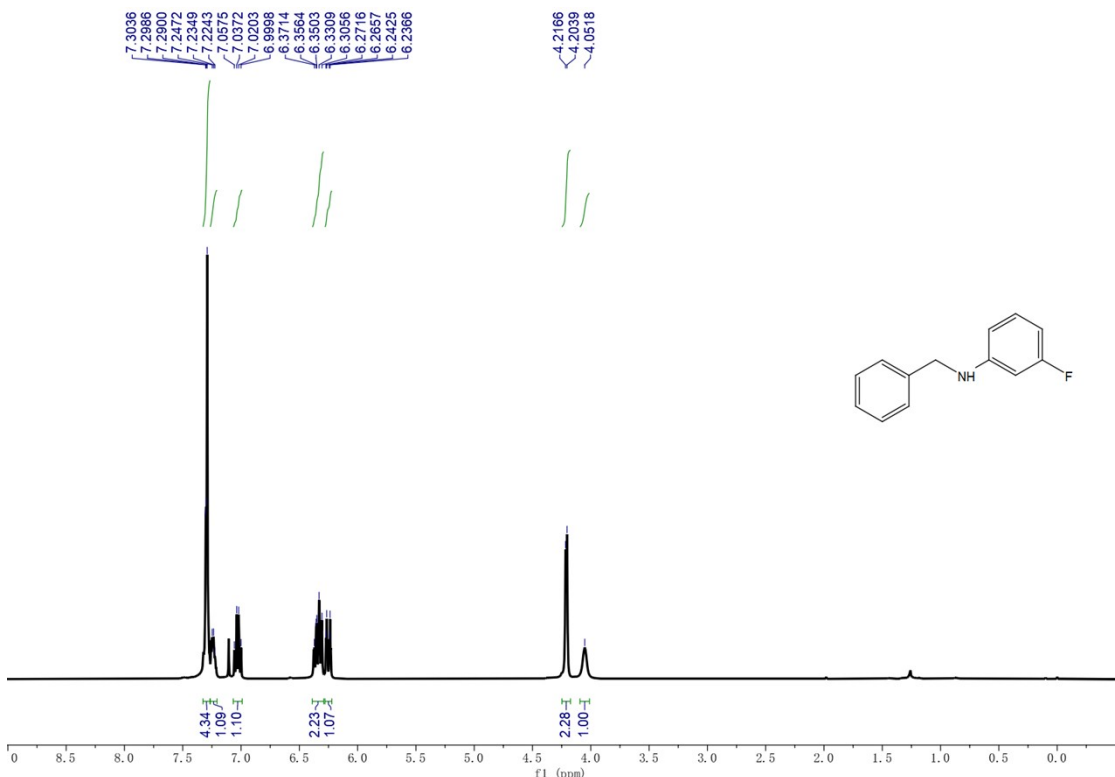
S4 NMR Image of the Products

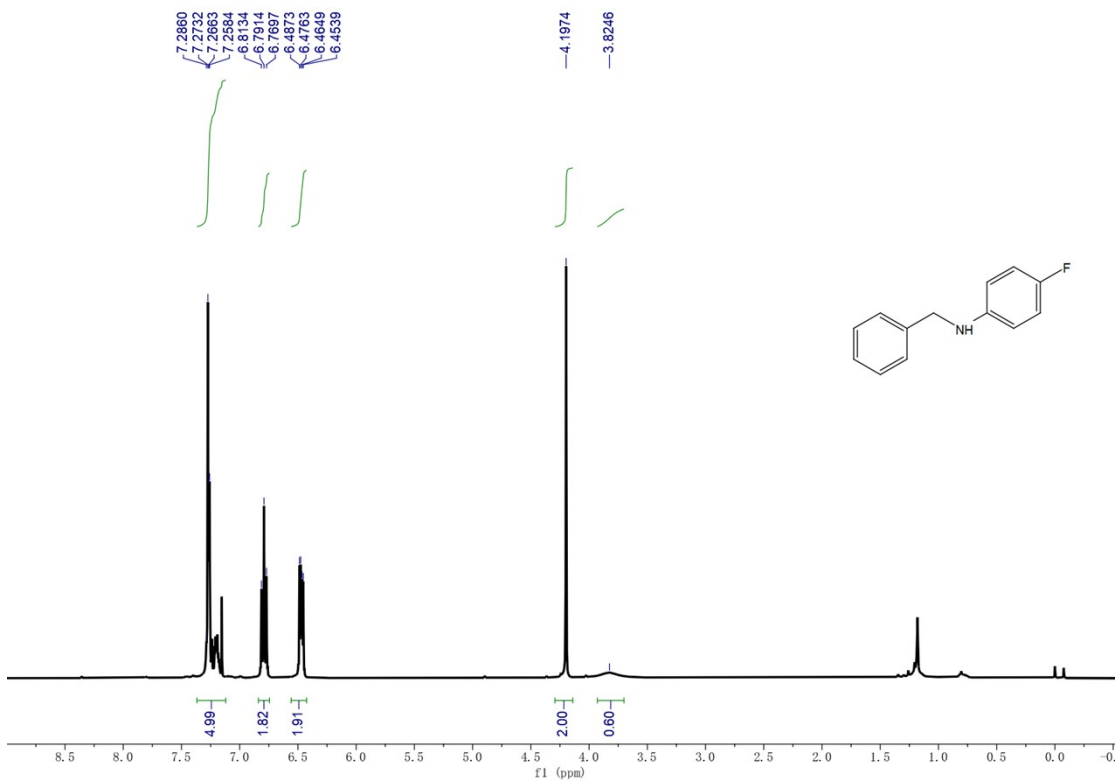
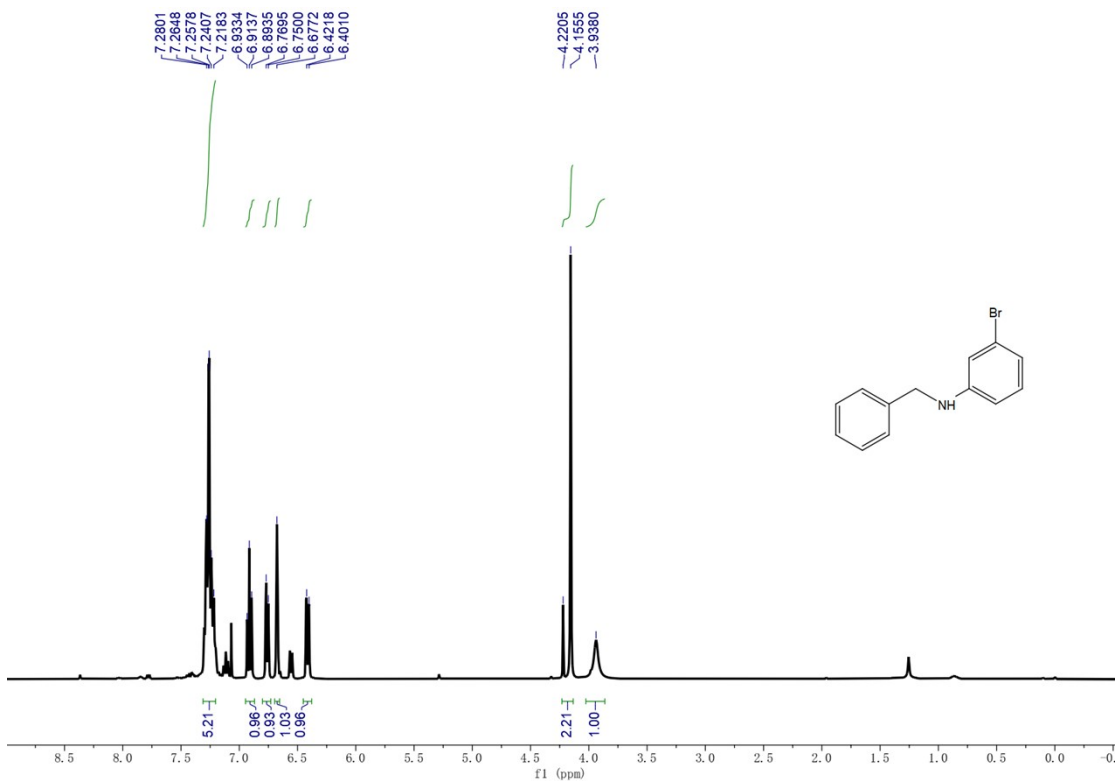


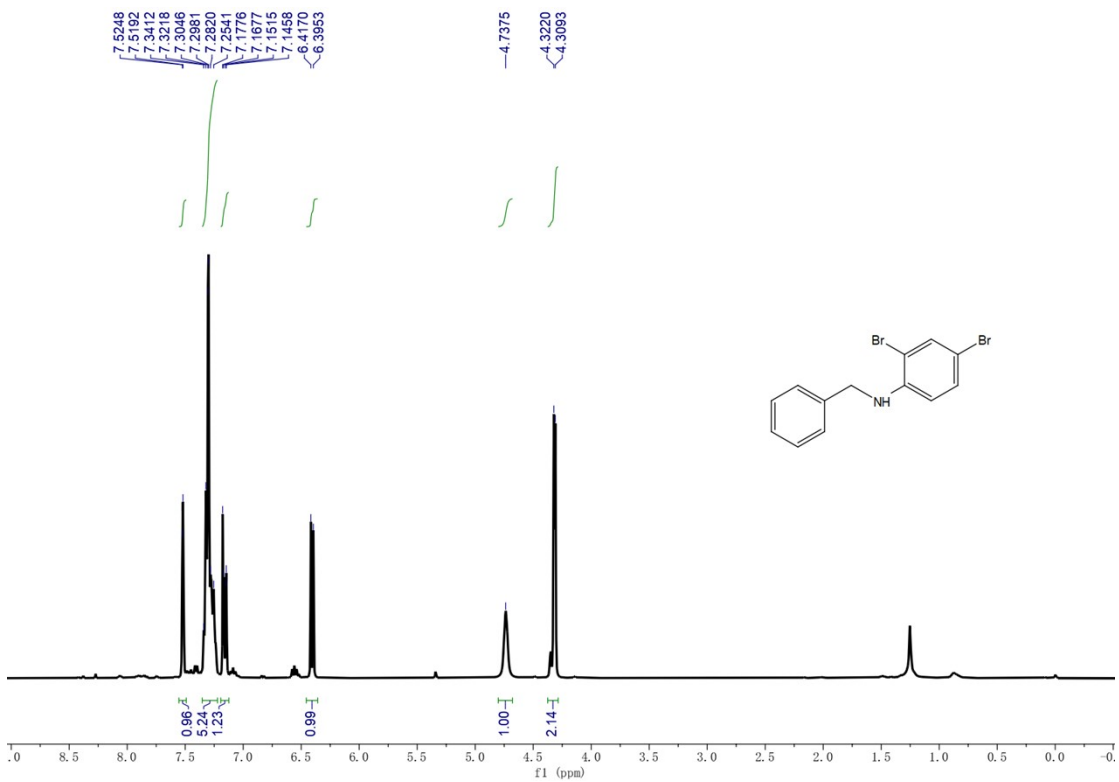
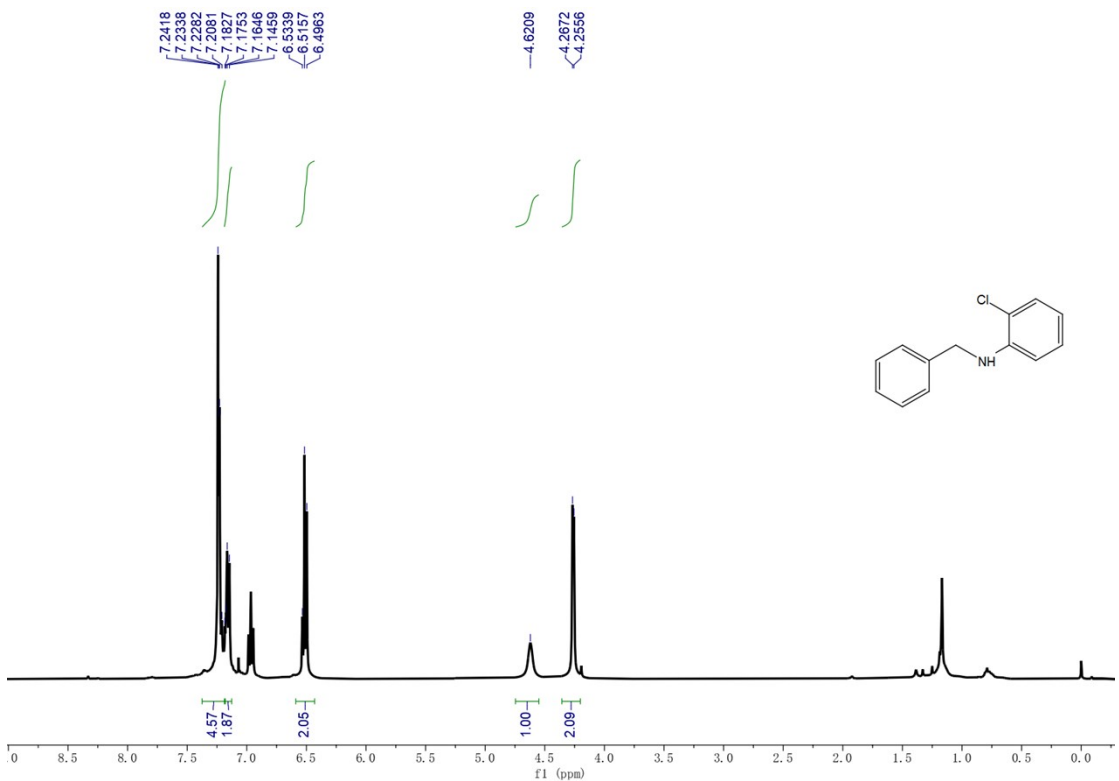


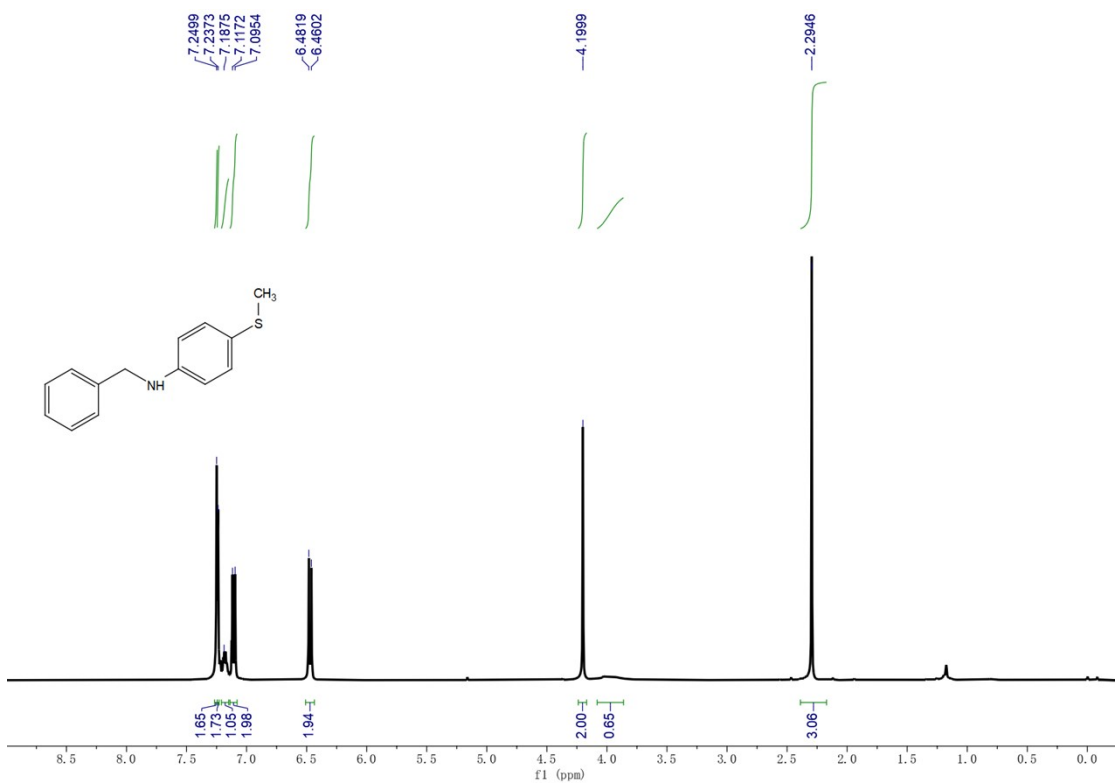
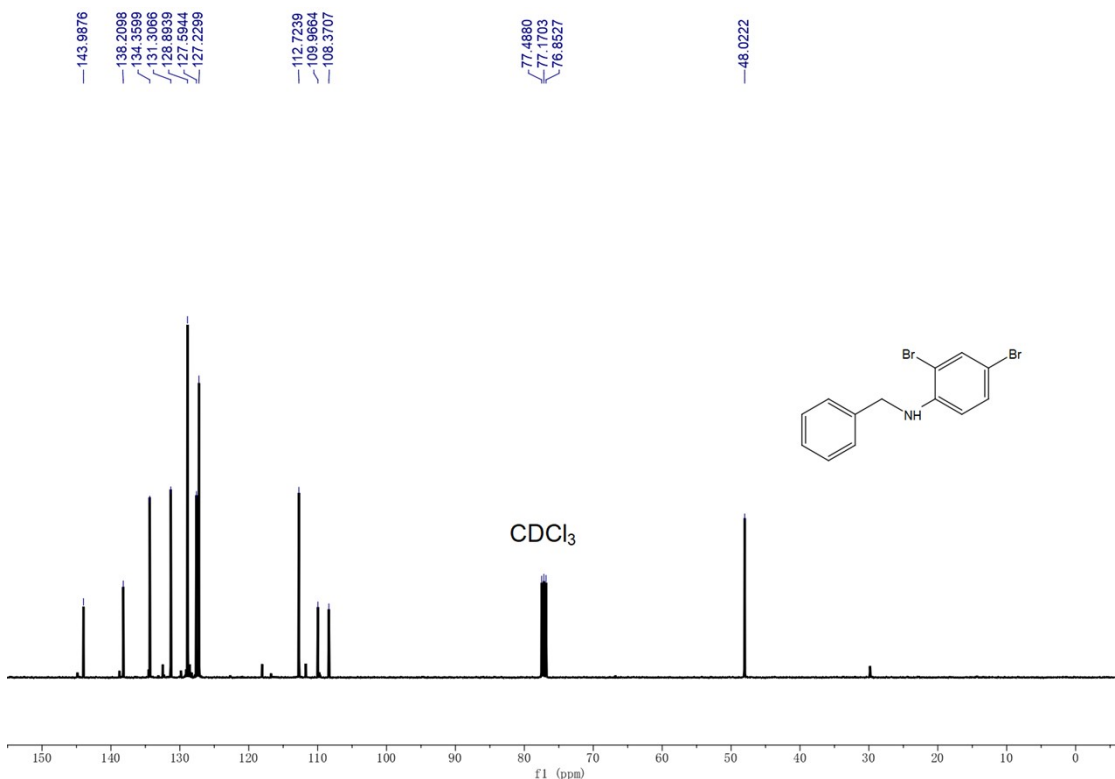


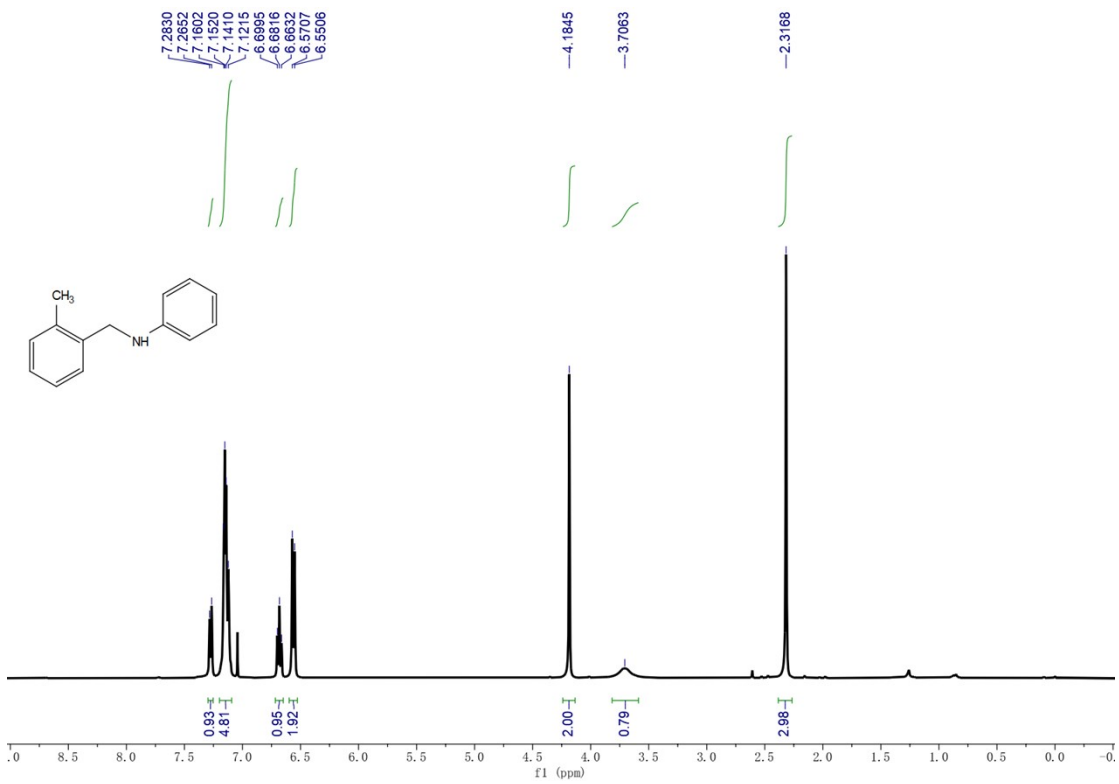
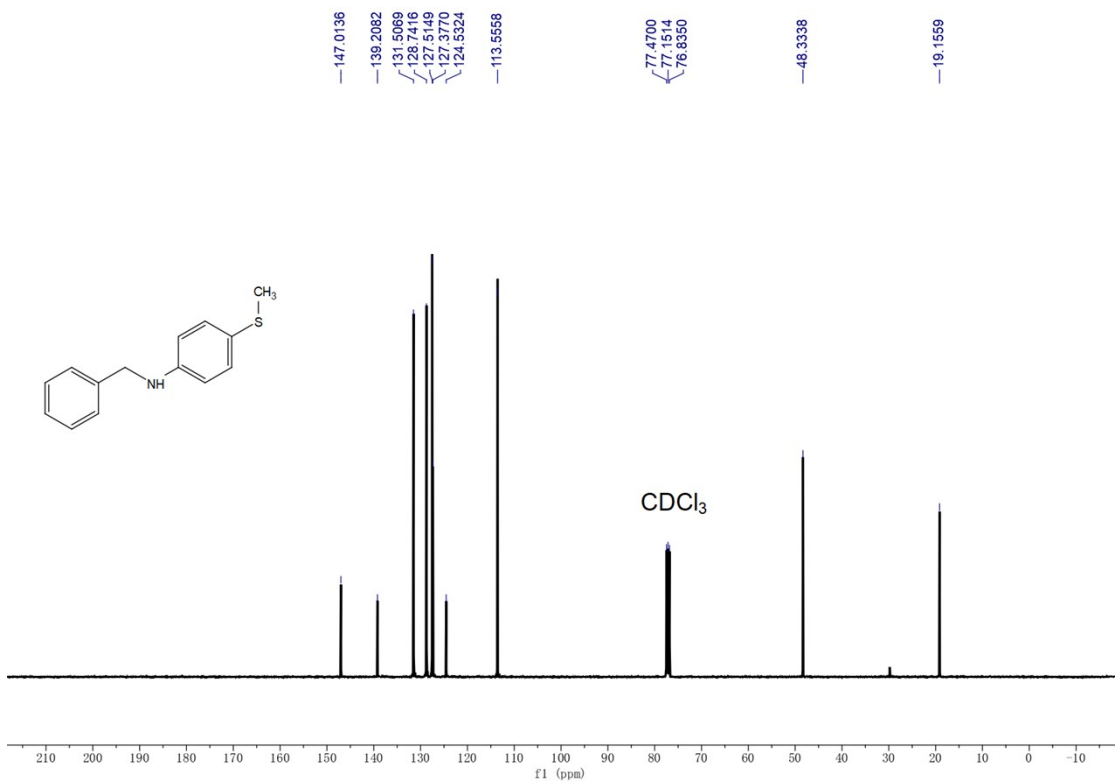


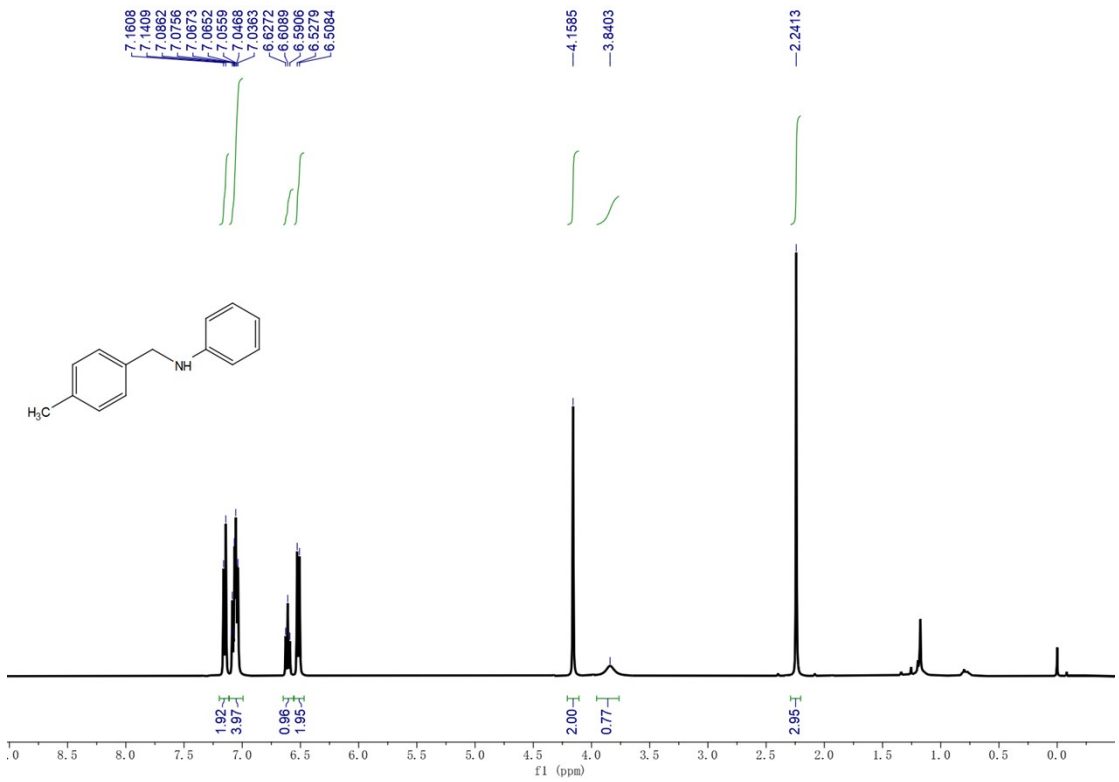
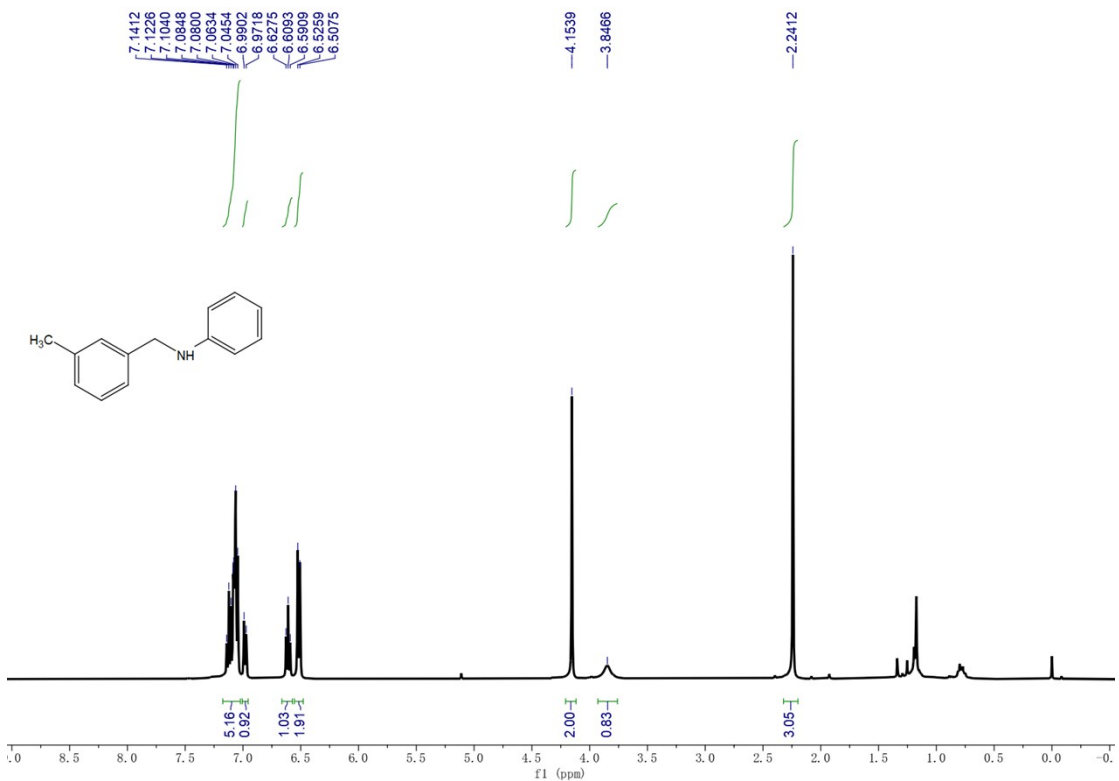


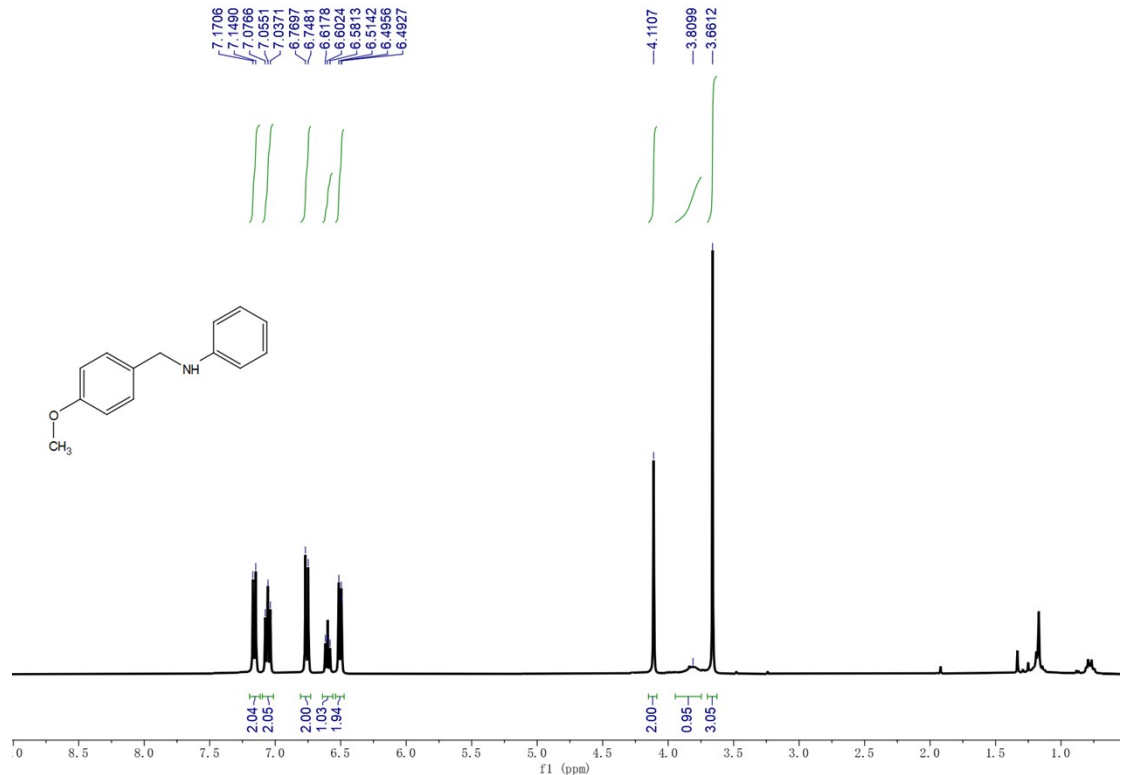
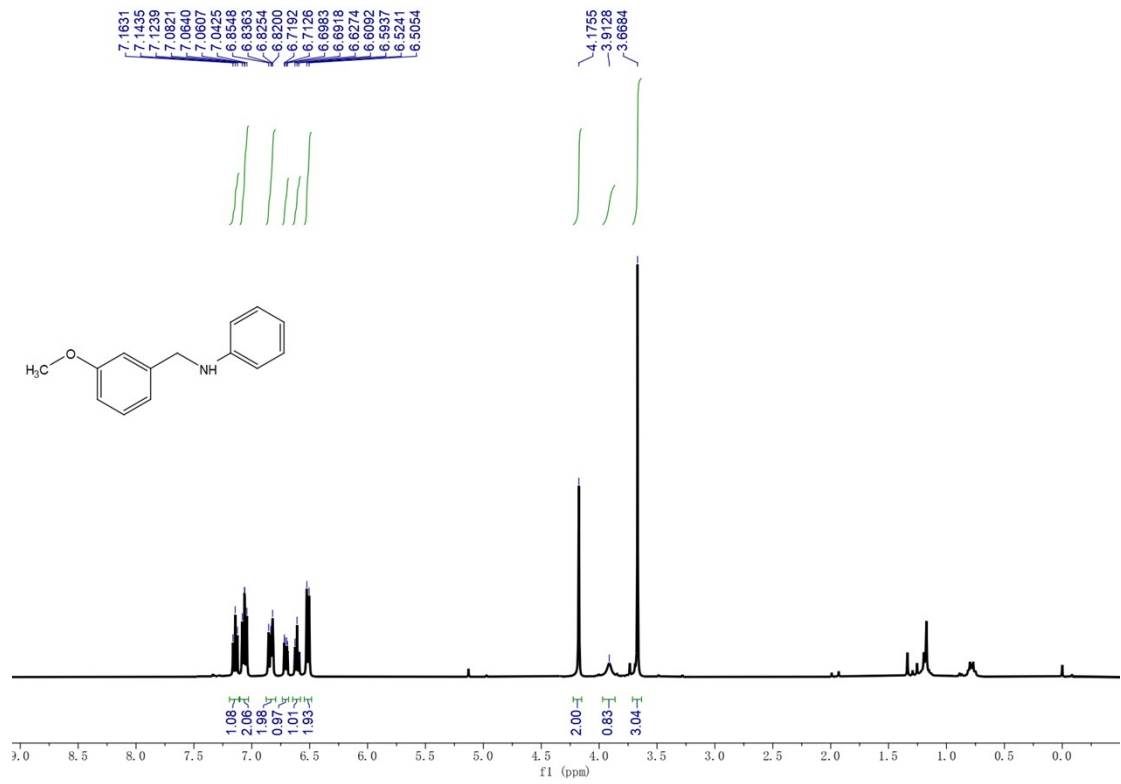


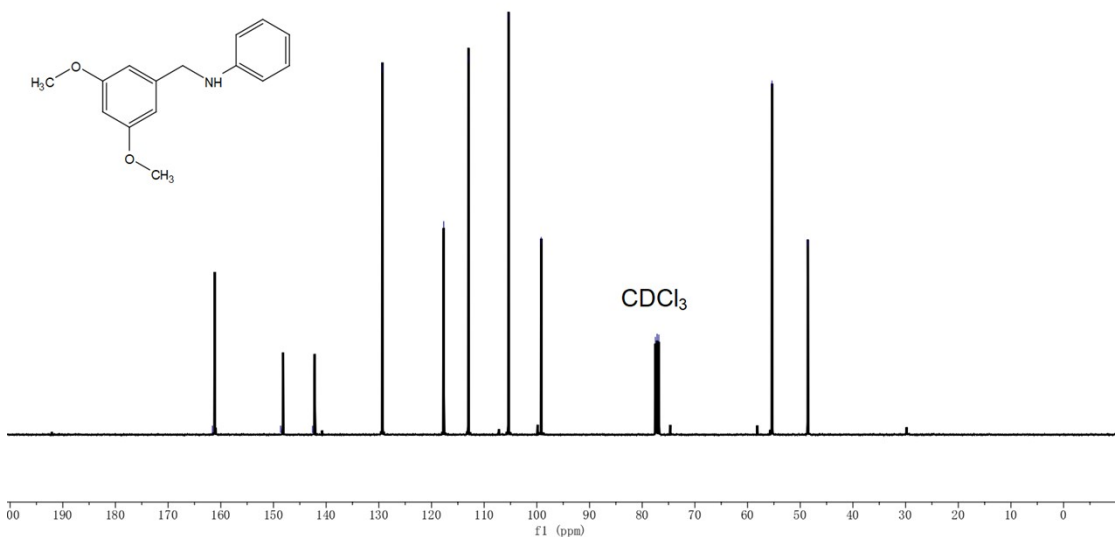
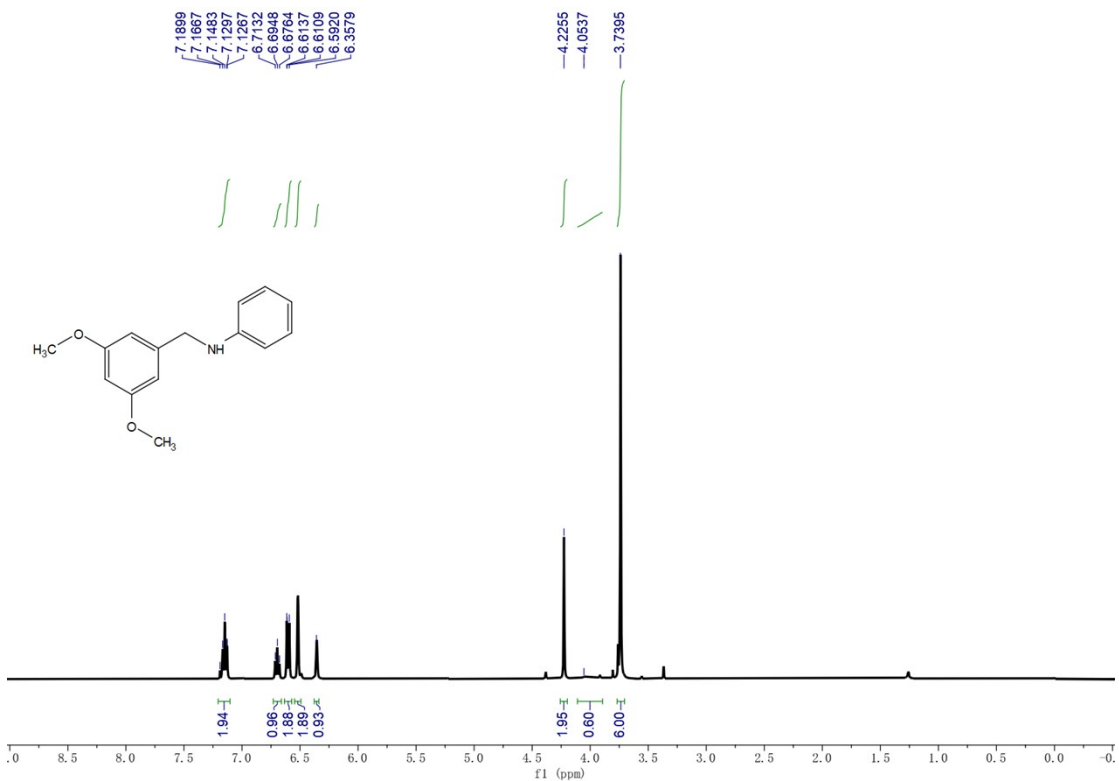


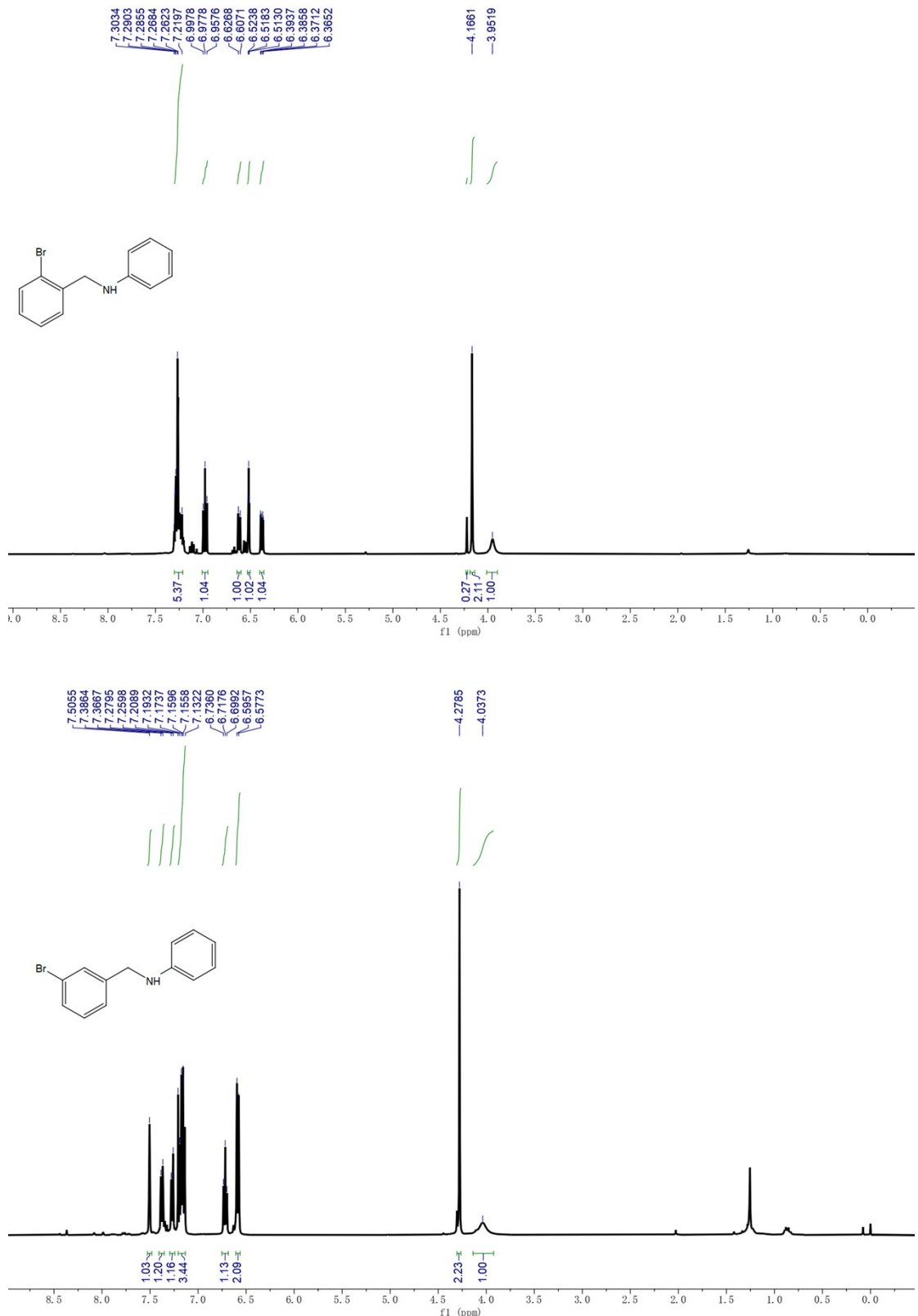


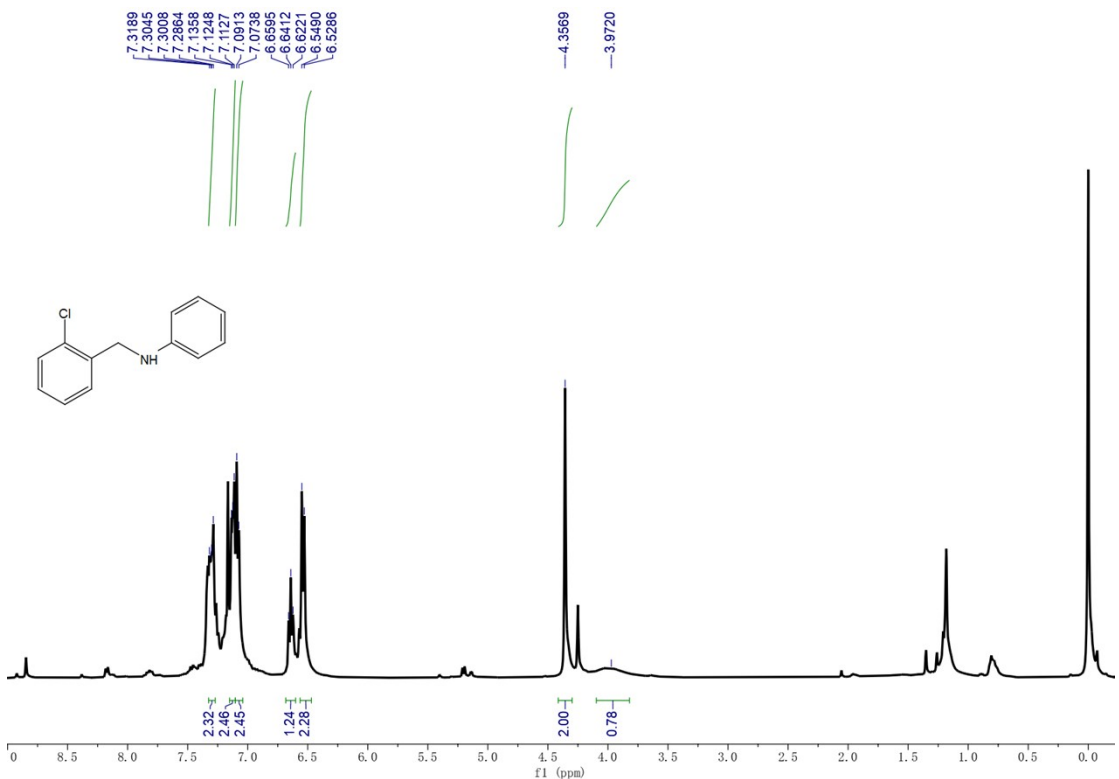
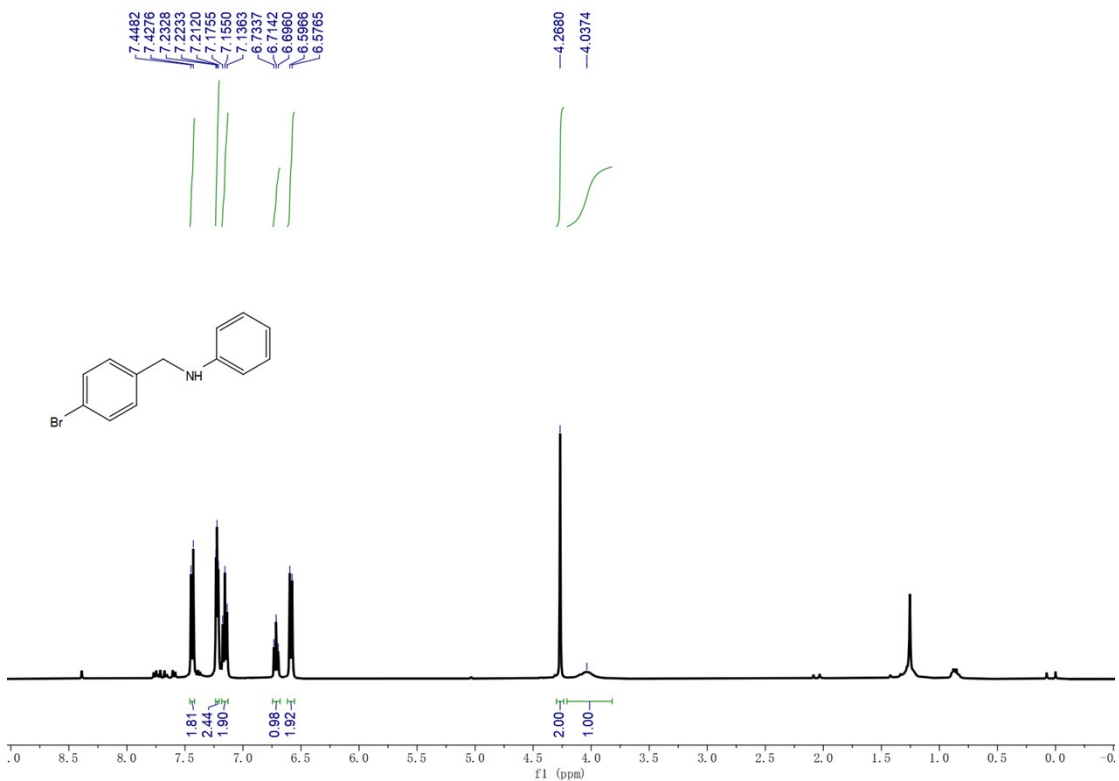


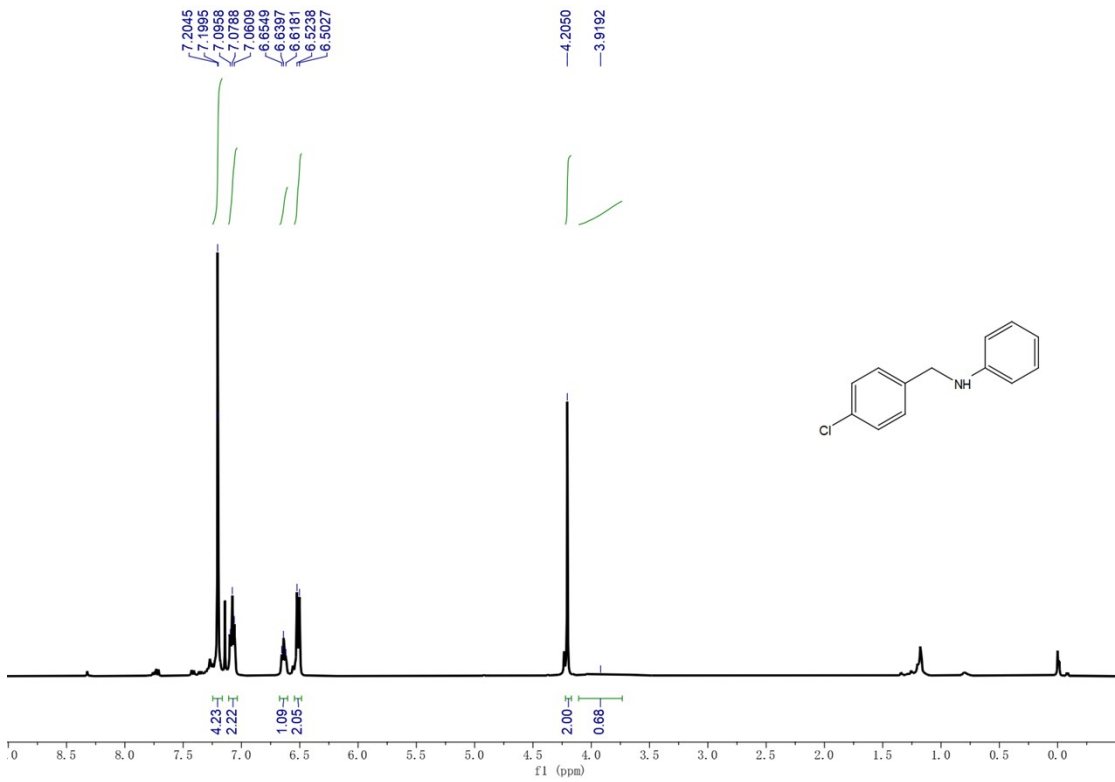
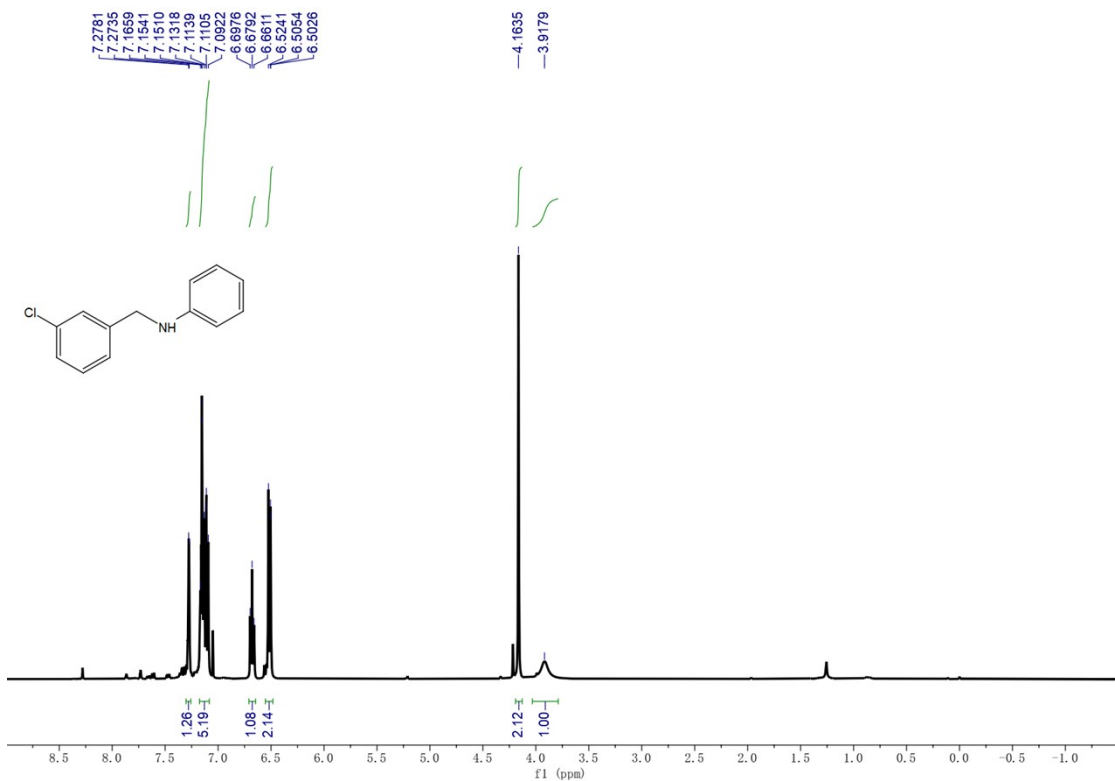


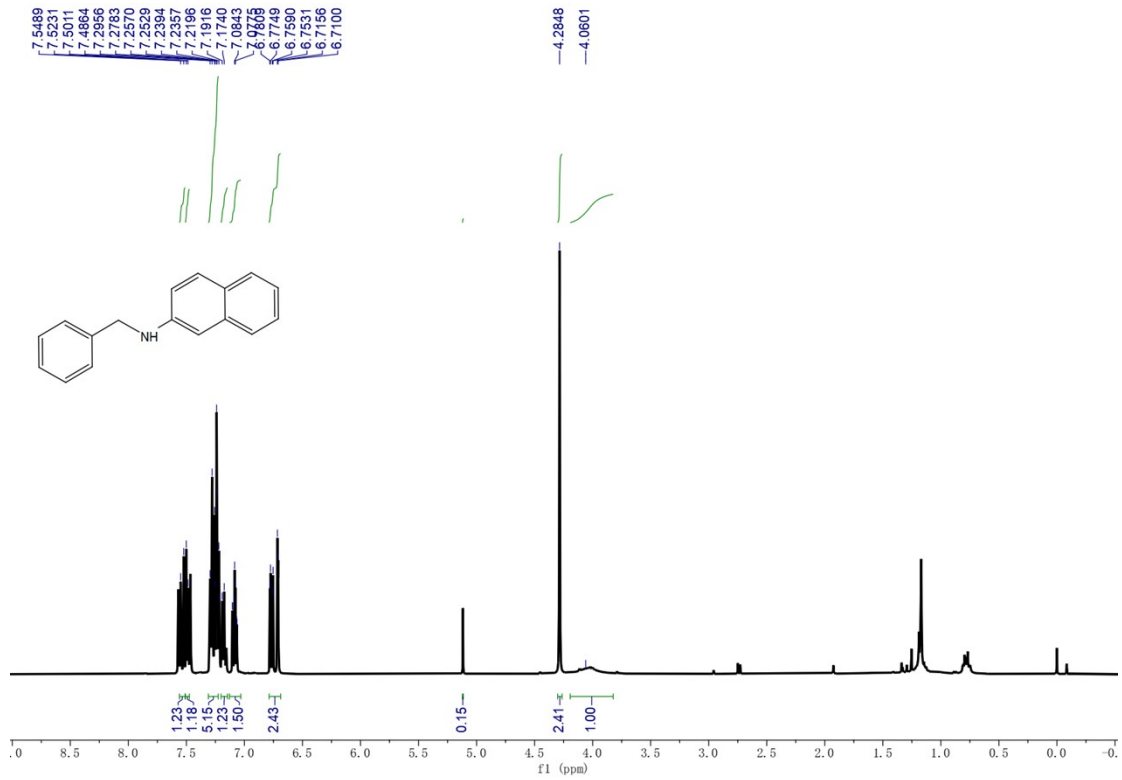
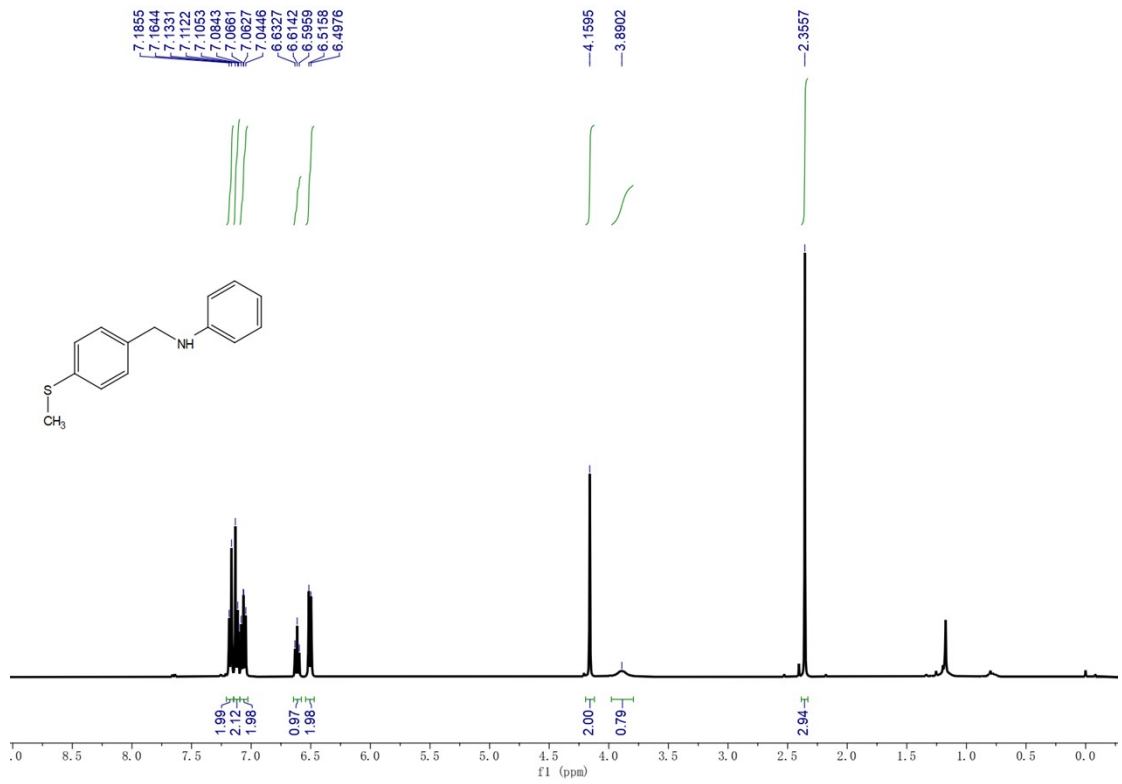


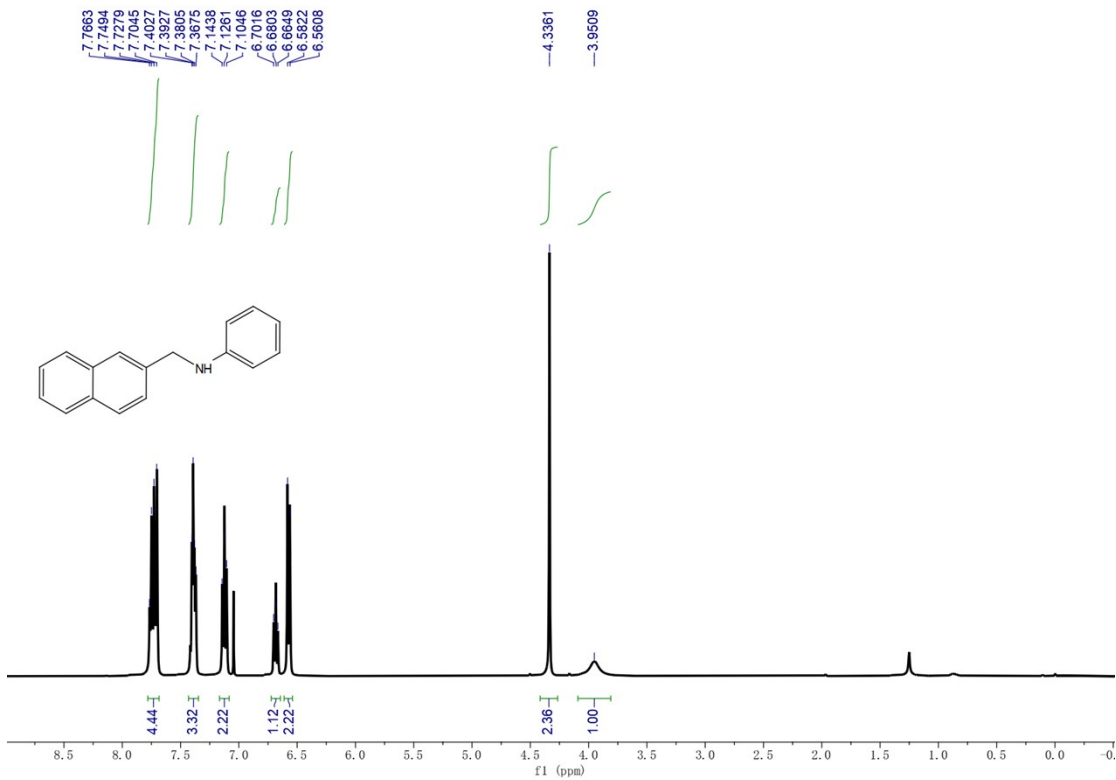
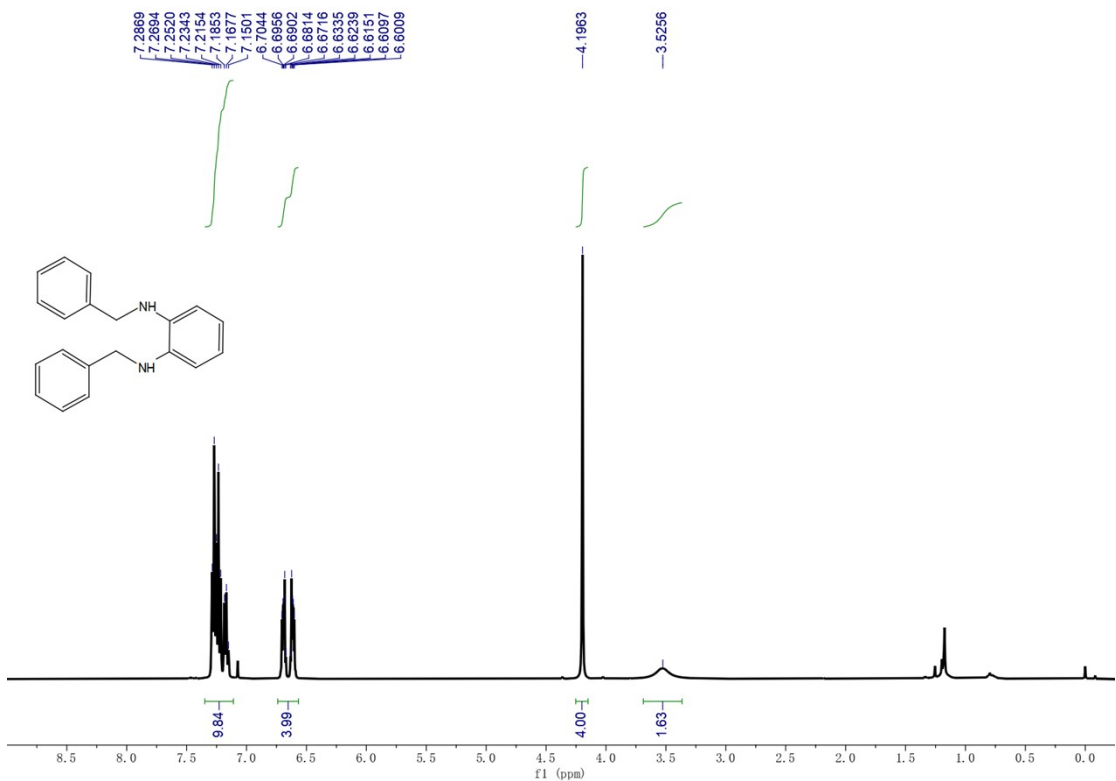


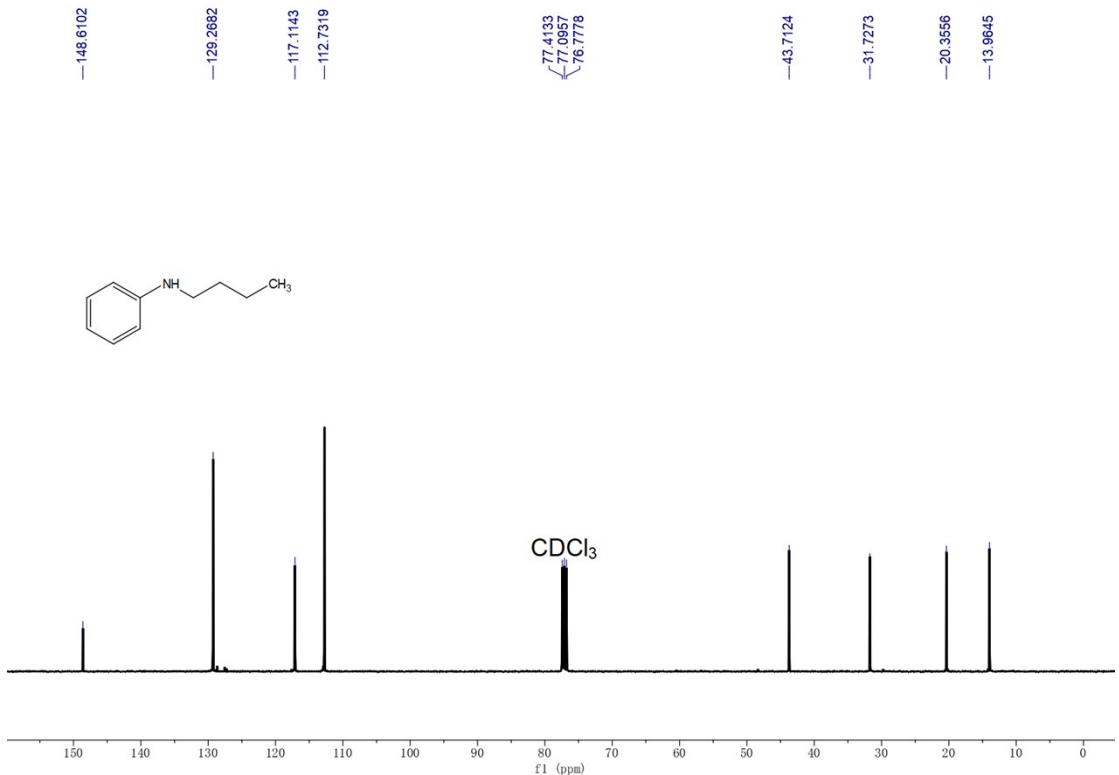
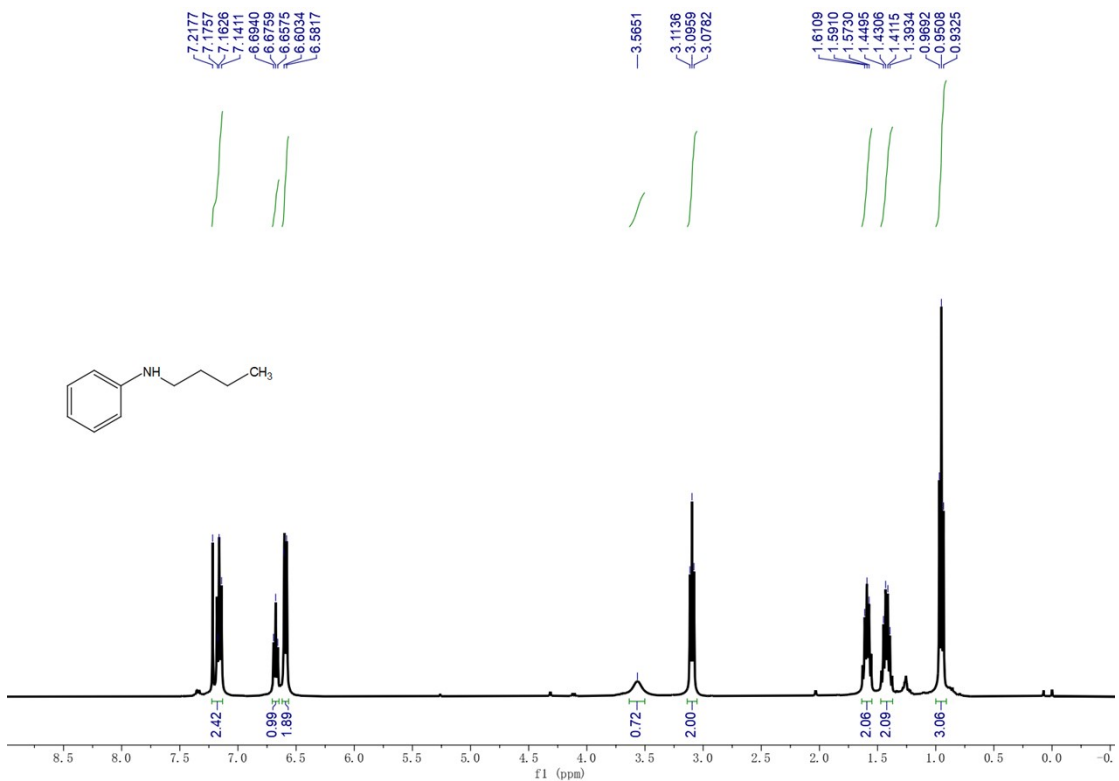


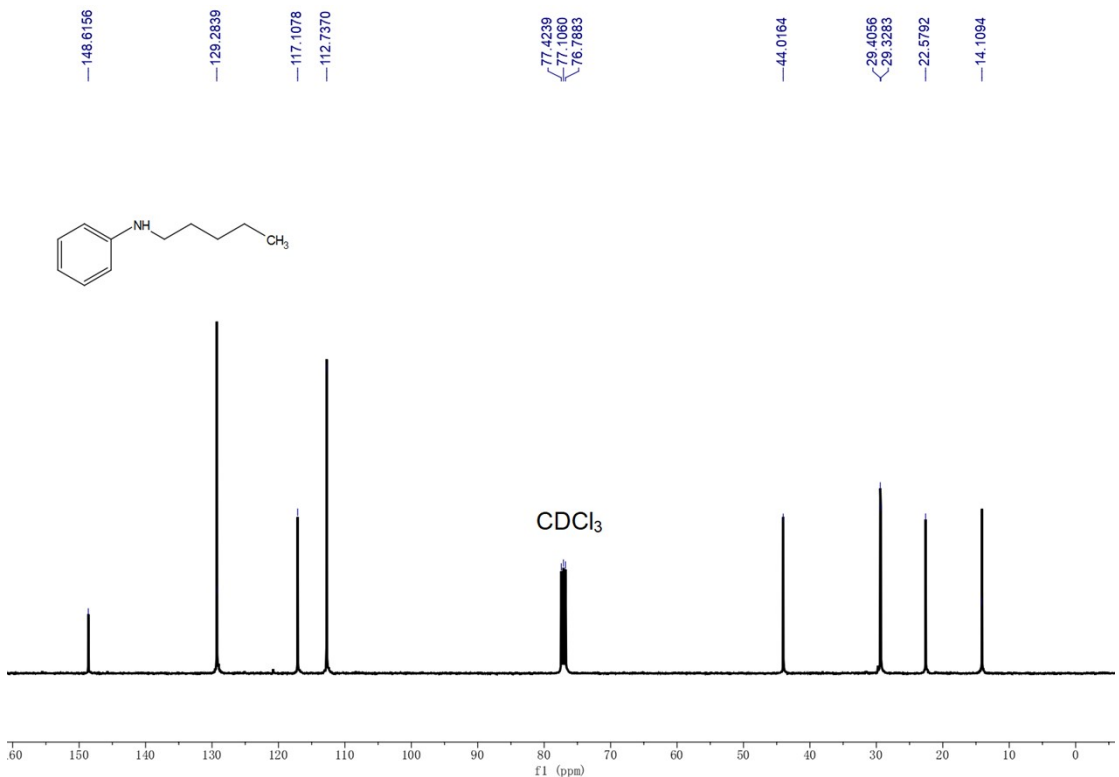
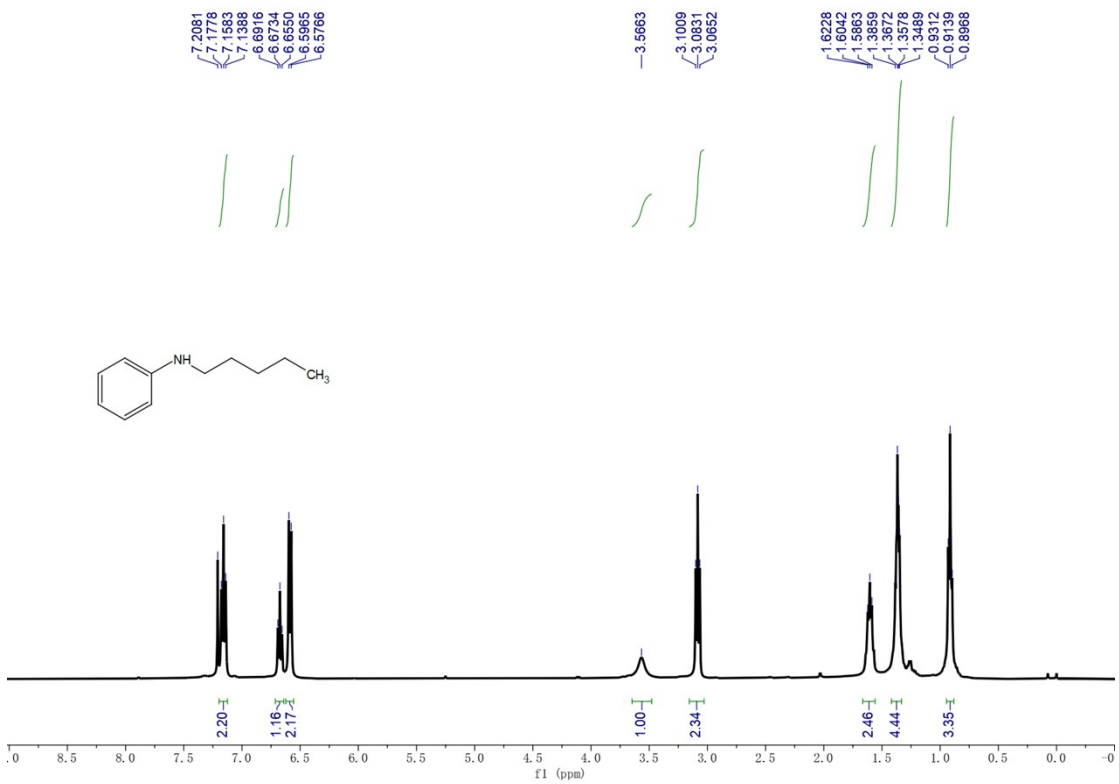


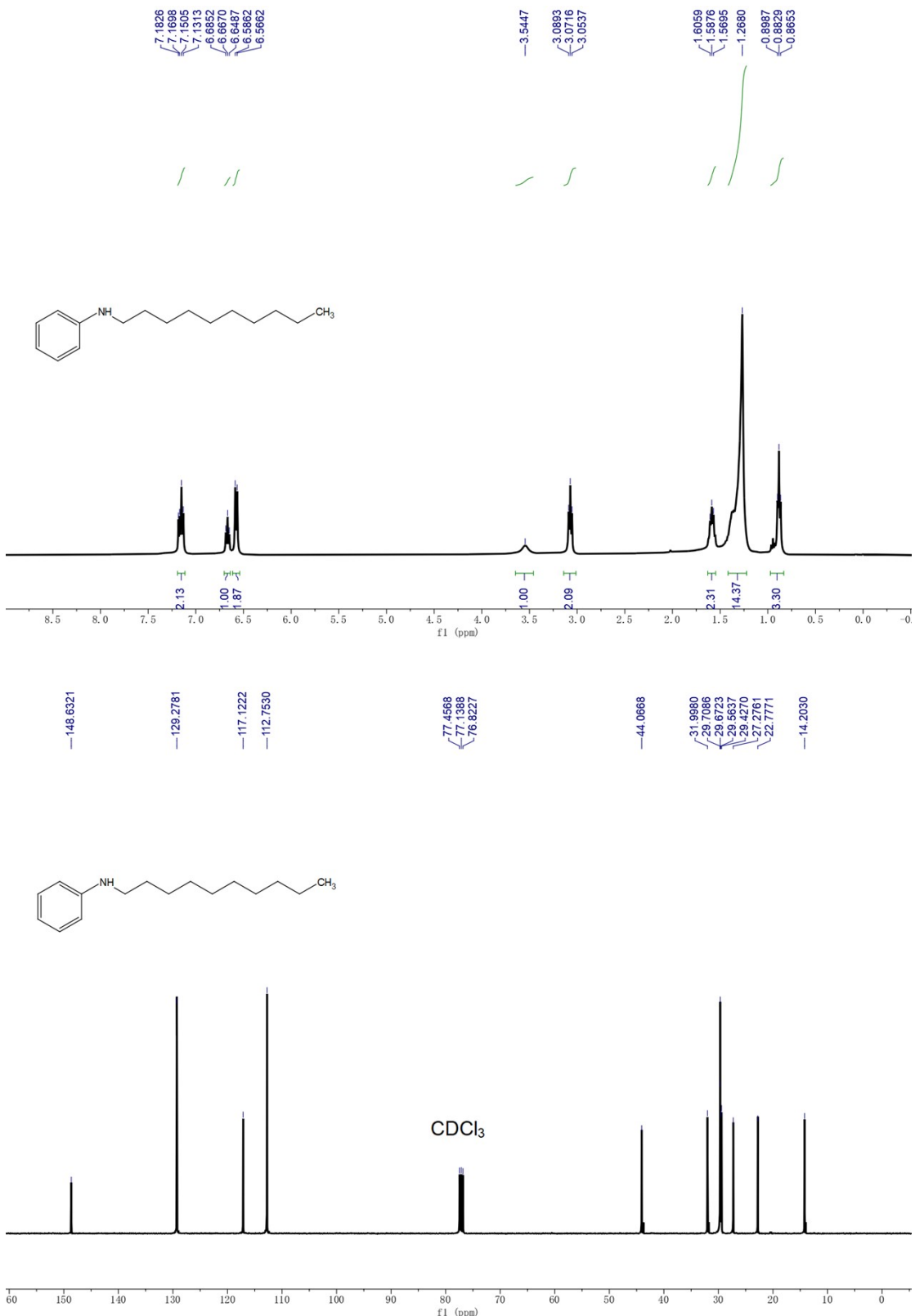


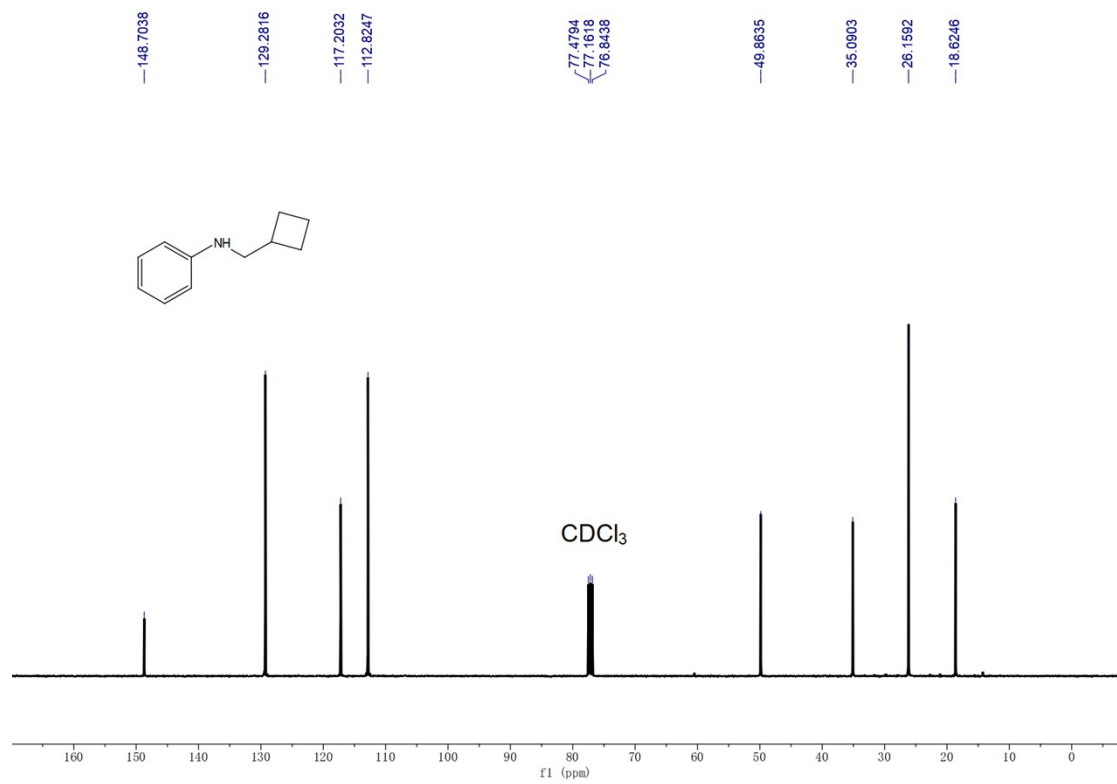
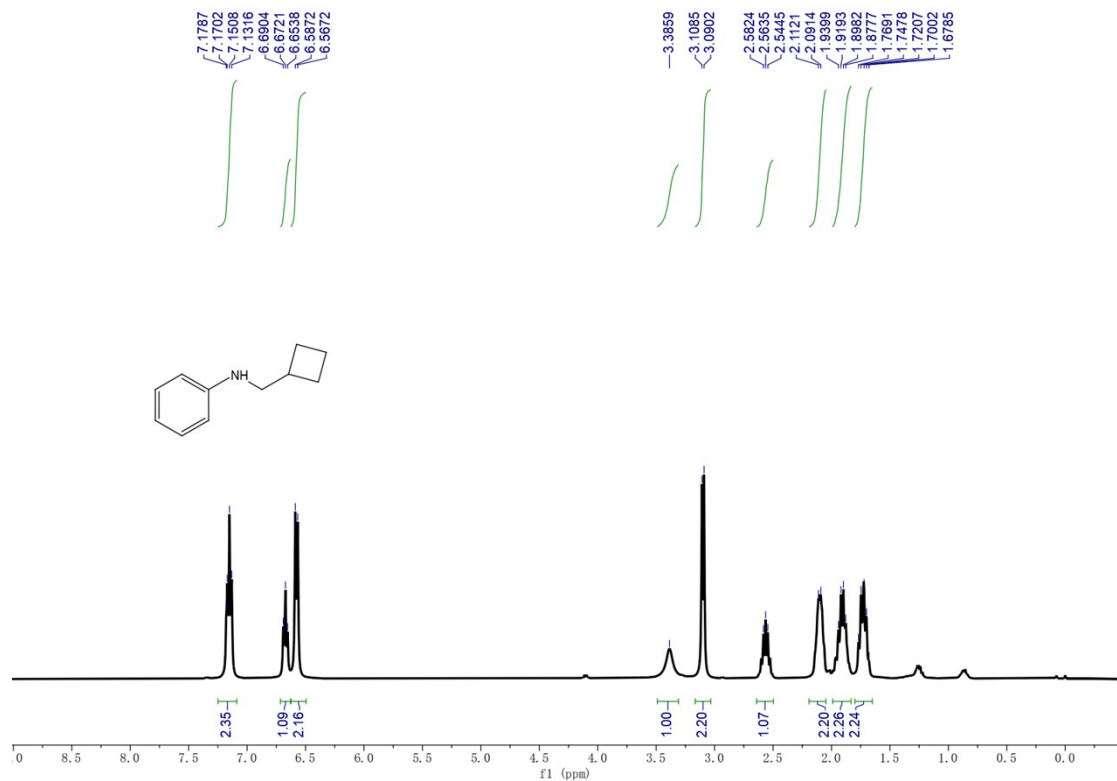


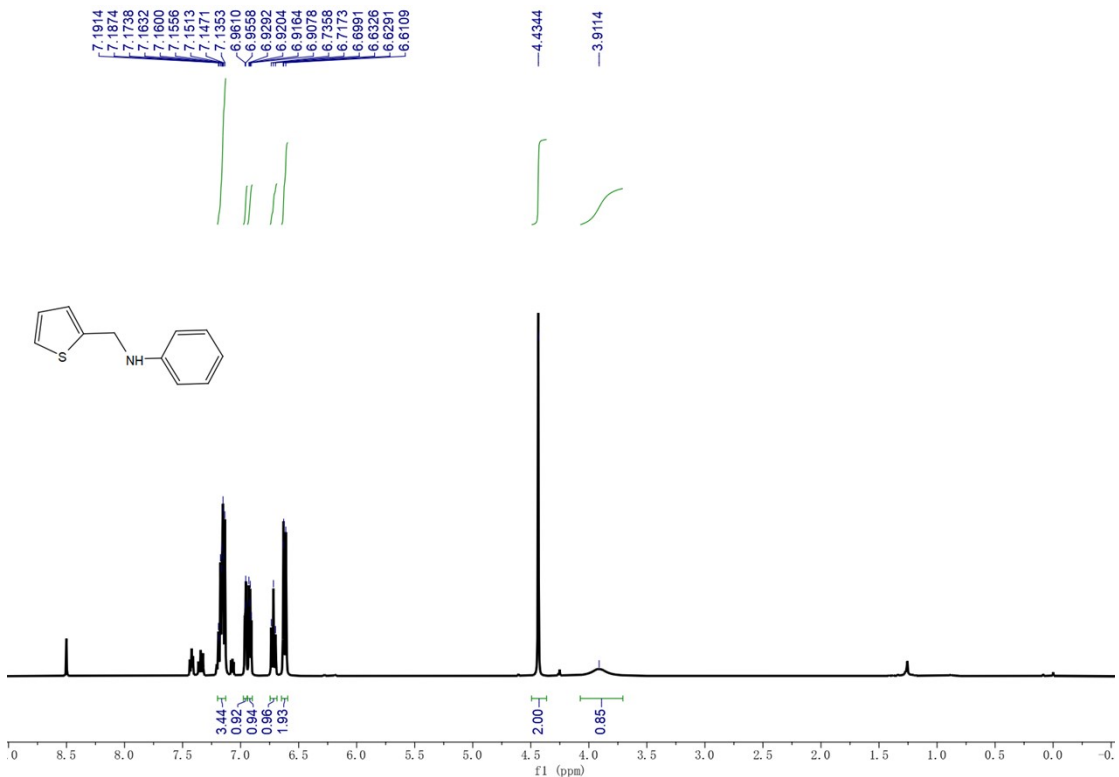
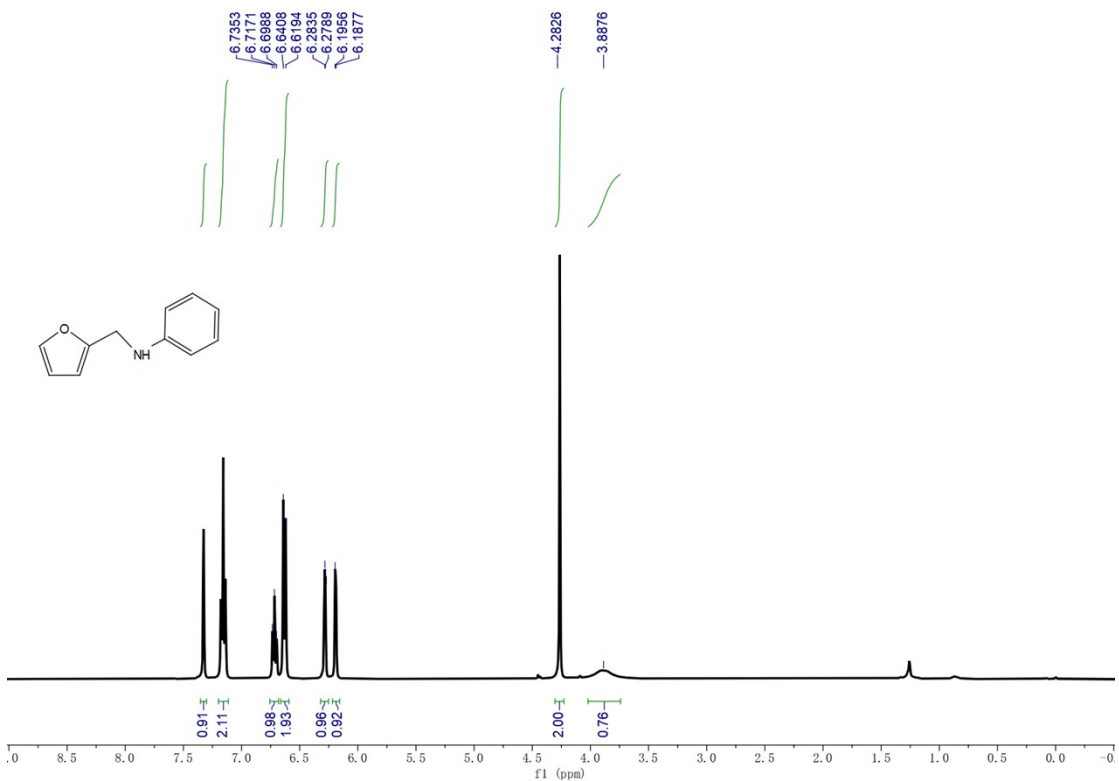


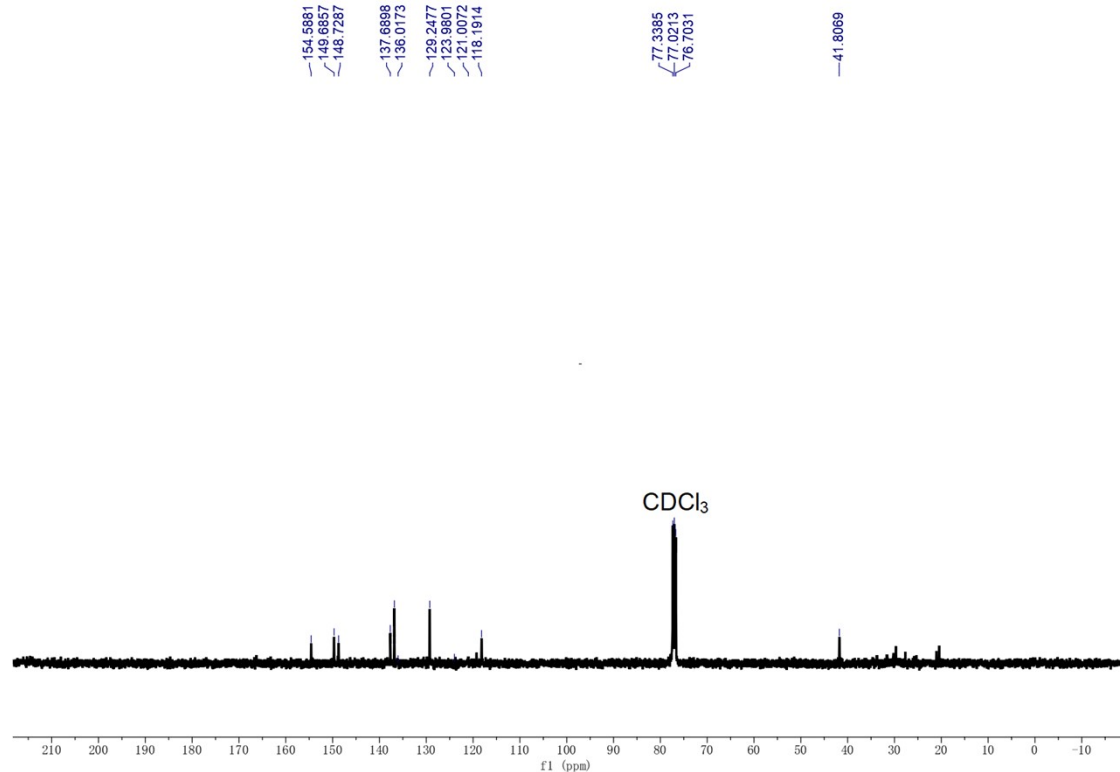
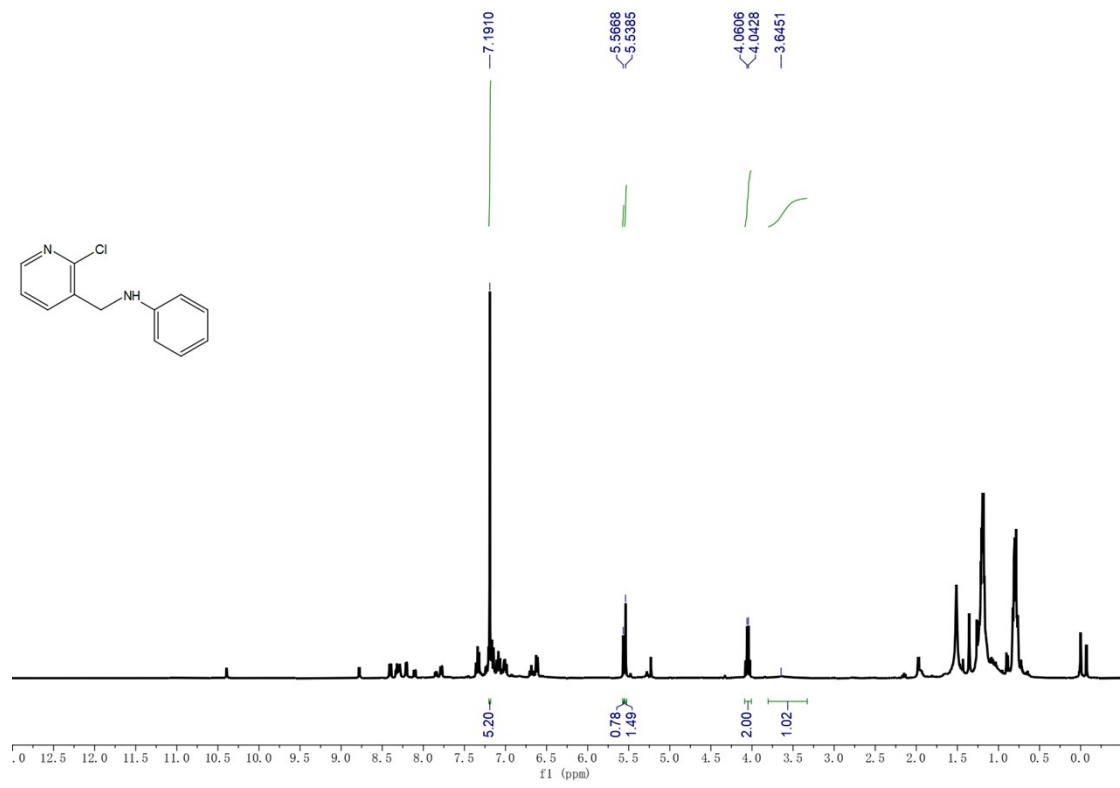


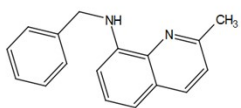
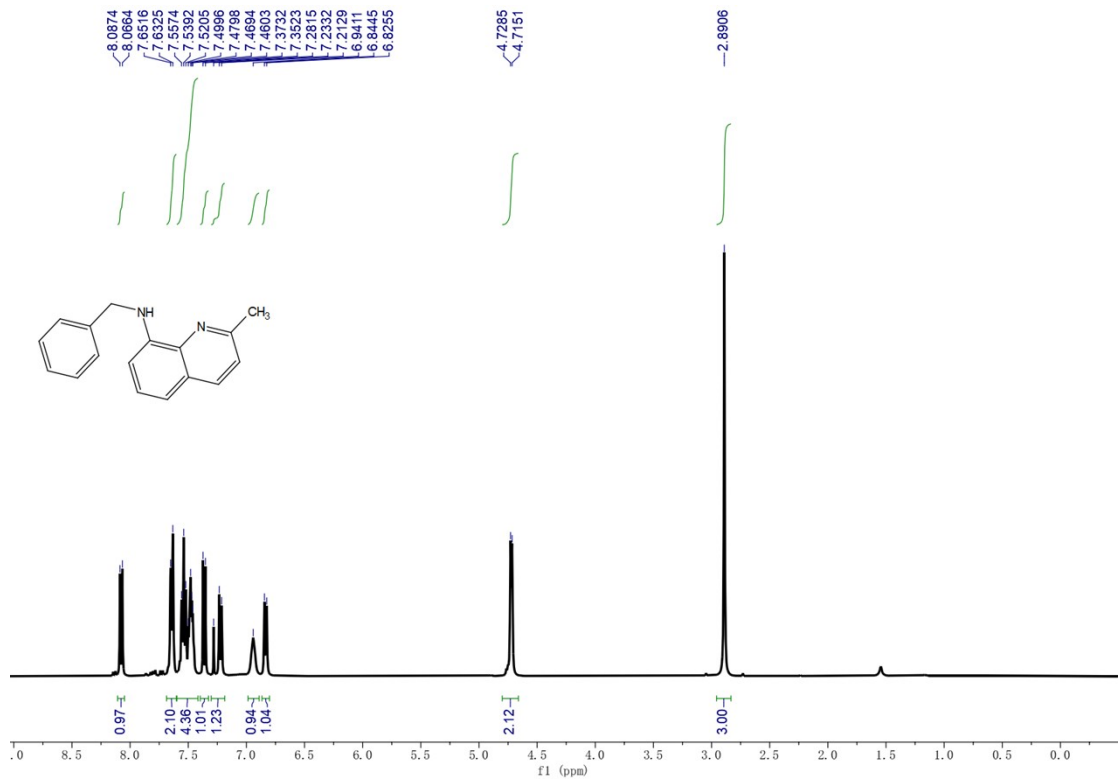
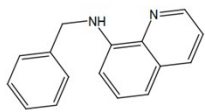
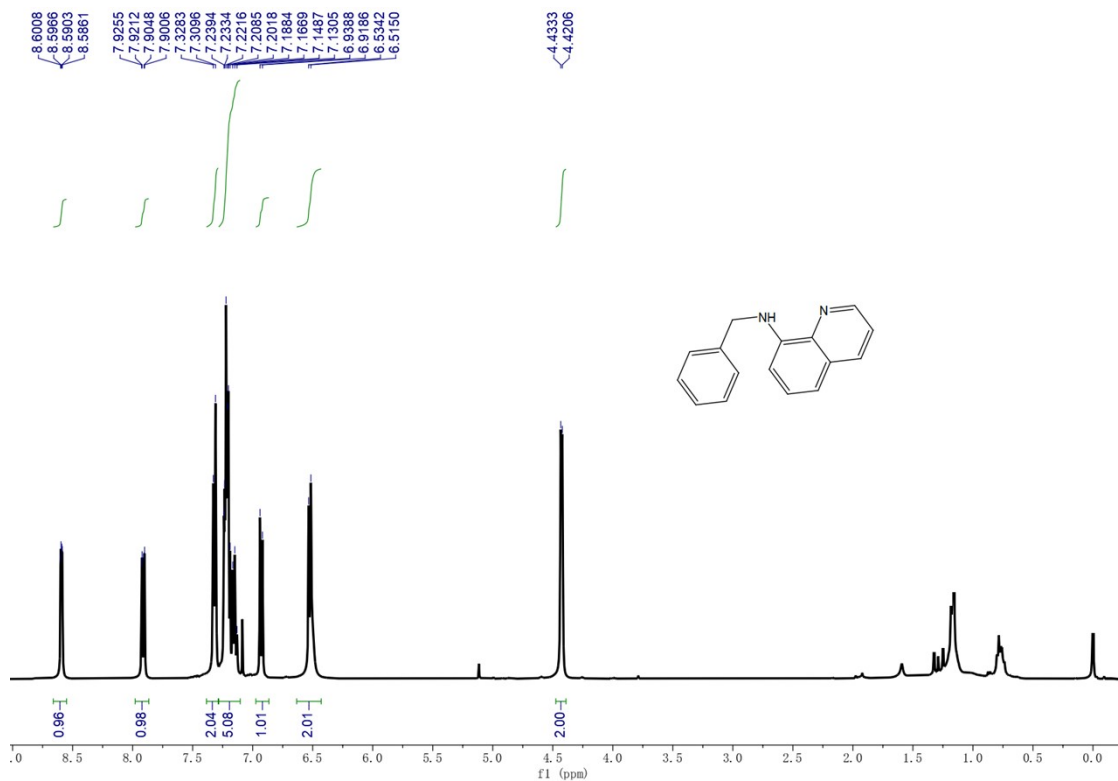


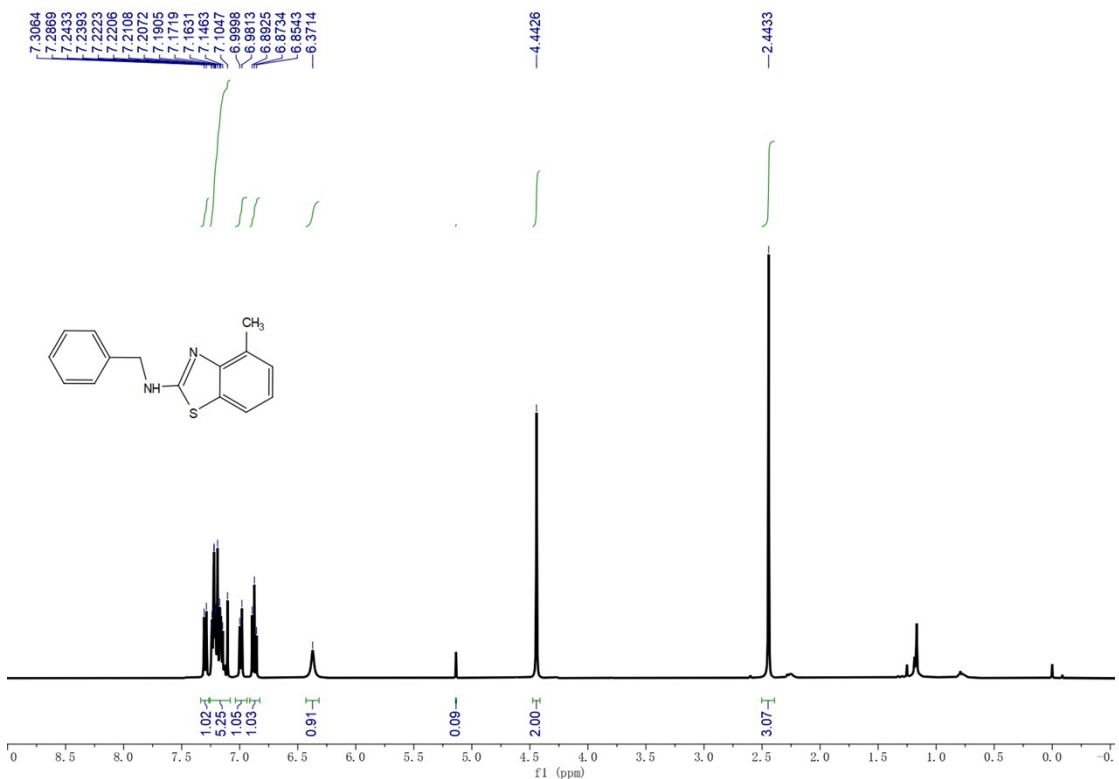
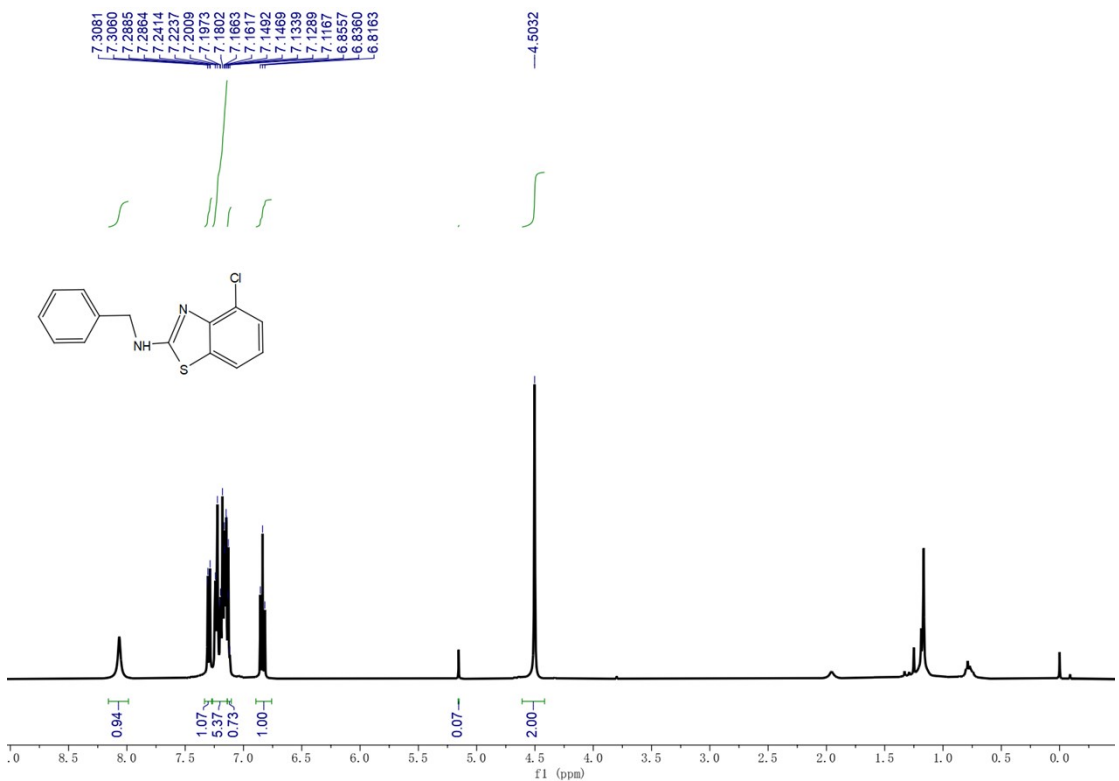












S5 Supplementary References

1. G. Kresse and J. Furthmüller, *Comput. Mater. Sci.*, 1996, **6**, 15-50.
2. J. P. Perdew, K. Burke and M. Ernzerhof, *Phys. Rev. Lett.*, 1996, **77**, 3865.
3. G. Kresse and D. Joubert, *Phys. Rev. B*, 1999, **59**, 1758.
4. P. E. Blöchl, *Phys. Rev. B*, 1994, **50**, 17953.
5. G. Henkelman, B. P. Uberuaga and H. Jónsson, *J. Chem. Phys.*, 2000, **113**, 9901-9904.
6. A. Heyden, A. T. Bell and F. J. Keil, *J. Chem. Phys.*, 2005, **123**.
7. S. Smidstrup, A. Pedersen, K. Stokbro and H. Jónsson, *J. Chem. Phys.*, 2014, **140**.
8. V. Wang, N. Xu, J.-C. Liu, G. Tang and W.-T. Geng, *Comput. Phys. Commun.*, 2021, **267**, 108033.
9. C. M. Wong, M. B. Peterson, I. Pernik, R. T. McBurney and B. A. Messerle, *Inorg. Chem.*, 2017, **56**, 14682-14687.
10. A. K. Bains, A. Kundu, S. Yadav and D. Adhikari, *ACS Catal.*, 2019, **9**, 9051-9059.
11. R. Fertig, T. Irrgang, F. Freitag, J. Zander and R. Kempe, *ACS Catal.*, 2018, **8**, 8525-8530.
12. T. C. Malig, D. Yu and J. E. Hein, *J. Am. Chem. Soc.*, 2018, **140**, 9167-9173.
13. R. Babu, S. Sukanya Padhy, R. Kumar and E. Balaraman, *Chem. Eur. J.*, 2023, **29**, e202302007.
14. W. Su, Y. Xie, M. Chen, Z. Xu, D. Shi, W. Yu, F. Jiang and H. Yu, *Eur. J. Inorg. Chem.*, 2023, **26**, e202200751.
15. S. Chakraborty, R. Mondal, S. Pal, A. K. Guin, L. Roy and N. D. Paul, *J. Org. Chem.*, 2022, **88**, 771-787.
16. S. Bauri, S. Donthireddy, P. M. Illam and A. Rit, *Inorg. Chem.*, 2018, **57**, 14582-14593.
17. S. Çakır, S. B. Kavukcu, O. Sahin, S. Gunnaz and H. Turkmen, *ACS Omega.*, 2023, **8**, 5332-5348.
18. D. Wu, Q. Bu, C. Guo, B. Dai and N. Liu, *Mol. Catal.*, 2021, **503**, 111415.
19. T. T. Dang, B. Ramalingam, S. P. Shan and A. M. Seayad, *ACS Catal.*, 2013, **3**, 2536-2540.
20. C.-C. Lee and S.-T. Liu, *ChemComm.*, 2011, **47**, 6981-6983.
21. M.-X. Fu, J.-H. Lin and J.-C. Xiao, *Org. Lett.*, 2024, **26**, 6065-6069.
22. S. Yang and B. M. Kim, *RSC Adv.*, 2022, **12**, 2436-2442.
23. A. Nandy and G. Sekar, *Eur. J. Org. Chem.*, 2022, **2022**, e202200982.
24. F. Freitag, T. Irrgang and R. Kempe, *J. Am. Chem. Soc.*, 2019, **141**, 11677-11685.
25. M. Huang, Y. Li, J. Liu, X.-B. Lan, Y. Liu, C. Zhao and Z. Ke, *RSC Green Chem.*, 2019, **21**, 219-224.
26. D. Pi, H. Zhou, Y. Zhou, Q. Liu, R. He, G. Shen and Y. Uozumi, *Tetrahedron*, 2018, **74**, 2121-2129.
27. Y. Xu, B. Li, X. Zhang and X. Fan, *J. Org. Chem.*, 2017, **82**, 9637-9646.

